Rethinking the Pruning Criteria for Convolutional Neural Network

Zhongzhan Huang[1] **Wenqi Shao**[2,3‡] **Xinjiang Wang**[3] **Liang Lin**[1] **Ping Luo**[4*]
[1]Sun Yat-Sen University, [2]The Chinese University of Hong Kong,
[3]SenseTime Research,[4]The University of Hong Kong

Abstract

Channel pruning is a popular technique for compressing convolutional neural networks (CNNs), where various pruning criteria have been proposed to remove the redundant filters. From our comprehensive experiments, we found two blind spots of pruning criteria: (1) Similarity: There are some strong similarities among several primary pruning criteria that are widely cited and compared. According to these criteria, the ranks of filters' *Importance Score* are almost identical, resulting in similar pruned structures. (2) Applicability: The filters' *Importance Score* measured by some pruning criteria are too close to distinguish the network redundancy well. In this paper, we analyze the above blind spots on different types of pruning criteria with layer-wise pruning or global pruning. We also break some stereotypes, such as that the results of ℓ_1 and ℓ_2 pruning are not always similar. These analyses are based on the empirical experiments and our assumption (*Convolutional Weight Distribution Assumption*) that the well-trained convolutional filters in each layer approximately follow a Gaussian-alike distribution. This assumption has been verified through systematic and extensive statistical tests.

1 Introduction

Pruning [1, 2, 3, 4] a trained neural network is commonly seen in network compression. In particular, for CNNs, channel pruning refers to the pruning of the filters in the convolutional layers. There are several critical factors for channel pruning. **Procedures**. One-shot method [5]: Train a network from scratch; Use a certain criterion to calculate filters' *Importance Score*, and prune the filters which have small *Importance Score*; After additional training, the pruned network can recover its accuracy to some extent. Iterative method [1, 6, 7]: Unlike One-shot methods, they prune and fine-tune a network alternately. **Criteria**. The filters' *Importance Score* can be definded by a given criterion. From different ideas, many types of pruning criteria have been proposed, such as Norm-based [5], Activation-based [8, 9], Importance-based [10, 11], BN-based [12] and so on. **Strategy**. Layer-wise pruning: In each layer, we can sort and prune the filters, which have small *Importance Score* measured by a given criterion. Global pruning: Different from layer-wise pruning, global pruning [12, 13] sort the filters from all the layers through their *Importance Score* and prune them.

In this work, we conduct our investigation on a variety of pruning criteria. As one of the simplest and most effective channel pruning criteria, ℓ_1 pruning [5] is widely used in practice. The core idea of this criterion is to sort the ℓ_1 norm of filters in one layer and then prune the filters with a small ℓ_1 norm. Similarly, there is ℓ_2 pruning which instead leverages the ℓ_2 norm [7, 6]. ℓ_1 and ℓ_2 can be seen as the criteria which use absolute *Importance Score* of filters. Through the study of the distribution of norm, [4] demonstrates that these criteria should satisfy two conditions: (1) the variance of the norm of the filters cannot be too small; (2) the minimum norm of the filters should be small enough. Since

[*]Corresponding author: pluo.lhi@gmail.com; [‡] co-first author.

35th Conference on Neural Information Processing Systems (NeurIPS 2021), Sydney, Australia.

Table 1: An example to illustrate the phenomenon that different criteria may select the similar sequence of filters for pruning. Taking VGG16 (3$^{\text{rd}}$ Conv) and ResNet18 (12$^{\text{th}}$ Conv) on Norm-based criteria as examples. The pruned filters' index (the ranks of filters' *Importance Score*) are almost the same, which lead to the similar pruned structures.

Criteria	Model	Pruned Filters' Index (Top 8)	Model	Pruned Filters' Index (Top 8)
ℓ_1	ResNet18	[111, 212, 33, 61, 68, 152, 171, 45]	VGG16	[102, 28, 9, 88, 66, 109, 86, 45]
ℓ_2	ResNet18	[111, 33, 212, 61, 171, 42, 243, 129]	VGG16	[102, 28, 88, 9, 109, 66, 86, 45]
GM	ResNet18	[111, 212, 33, 61, 68, 45, 171, 42]	VGG16	[102, 28, 9, 88, 109, 66, 45, 86]
Fermat	ResNet18	[111, 212, 33, 61, 45, 171, 42, 68]	VGG16	[102, 28, 88, 9, 109, 66, 45, 86]

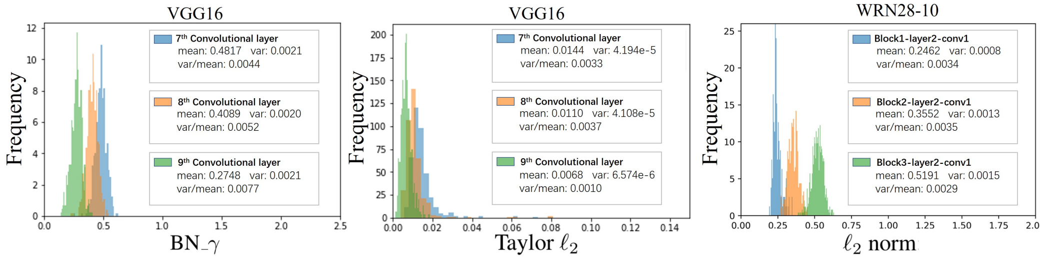

Figure 1: Visualization of Applicability problem, *i.e.,* the histograms of the *Importance Score* measured by different types of pruning criteria (like BN_γ, Taylor ℓ_2 and ℓ_2 norm). The *Importance Score* in each layer are close enough, which implies that it is hard for these criteria to distinguish redundant filters well in layer-wise pruing.

these two conditions do not always hold, a new criterion considering the relative *Importance Score* of the filters is proposed [4]. Since this criterion uses the Fermat point (*i.e.*, geometric median [14]), we call this method **Fermat**. Due to the high calculation cost of Fermat point, [4] further relaxed the **Fermat** and then introduced another criterion denotes as **GM**. To illustrate each of the pruning criteria, let $F_{ij} \in \mathbb{R}^{N_i \times k \times k}$ represent the j^{th} filter of the i^{th} convolutional layer, where N_i is the number of input channels for i^{th} layer and k denotes the kernel size of the convolutional filter. In i^{th} layer, there are N_{i+1} filters. For each criteria, details are shown in Table 2, where $\mathbf{F}$ denotes the Fermat point of F_{ij} in Euclidean space. These four pruning criteria are called Norm-based pruning in this paper as they utilize norm in their design.

Previous works [15, 3, 16, 17, 18], including the criteria mentioned above, the main concerns commonly consist of (a) How much the model was compressed; (b) How much performance was restored; (c) The inference efficiency of the pruned network and (d) The cost of finding the pruned network. However, few works discussed the following two blind spots about the pruning criteria:

(1) Similarity: What are the actual differences among these pruning criteria? Taking the VGG16 and ResNet18 on ImageNet as an example, we show the ranks of filters' *Importance Score* under different criteria in Table 1. It is obvious that they have almost the same sequence, leading to similar pruned structures. In this situation, the criteria used absolute *Importance Score* of filters (ℓ_1,ℓ_2) and the criteria used relative *Importance Score* of filters (**Fermat**, **GM**) may not be significantly different.

Table 2: Norm-based pruning criteria.

Criterion	Details of *Importance Score*
ℓ_1 [5]	$\|\|F_{ij}\|\|_1$
ℓ_2 [7]	$\|\|F_{ij}\|\|_2$
Fermat [4]	$\|\|\mathbf{F} - F_{ij}\|\|_2$
GM [4]	$\sum_{k=1}^{N_{i+1}} \|\|F_{ik} - F_{ij}\|\|_2$

(2) Applicability: What is the applicability of these pruning criteria to prune the CNNs? There is a toy example w.r.t. ℓ_2 criterion. If the ℓ_2 norm of the filters in one layer are 0.9, 0.8, 0.4 and 0.01, according to *smaller-norm-less-informative assumption* [19], it's apparent that we should prune the last filter. However, if the norm are close, such as 0.91, 0.92, 0.93, 0.92, it is hard to determine which filter should be pruned even though the first one is the smallest. In Fig. 1, we demonstrate some real examples, *i.e.,* the visualization of Applicability problem under different networks and criteria.

In this paper, we provide comprehensive observations and in-depth analysis of these two blind spots. Before that, in Section 2, we propose an assumption about the parameters distribution of CNNs, called *Convolution Weight Distribution Assumption* (CWDA), and use it as a theoretical tool to analyze the two blind spots. We explore the Similarity and Applicability problem of pruning criteria in the following order: (1) Norm-based criteria (layer-wise pruning) in Section 3; (2) Other types of criteria (layer-wise pruning) in Section 4; (3) and different types of criteria (global pruning) in Section 5. Last but not least, we provide further discussion on: (i) the conditions for CWDA to be satisfied, (ii) how our findings help the community in Section 6. In order to focus on the pruning criteria, all the pruning experiments are based on the relatively simple pruning procedure, *i.e.,* one-shot method.

The main **contributions** of this work are two-fold:

(1) We analyze the Applicability problem and the Similarity of different types of pruning criteria. These two blind spots can guide and motivate researchers to design more reasonable criteria. We also break some stereotypes, such as that the results of ℓ_1 and ℓ_2 pruning are not always similar.

(2) We propose and verify an assumption called CWDA, which reveals that the well-trained convolutional filters approximately follow a Gaussian-alike distribution. Using CWDA, we succeeded in explaining the multiple observations about these two blind spots theoretically.

2 Weight Distribution Assumption

In this section, we propose and verify an assumption about the parameters distribution of the convolutional filters.

(Convolution Weight Distribution Assumption) Let $F_{ij} \in \mathbb{R}^{N_i \times k \times k}$ be the j^{th} well-trained filter of the i^{th} convolutional layer. In general[2], in i^{th} layer, F_{ij} $(j = 1, 2, ..., N_{i+1})$ are i.i.d and follow such a distribution:

$$F_{ij} \sim \mathbf{N}(\mathbf{0}, \mathbf{\Sigma}^i_{\text{diag}} + \epsilon \cdot \mathbf{\Sigma}^i_{\text{block}}), \tag{1}$$

where $\mathbf{\Sigma}^i_{\text{block}} = \text{diag}(K_1, K_2, ..., K_{N_i})$ is a block diagonal matrix and the diagonal elements of $\mathbf{\Sigma}^i_{\text{block}}$ are 0. ϵ is a small constant. The values of the off-block-diagonal elements are 0 and $K_l \in R^{k^2 \times k^2}, l = 1, 2, ..., N_i$. $\mathbf{\Sigma}^i_{\text{diag}} = \text{diag}(a_1, a_2, ..., a_{N_i \times k \times k})$ is a diagonal matrix and the elements of $\mathbf{\Sigma}^i_{\text{diag}}$ are close enough.

This assumption is based on the observation shown in the Fig. 2. To estimate $\mathbf{\Sigma}^i_{\text{diag}} + \epsilon \cdot \mathbf{\Sigma}^i_{\text{block}}$, we use the correlation matrix FF^T where $F \in \mathbb{R}^{(N_i \times k \times k) \times N_{i+1}}$ denotes all the parameters in i^{th} layer. Taking a convolutional layer of ResNet18 trained on ImageNet as an example, we find that FF^T is a block diagonal matrix. Specifically, each block is a $k^2 \times k^2$ matrix and the off-diagonal elements are close to 0. We visualize the j^{th} filter $F_{ij} \in \mathbb{R}^{N_i \times k \times k}$ in i^{th} layer in Fig. 2(c), and this phenomenon reveals that the parameters in the same channel of F_{ij} tend to be linearly correlated, and the parameters of any two different channels (yellow and green channel in Fig. 2(c)) in F_{ij} only have a low linear correlation.

2.1 Statistical test for CWDA

In fact, CWDA is not easy to be verified, *e.g.*, for ResNet164 trained on Cifar100, the number of filters in the first stage is only 16, which is too small to be used to estimate the statistics in CWDA accurately. Thus, We consider verifying four **necessary conditions** of CWDA:

(1) **Gaussian.** Whether the weights of F_{ij} approximately follows a Gaussian-alike distribution; (2) **Variance.** Whether the variance of the diagonal elements of Σ_{diag} are small enough; (3) **Mean.** Whether the mean of weights of F_{ij} is close to 0. (4) **The magnitude of** ϵ**.** Whether ϵ is small enough.

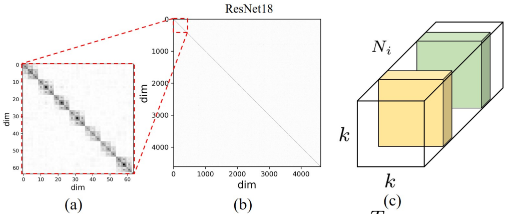

Figure 2: (a-b) Visualization of FF^T in ResNet-18 trained on ImageNet dataset. More experiments can be found in Appendix N. These experiments are based on torchvison model zoo [20], which can guarantee the generality and reproducibility. (c) A convolutional filter. k is the kernel size and N_i denotes the number of input channels.

The results of the tests are shown in Appendix P, where we consider a variety of factors for the statistical tests, including different network structure, optimizer, regularization, initialization, dataset,

[2] In Section 6, we make further discussion and analysis on the conditions for CWDA to be satisfied.

training strategy, and other tasks in computer vision (*e.g.*, semantic segmentation, detection and so on). The test results show that CWDA has a great generality for CNNs.

3 About the Norm-based criteria

We start from the criteria in Table 2, which are widely cited and compared [21, 22, 23, 24, 25].

3.1 Similarity

In this section, we further verify the observation that the Norm-based pruning criteria in Table 2 are highly similar from two perspectives. Empirically, we conducted large amount of experiments on image classification to investigate the similarities. Theoretically, we rigorously prove the similarities of the criteria in Table 2 in layer-wise pruning under CWDA.

Empirical Analysis. (1) In Fig. 3, we show the test accuracy of the ResNet56 after pruning and fine-tuning under different pruning ratios and datasets. The test accuracy curves of different pruning criteria at different stages are very close under different pruning ratios. This phenomenon implies that those pruned networks using different Norm-based criteria are very similar, and there are strong similarities among these pruning criteria. The experiments about other commonly used configs of pruning ratio can be found in Appendix L. (2) In Fig. 4, we show the Spearman's rank correlation coefficient[3] (Sp) between different pruning criteria. The Sp in most convolutional layers are more than 0.9, which means the network structures are almost the same after pruning. Note that the Sp in transition layer are relatively small, and the transition layer refers to the layer where the dimensions of the filter change, like the layer between stage 1 and stage 2 of a ResNet. The reason for this phenomenon may be that the layers in these areas are sensitive. It is interesting but will not greatly impact the structural similarity of the whole pruned network. The similar observations are shown in Fig. 2 in [16], Fig. 6 and Fig. 10 in [5].

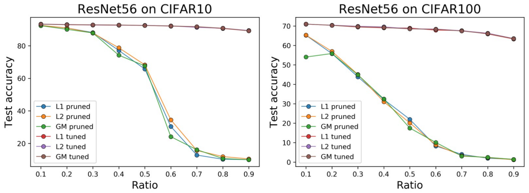

Figure 3: Test accuracy of the ResNet56 on CIFAR10/100 while using different pruning ratios. "L1 pruned" and "L1 tuned" denote the test accuracy of the ResNet56 after ℓ_1 pruning and fine-tuning, respectively. If ratio is 0.5, we prune 50% filters in all layers.

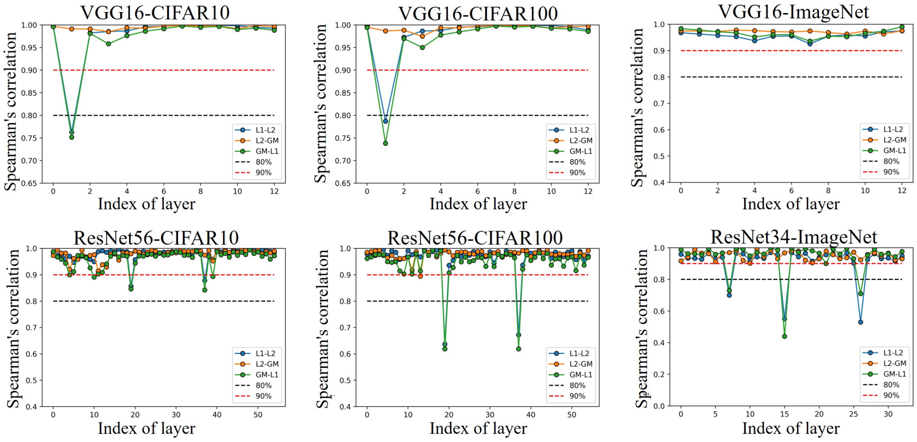

Figure 4: Spearman's rank correlation coefficient (Sp) between different pruning criteria on several networks and datasets (more experiments can be found in Appendix R).

[3] Sp is a nonparametric measurement of ranking correlation, and it assesses how well the relationship between two variables can be described using a monotonic function, *i.e.*, filters ranking sequence in the same layer under two criteria in this paper.

Theoretical Analysis. Besides the experimental verification, the similarities via using layer-wise pruning among the criteria in Table 2 can also be proved theoretically in this section. Let C_1 and C_2 be two pruning criteria to calculate the *Importance Score* for all convolutional filters in one layer. If they can produce the similar ranks of *Importance Score*, we define that C_1 and C_2 are *approximately monotonic* to each other and use $C_1 \cong C_2$ to represent this relationship. In Section 3.1, we use the Sp to describe this relationship but it's hard to be analyzed theoretically. Therefore, we focus on a stronger condition. Let $\mathbf{X} = (x_1, x_2, ..., x_k)$ and $\mathbf{Y} = (y_1, y_2, ..., y_k)$ be two given sequences[4]. we first normalize their magnitude, *i.e.*, let $\widehat{\mathbf{X}} = \mathbf{X}/\mathbb{E}(\mathbf{X})$ and $\widehat{\mathbf{Y}} = \mathbf{Y}/\mathbb{E}(\mathbf{Y})$. This operation does not change the ranking sequence of the elements of $\mathbf{X}$ and $\mathbf{Y}$, because $\mathbb{E}(\mathbf{X})$ and $\mathbb{E}(\mathbf{Y})$ are constants, *i.e.*, $\widehat{\mathbf{X}} \cong \widehat{\mathbf{Y}} \Leftrightarrow \mathbf{X} \cong \mathbf{Y}$. After that, if both $\mathbf{Var}(\widehat{\mathbf{X}}/\widehat{\mathbf{Y}})$ and $\mathbf{Var}(\widehat{\mathbf{Y}}/\widehat{\mathbf{X}})$ are small enough, then the Sp between $\mathbf{X}$ and $\mathbf{Y}$ is close to 1, where $\widehat{\mathbf{X}}/\widehat{\mathbf{Y}} = (\widehat{x_1}/\widehat{y_1}, .., \widehat{x_k}/\widehat{y_k})$. The reason is that in these situations, the ratio $\widehat{\mathbf{X}}/\widehat{\mathbf{Y}}$ and $\widehat{\mathbf{Y}}/\widehat{\mathbf{X}}$ will be close to two constants a, b. For any $1 \leq i \leq k$, $\widehat{x_i} \approx a \cdot \widehat{y_i}$ and $\widehat{y_i} \approx b \cdot \widehat{x_i}$. So, $ab \approx 1$ and $a, b \neq 0$. Therefore, there exists an *approximately monotonic* mapping from $\widehat{y_i}$ to $\widehat{x_i}$ (linear function), which makes the Sp between $\mathbf{X}$ and $\mathbf{Y}$ close to 1. With this basic fact, we propose the Theorem 1, which implies that many Norm-based pruning criteria produces almost the same ranks of *Importance Score*.

Theorem 1. *Let $n-$dimension random variable X meet CWDA, and the pair of criteria (C_1, C_2) is one of (ℓ_1, ℓ_2), $(\ell_2, \mathbf{Fermat})$ or $(\mathbf{Fermat}, \mathbf{GM})$, we have*

$$\mathbf{max}\left\{\mathbf{Var}_X\left(\frac{\widehat{C}_2(X)}{\widehat{C}_1(X)}\right), \mathbf{Var}_X\left(\frac{\widehat{C}_1(X)}{\widehat{C}_2(X)}\right)\right\} \lesssim B(n), \tag{2}$$

where $\widehat{C}_1(X)$ denotes $C_1(X)/\mathbb{E}(C_1(X))$ and $\widehat{C}_2(X)$ denotes $C_2(X)/\mathbb{E}(C_2(X))$. $B(n)$ denotes the upper bound of left-hand side and when n is large enough, $B(n) \to 0$.

Proof. (See Appendix C). □

In specific, for i^{th} convolutional layer of a CNN, since $F_{ij} \in \mathbb{R}^n$, $j = 1, 2, ...N_{i+1}$, meet CWDA and the dimension n is generally large, we can obtain $\ell_1 \cong \ell_2$, $\ell_2 \cong \mathbf{Fermat}$ and $\mathbf{Fermat} \cong \mathbf{GM}$ according to Theorem 1. Therefore, we have $\ell_1 \cong \ell_2 \cong \mathbf{Fermat} \cong \mathbf{GM}$, which verifies the strong similarities among the criteria shown in Table 2.

3.2 Applicability

In this section, we analyze the Applicability problem of the Norm-based criteria. In Fig. 1 (Right), we know that there are some cases where the values of *Importance Score* measured by ℓ_2 criterion are very close (e.g., the distribution looks sharp), which make ℓ_2 criterion cannot distinguish the redundant filters well. It's related to the variance of *Importance Score*. [4] argue that a *small norm deviation* (the values of variance of *Importance Score* are small) makes it difficult to find an appropriate threshold to select filters to prune. However, even if the values of the variance are large, it still cannot guarantee to solve this problem. Since the magnitude of these *Importance Score* may be much greater than the values of the variance, we can use the mean of *Importance Score* to represent their magnitude. Therefore, we consider using a relative variance $\mathbf{Var}_r[C(F_A)]$ to describe the Applicability problem. Let $\mathbb{E}[C(F_A)] > 0$ and

$$\mathbf{Var}_r[C(F_A)] = \mathbf{Var}[C(F_A)]/\mathbb{E}[C(F_A)], \tag{3}$$

where C is a given pruning criterion and F_A denotes the filters in layer A. The criterion C for layer A has Applicability problem when $\mathbf{Var}_r[C(F_A)]$ is close to 0. Then we introduce the Proposition 1 to provide the estimation of the mean and variance w.r.t. different criteria when the CWDA is hold:

Proposition 1. *If the convolutional filters F_A in layer A meet CWDA, then we have following estimations:*

Criterion	Mean	Variance
$\ell_1(F_A)$	$\sqrt{2/\pi}\sigma_A d_A$	$(1-\frac{2}{\pi})\sigma_A^2 d_A$
$\ell_2(F_A)$	$\sqrt{2}\sigma_A\Gamma(\frac{d_A+1}{2})/\Gamma(\frac{d_A}{2})$	$\sigma_A^2/2$
$\mathbf{Fermat}(F_A)$	$\sqrt{2}\sigma_A\Gamma(\frac{d_A+1}{2})/\Gamma(\frac{d_A}{2})$	$\sigma_A^2/2$

[4] Since $\mathbf{X}$ is not random variables here, $\mathbb{E}(\mathbf{X})$ and $\mathbf{Var}(\mathbf{X})$ denote the average value $\sum_{i=1}^{k} x_i/k$ and the sample variance $\sum_{i=1}^{k}(x_i - \mathbb{E}(\mathbf{X}))/(k-1)$, respectively.

where d_A and σ_A^2 denote the dimension of F_A and the variance of the weights in layer A, respectively.

Proof. (See Appendix A). □

Based on the Proposition 1, we further provide the theoretical analysis for each criteria:

(i) For $\ell_2(F_A)$. From Proposition 1, we can obtain that

$$\mathbf{Var}_r[\ell_2(F_A)] = \frac{\sigma_A^2}{2} / [\sqrt{2}\sigma_A \Gamma(\frac{d_A+1}{2}) / \Gamma(\frac{d_A}{2})] = O(\sigma_A / g(d_A)), \tag{4}$$

where $g(d_A) = \Gamma(\frac{d_A+1}{2})/\Gamma(\frac{d_A}{2})$ is a monotonically increasing function w.r.t d_A. From Eq. (4), $\mathbf{Var}_r[\ell_2(F_A)]$ depend on σ_A and d_A. When σ_A is small or d_A is large enough, $\mathbf{Var}_r[\ell_2(F_A)]$ tends to be 0.

(ii) For $\mathbf{Fermat}(F_A)$. From the proof in Appendix D, we know that the Fermat point $\mathbf{F}$ of F_A and the origin $\mathbf{0}$ approximately coincide. From Table 1, $||\mathbf{F} - F_A||_2 \approx ||\mathbf{0} - F_A||_2 = ||F_A||_2$. Therefore, the mean and variance of $\mathbf{Fermat}(F_A)$ are the same as $\ell_2(F_A)$'s in Proposition 1. Hence, a similar conclusion can be obtained for **Fermat** criterion. *i.e.,* the *Importance Score* tends to be identical and it's hard to distinguish the network redundancy well when σ_A is small or d_A is large enough.

(iii) For $\ell_1(F_A)$. Intuitively, the ℓ_1 criterion should have the same conclusion as the ℓ_2 criterion. However, given the Proposition 1, we can obtain that

$$\mathbf{Var}_r[\ell_1(F_A)] = (1 - \frac{2}{\pi})\sigma_A^2 d_A / [\sqrt{2/\pi}\sigma_A d_A] = \epsilon(\pi) \cdot \sigma_A, \tag{5}$$

where $\epsilon(\pi) < 1$ is a constant w.r.t π. Note that $\mathbf{Var}_r[\ell_1(F_A)]$ only depend on σ_A, but not the dimension n. Moreover, for the common network structures, like VGG, ResNet shown in Fig. 6 (b) and (d), the dimension of the filters are usually large enough. Therefore, compared with ℓ_2, ℓ_1 criterion is relatively not prone to have Applicability problems, unless the σ_A is very small.

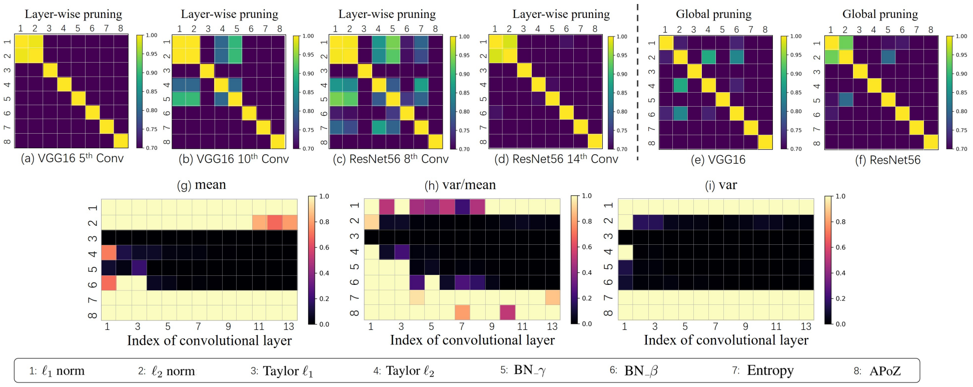

(a) VGG16 5th Conv (b) VGG16 10th Conv (c) ResNet56 8th Conv (d) ResNet56 14th Conv (e) VGG16 (f) ResNet56

(g) mean (h) var/mean (i) var

Figure 5: The Similarity and Applicability problem for different types of pruning criteria in layer-wise or global pruning.

4 About other types of pruning criteria

In this section, we study the Similarity and Applicability problem in other types of pruning criteria through numerical experiments, such as Activation-based pruning [8, 9], Importance-based pruning [10, 11] and BN-based pruning [12]. For each type, we choose two representative criteria and we call them: (1) Norm-based: ℓ_1 and ℓ_2; (2) Importance-based: Taylor ℓ_1 and Taylor ℓ_2 [10, 11, 26]; (3) BN-based: BN_γ[5] and BN_β [12]; (4) Activation-based: Entropy [9] and APoZ [8]. The details of these criteria can be found in Appendix K.

The Similarity for different types of pruning criteria. In Fig. 5 (a-d), we show the Sp between different types of pruning criteria, and only the Sp greater than 0.7 are shown because if Sp < 0.7, it means that there is no strong similarity between two criteria in the current layer.

[5] The empirical result for slimming training [12] is shown in Appendix Q.

According to the Sp shown in Fig. 5 (a-d), we obtain the following observations: (1) As verified in Section 3.1, ℓ_1 and ℓ_2 can maintain a strong similarity in each layer; (2) In the layers shown in Fig. 5 (a) and Fig. 5 (d), the Sp between most different pruning criteria are not large in these layers, which indicates that these criteria have great differences in the redundancy measurement of convolutional filters. This may lead to a phenomenon that one criterion considers a convolutional filter to be important, while another considers it redundant. We find a specific example which is shown in Appendix J; (3) Intuitively, the same type of criteria should be similar. However, Fig. 5 (b) and Fig. 5 (c) show that the Sp between Taylor ℓ_1 and Taylor ℓ_2 is not large, but Taylor ℓ_2 has strong similarity with both two Norm-based criteria. Moreover, the Sp between BN_γ and each Norm-based criteria exceeds 0.9, but it is not large in other layers (Fig. 5 (a) and Fig. 5 (d)). These phenomena are worthy of further study.

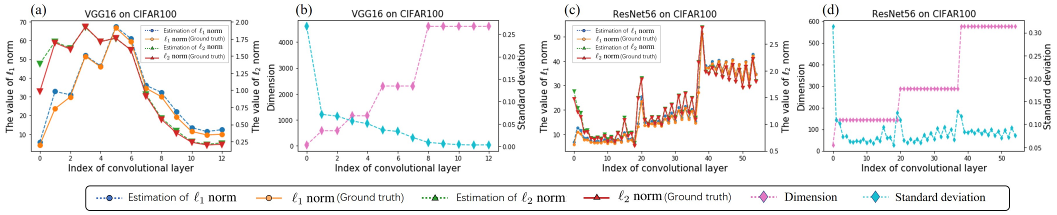

Figure 6: The magnitude of the *Importance Score* measured by ℓ_1 and ℓ_2 criteria.

The Applicability for different types of pruning criteria. According to the analysis in Section 3.2, the Applicability problem depends on the mean and variance of the *Importance Score*. Fig. 5 (g-i) shows the result of the *Importance Score* measured by different pruning criteria on each layer of VGG16. Due to the difference in the magnitude of *Importance Score* for different criteria, for the convenience of visualization, the value greater than 1 is represented by 1.

First, we analyze the Norm-based criteria. In most layers, the relative variance $\mathbf{Var}_r[\ell_2]$ is much smaller than that of $\mathbf{Var}_r[\ell_1]$, which means that the ℓ_2 pruning has Applicability problem in VGG16, while the ℓ_1 does not. This is consistent with our conclusion in Section 3.2. Next, for the Activation-based criteria, the relative variance $\mathbf{Var}_r$ is large in each layer, which means that these two Activation-based criteria can distinguish the network redundancy well from their measured filters' *Importance Score*. However, for the Importance-based and BN-based criteria, their relative variance $\mathbf{Var}_r$ are close to 0. According to Section 3.2, these criteria have Applicability problem, especially in the deeper layers (e.g., from 6$^{\text{th}}$ layer to the last layer).

5 About global pruning

Compared with layer-wise pruning, global pruning is more widely [27, 10, 12] used in the current research of channel pruning. Therefore, in this section we may also analyze the Similarity and Applicability problem of global pruning.

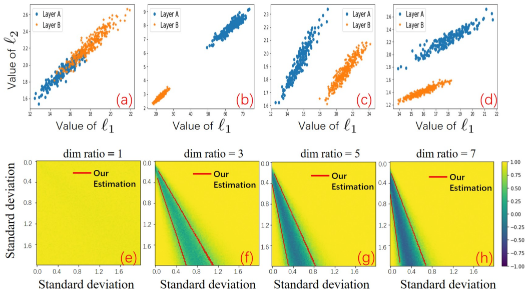

Figure 7: The global pruning simulation for the unpruned network with only two layers.

Applicability while using global pruning. In fact, for global pruning, both ℓ_1 and ℓ_2 criteria are not prone to Applicability problems. From Proposition 1, we show that the estimations for the mean of *Importance Score* in layer A for ℓ_1 and ℓ_2 are $\sigma_A \cdot d_A\sqrt{\frac{2}{\pi}}$ and $\sqrt{2}\sigma_A \cdot \Gamma(\frac{d_A+1}{2})/\Gamma(\frac{d_A}{2})$, respectively. Since σ_A and d_A are quite different, shown in Fig. 6 (b) and (d), hence the variance of the *Importance Score* may be large in this situation. Fig. 6 (a) and (c) show such kind of difference of the magnitude on different convolutional layers. In addition, from our estimations in Fig. 6 (c), this inconsistent magnitude can be explained for another common problem in practical applications of global pruning: the ResNet is easily pruned off. As shown in Fig. 6 (c), we take ResNet56 as an example. Since the *Importance Score* in first stage is much smaller than the *Importance Score* in the deeper layer, global pruning will give priority to prune the convolutional filters of the first stage. For problem, we suggest that some normalization tricks should be implemented or a protection mechanism should be established, *e.g.*, a mechanism which can ensure that each layer has at least a certain number of convolutional filters that will not be pruned. Unlike some previous works [13, 28, 29], which make suggestions from qualitative observation, we provide a quantitative view to illustrate that these tricks are necessary.

Similarity while using global pruning. In Fig. 5 (e-f), we show the similarity of different types of pruning criteria using global pruning on VGG16 and ResNet56. Comparing to the results from the layer-wise pruning shown in Fig. 5 (a-d), we can find that the similarities of most pruning criteria are quite different in global pruning. In addition, the same criteria may have different results for different network structures in global pruning, *e.g.,* in Fig. 5 (e), we can find $\ell_2 \cong$ Taylor ℓ_2 and BN$_\gamma \cong \ell_2$, but this observation does not hold in Fig. 5 (f). In particular, different from the result about ResNet56 in Fig. 5 (f), the similarity between ℓ_1 and ℓ_2 is not as strong as the one in the layer-wise case. This phenomenon is counter intuitive.

To understand this phenomenon, we first consider about a simple case, *i.e.,* the unpruned network has only two convolutional layers (layer A and layer B). The filters in these two layers are $F_A = (F_A^1, F_A^2, ..., F_A^n)$ and $F_B = (F_B^1, F_B^2, ..., F_B^m)$. According to CWDA, for $1 \leq i \leq n$ and $1 \leq j \leq m$, F_A^i and F_B^j can follow $N(\mathbf{0}, \sigma_A^2 \mathbf{I}_{d_A})$ and $N(\mathbf{0}, \sigma_B^2 \mathbf{I}_{d_B})$, respectively. Next, we show Sp between *Importance Score* measured by ℓ_1 and ℓ_2 pruning in different dimension ratio d_A/d_B, σ_A and σ_B in Fig. 7 (e-h). Moreover, to analyze this phenomenon concisely, we draw some scatter plots as shown in Fig. 7 (a-d), where the coordinates of each point are given by (value of ℓ_1, value of ℓ_2). The set of the points consisting of the filters in layer A is called group-A. Then we introduce the Proposition 2.

Proposition 2. *If the convolutional filters F_A in layer A meet CWDA, then $\mathbb{E}[\ell_1(F_A)/\ell_2(F_A)]$ and $\mathbb{E}[\ell_2(F_A)/\ell_1(F_A)]$ only depend on their dimension d_A.*

Proof. (See Appendix A). □

Now we analyze the simple case under different situations:

(1) For $d_A/d_B = 1$. If $\sigma_A^2 = \sigma_B^2$, in fact, it's the same situation as layer-wise pruning. From Theorem 1, we know that group-A and group-B coincide and approximately lie on the same line, resulting $\ell_1 \cong \ell_2$. If $\sigma_A^2 \neq \sigma_B^2$, group-$A$ and group-B lie on two lines, respectively. However, these two lines have the same slope based on Proposition 2, as shown in Fig. 7 (a). For these reasons, we have $\ell_1 \cong \ell_2$ when $d_A/d_B = 1$.

(2) For $d_A/d_B \neq 1$. In Fig. 7 (b-d), there are three main situations about the position relationship between group-A and group-B. In Fig. 7 (b), according to Theorem 1, the points in group-A and group-B are monotonic respectively. Moreover, their *Importance Score* measured by ℓ_1 and ℓ_2 do not overlap, which make ℓ_1 and ℓ_2 are *approximately monotonic* overall. Thus, $\ell_1 \cong \ell_2$. However, for Fig. 7 (c-d), the Sp is small since the points in these two group are not monotonic (the *Importance Score* measured by ℓ_1 or ℓ_2 has a large overlap). From Proposition 1 and the approximation $\Gamma(\frac{d_A+1}{2})/\Gamma(\frac{d_A}{2}) \approx \sqrt{d_A/2}$ (Appendix D), these two situations can be described as:

$$\sigma_A d_A \approx \sigma_B d_B \quad or \quad \sigma_A \sqrt{d_A} \approx \sigma_B \sqrt{d_B}, \tag{6}$$

where $d_A \neq d_B$. Through Eq. (6) we can obtain the two red lines shown in Fig. 7 (f-h). It can be seen that the area surrounded by these two red lines is consistent with the area where the Sp is relatively small, which means our analysis is reasonable. Based on the above analysis, we can summarize the conditions about $\ell_1 \cong \ell_2$ in global pruning for two convolutional layers as shown in Table 3.

Next, we go back to the the situation about real neural networks in Fig. 5 (e-f). (1) For ResNet56. As shown in Fig.6 (d), the dimensions of the filters in each stage are almost the same. From Table 3 (1), the pruning results after ℓ_1 and ℓ_2 pruning in each stage are similar. And, the magnitudes of the *Importance Score* in each stage are very different, since Table 3 (2), we can obtain that $\ell_1 \cong \ell_2$ for ResNet56.

Table 3: The conditions about $\ell_1 \cong \ell_2$ in global pruning for two layers (layer A and layer B)

	$d_A = d_B$?	$\frac{\sigma_A}{\sigma_B} \approx \frac{d_B}{d_A}$?	$\frac{\sigma_A}{\sigma_B} \approx \frac{\sqrt{d_B}}{\sqrt{d_A}}$?	$\ell_1 \cong \ell_2$?
(1)	✓	–	–	✓
(2)	✗	✗	✗	✓
(3)	✗	✓	–	✗
(4)	✗	–	✓	✗

(2) For VGG16. As shown in Fig.6 (a-b), compared with ResNet56, VGG16 has some layers with different dimensions but similar *Importance Score* measured by ℓ_1 or ℓ_2, such as "layer 2" and "layer

8” for ℓ_2 criterion in Fig.6 (a). From Table 3 (3-4), these pairs of layers make the Sp small, which explain why the result of ℓ_1 and ℓ_2 pruning is not similar in Fig. 5 (e) for VGG16. In Appendix O, more experiments show that we can increase the Sp in global pruning by ignoring part of these pairs of layers, which support our analysis.

6 Discussion

6.1 Why CWDA sometimes does not hold?

CWDA may not always hold. As shown in Appendix P, a small number of convolutional filters may not pass all statistical tests. In this section, we try to analyze this phenomenon.

(1) **The network is not trained well enough**. The distribution of parameters should be discussed **only when** the network is trained well. If the network does not converge, it is easy to construct a scenario which does not satisfy CWDA, *e.g.*, for a network with uniform initialization, when it is only be trained for a few epochs, the distribution of parameters may be still close to a uniform distribution. At this time, the distribution obviously does not satisfy CWDA. A specific example is in Appendix I.

(2) **The number of filters is insufficient.** In Appendix P, the layers that can not pass the statistical tests are almost those whose position is in the front of the network. A common characteristic of these layers is that they have a few filters, which may not estimate statistics well. Taking the second convolutional layer (64 filters) in VGG16 on CIFAR10 as an example, first, the filters in this layer can not pass all the statistical tests. And then the Sp in this transition layer is relatively small, as shown in Fig. 4. However, in Fig. 8, we change the number of filters in this layer from 64 to 128 or 256. After that, the Sp increases significantly, and the filters can pass all the statistical tests when the number of filters is 256. These observations suggest that the number of filters is a major factor for CWDA to be hold.

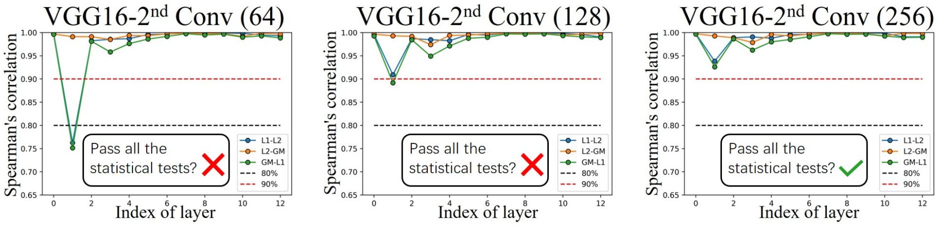
VGG16-2nd Conv (64)
VGG16-2nd Conv (128)
VGG16-2nd Conv (256)

Figure 8: The Sp between different pruning criteria on VGG16 (CIFAR10). The number of filters in the second convolutional layers is changed from 64 to 256. The filters in this layer can pass all the statistical tests when the number of filters is 256.

6.2 How our findings help the community?

(1) We propose an assumption about the parameters distribution of the CNNs called CWDA, which is an effective theoretical tool for analyzing convolutional filter. In this paper, CWDA is successfully used to explain many phenomena in the Similarity and Applicability of pruning criteria. In addition, it also explains why the ResNet is easily pruned off in global pruning. In Section 2.1, since CWDA can pass statistical tests in various situations, it can be expected that it can also be used as an effective and concise analysis tool for other CNNs-related areas, **not just** pruning area.

(2) In this paper, we study the Similarity and Applicability problem about pruning criteria, which can guide and motivate the researchers to design more reasonable criteria. For Applicability problem, we suggest that, intuitively, it is reasonable that the *Importance Score* should be distinguishable for the proposed novel criteria. For Similarity, as more and more criteria are proposed, these criteria can be used for ensemble learning to enhance their pruning performance [23]. In this case, the similarity analysis between criteria in this paper is important, because highly similar criteria cannot bring gains to ensemble learning.

(3) In pruning area, ℓ_1 and ℓ_2 are usually regarded as the same pruning criteria, which is intuitive. In layer-wise pruning, we do prove that the ℓ_1 and ℓ_2 pruning are almost the same. However, in global pruning, the pruning results by these two criteria are sometimes very different. In addition, compared

with ℓ_1 criterion, ℓ_2 criterion is prone to Applicability problems. These counter-intuitive phenomena enlighten us that we can't just rely on intuition when analyzing problems.

Table 4: The random pruning results of VGGNet with different criteria which have the Applicability problem. The VGG16 and VGG19 are trained on CIFAR100. The unpruned baseline accuracy of VGG16 and VGG19 are 72.99 and 73.42, respectively.

Model	criterion	min (r=10%)	max (r=10%)	mean (r=10%)	Δ	min (r=20%)	max (r=20%)	mean (r=20%)	Δ
VGG16	ℓ_2	71.41	72.65	71.75	1.24	71.01	72.47	71.32	1.46
	Taylor ℓ_1	71.67	72.34	71.89	0.67	71.32	72.32	71.45	1.01
	Taylor ℓ_2	71.87	72.37	71.91	0.5	71.66	72.27	71.65	0.61
	BN_γ	71.09	71.66	71.36	0.57	71.02	71.57	71.12	0.55
	BN_β	71.15	72.58	71.43	1.43	71.06	72.11	71.87	1.05
VGG19	ℓ_2	71.99	73.15	72.26	1.16	71.11	73.02	72.15	1.91
	Taylor ℓ_1	71.67	73.04	72.23	1.37	71.6	72.98	72.24	1.38
	Taylor ℓ_2	72.12	72.99	72.28	0.87	72.04	72.83	72.54	0.79
	BN_γ	72.01	73.23	72.25	1.22	71.98	72.32	72.12	0.34
	BN_β	72.25	73.23	72.41	0.98	72.04	72.65	72.33	0.61

(4) Similar to the setting in Fig. 5, we can explore the effect of pruning filters with similar *Importance Score* on the performance. First, we find that the criteria (ℓ_2,Taylor ℓ_1, Taylor ℓ_2, BN_γ and BN_β) for VGGNet can cause the Applicability problem in most layers (Fig. 5). As such, we randomly select 10% or 20% filters to be pruned by the uniform distribution $U[0, 1]$ in each layer, and the selective filters will be in similar *Importance Score*. Finally, we finetune the pruned model (there are 20 random repeated experiments). Δ denotes the difference between max acc. and min acc. (*i.e.* max acc. - min acc.) . Since their *Importance Score* are very similar, when the network is pruned and finetuned, it can be expected that the performance should be similar in these repeated experiments. However, from the results in the above table, although the *Importance Score* of the pruned filters is very close, we can still get pruning results with very different results (*e.g.* the Δ of VGG16 on ℓ_2 are more than 1). It means that these criteria may not really represent the importance of convolutional filters. Therefore, it is necessary to re-evaluate the correctness of the existing pruning criteria.

Acknowledgments. Z. Huang gratefully acknowledges the technical and writing support from Mingfu Liang (Northwestern University), Senwei Liang (Purdue University) and Wei He (Nanyang Technological University). Moreover, he sincerely thanks Mingfu Liang for offering his self-purchasing GPUs and Qinyi Cai (NetEase, Inc.) for checking part of the proof in this paper. This work was supported in part by the General Research Fund of Hong Kong No.27208720, the National Key R&D Program of China under Grant No. 2020AAA0109700, the National Science Foundation of China under Grant No.61836012 and 61876224, the National High Level Talents Special Support Plan (Ten Thousand Talents Program), and GD-NSF (no.2017A030312006).

References

[1] Yann LeCun, John S Denker, and Sara A Solla. Optimal brain damage. In *Advances in neural information processing systems*, pages 598–605, 1990.

[2] Babak Hassibi and David G Stork. Second order derivatives for network pruning: Optimal brain surgeon. In *Advances in neural information processing systems*, pages 164–171, 1993.

[3] Song Han, Huizi Mao, and William J Dally. Deep compression: Compressing deep neural networks with pruning, trained quantization and huffman coding. *arXiv preprint arXiv:1510.00149*, 2015.

[4] Yang He, Ping Liu, Ziwei Wang, Zhilan Hu, and Yi Yang. Filter pruning via geometric median for deep convolutional neural networks acceleration. In *Proceedings of the IEEE Conference on Computer Vision and Pattern Recognition*, pages 4340–4349, 2019.

[5] Hao Li, Asim Kadav, Igor Durdanovic, Hanan Samet, and Hans Peter Graf. Pruning filters for efficient convnets. *arXiv preprint arXiv:1608.08710*, 2016.

[6] Yang He, Guoliang Kang, Xuanyi Dong, Yanwei Fu, and Yi Yang. Soft filter pruning for accelerating deep convolutional neural networks. *arXiv preprint arXiv:1808.06866*, 2018.

[7] Jonathan Frankle and Michael Carbin. The lottery ticket hypothesis: Finding sparse, trainable neural networks. In *International Conference on Learning Representations*, 2019.

[8] Hengyuan Hu, Rui Peng, Yu-Wing Tai, and Chi-Keung Tang. Network trimming: A data-driven neuron pruning approach towards efficient deep architectures. *arXiv preprint arXiv:1607.03250*, 2016.

[9] Jian-Hao Luo and Jianxin Wu. An entropy-based pruning method for cnn compression. *arXiv preprint arXiv:1706.05791*, 2017.

[10] Pavlo Molchanov, Stephen Tyree, Tero Karras, Timo Aila, and Jan Kautz. Pruning convolutional neural networks for resource efficient inference. *arXiv preprint arXiv:1611.06440*, 2016.

[11] Pavlo Molchanov, Arun Mallya, Stephen Tyree, Iuri Frosio, and Jan Kautz. Importance estimation for neural network pruning. In *Proceedings of the IEEE Conference on Computer Vision and Pattern Recognition*, pages 11264–11272, 2019.

[12] Zhuang Liu, Jianguo Li, Zhiqiang Shen, Gao Huang, Shoumeng Yan, and Changshui Zhang. Learning efficient convolutional networks through network slimming. In *Proceedings of the IEEE International Conference on Computer Vision*, pages 2736–2744, 2017.

[13] Wei He, Meiqing Wu, Mingfu Liang, and Siew-Kei Lam. Cap: Context-aware pruning for semantic segmentation. In *Proceedings of the IEEE/CVF Winter Conference on Applications of Computer Vision*, pages 960–969, 2020.

[14] Michael B Cohen, Yin Tat Lee, Gary Miller, Jakub Pachocki, and Aaron Sidford. Geometric median in nearly linear time. In *Proceedings of the forty-eighth annual ACM symposium on Theory of Computing*, pages 9–21. ACM, 2016.

[15] Jian-Hao Luo, Jianxin Wu, and Weiyao Lin. Thinet: A filter level pruning method for deep neural network compression. In *Proceedings of the IEEE international conference on computer vision*, pages 5058–5066, 2017.

[16] Xiaohan Ding, Xiangxin Zhou, Yuchen Guo, Jungong Han, Ji Liu, et al. Global sparse momentum sgd for pruning very deep neural networks. In *Advances in Neural Information Processing Systems*, pages 6379–6391, 2019.

[17] Xin Dong, Shangyu Chen, and Sinno Pan. Learning to prune deep neural networks via layer-wise optimal brain surgeon. In *Advances in Neural Information Processing Systems*, pages 4857–4867, 2017.

[18] Alex Renda, Jonathan Frankle, and Michael Carbin. Comparing fine-tuning and rewinding in neural network pruning. In *International Conference on Learning Representations*, 2020.

[19] Jianbo Ye, Xin Lu, Zhe Lin, and James Z. Wang. Rethinking the smaller-norm-less-informative assumption in channel pruning of convolution layers. In *International Conference on Learning Representations*, 2018.

[20] Adam Paszke, Sam Gross, Francisco Massa, Adam Lerer, James Bradbury, Gregory Chanan, Trevor Killeen, Zeming Lin, Natalia Gimelshein, Luca Antiga, Alban Desmaison, Andreas Kopf, Edward Yang, Zachary DeVito, Martin Raison, Alykhan Tejani, Sasank Chilamkurthy, Benoit Steiner, Lu Fang, Junjie Bai, and Soumith Chintala. Pytorch: An imperative style, high-performance deep learning library. In H. Wallach, H. Larochelle, A. Beygelzimer, F. d'Alché-Buc, E. Fox, and R. Garnett, editors, *Advances in Neural Information Processing Systems 32*, pages 8024–8035. Curran Associates, Inc., 2019.

[21] Zechun Liu, Xiangyu Zhang, Zhiqiang Shen, Zhe Li, Yichen Wei, Kwang-Ting Cheng, and Jian Sun. Joint multi-dimension pruning. *arXiv preprint arXiv:2005.08931*, 2020.

[22] Yawei Li, Shuhang Gu, Christoph Mayer, Luc Van Gool, and Radu Timofte. Group sparsity: The hinge between filter pruning and decomposition for network compression. In *Proceedings of the IEEE/CVF Conference on Computer Vision and Pattern Recognition*, pages 8018–8027, 2020.

[23] Yang He, Yuhang Ding, Ping Liu, Linchao Zhu, Hanwang Zhang, and Yi Yang. Learning filter pruning criteria for deep convolutional neural networks acceleration. In *Proceedings of the IEEE/CVF Conference on Computer Vision and Pattern Recognition*, pages 2009–2018, 2020.

[24] Yuchen Liu, David Wentzlaff, and SY Kung. Rethinking class-discrimination based cnn channel pruning. *arXiv preprint arXiv:2004.14492*, 2020.

[25] Bailin Li, Bowen Wu, Jiang Su, Guangrun Wang, and Liang Lin. Eagleeye: Fast sub-net evaluation for efficient neural network pruning. *arXiv preprint arXiv:2007.02491*, 2020.

[26] Pavlo Molchanov, Arun Mallya, Stephen Tyree, Iuri Frosio, and Jan Kautz. Importance estimation for neural network pruning. In *Proceedings of the IEEE Conference on Computer Vision and Pattern Recognition*, 2019.

[27] Zhuang Liu, Mingjie Sun, Tinghui Zhou, Gao Huang, and Trevor Darrell. Rethinking the value of network pruning. *arXiv preprint arXiv:1810.05270*, 2018.

[28] Ting-Wu Chin, Ruizhou Ding, Cha Zhang, and Diana Marculescu. Towards efficient model compression via learned global ranking. In *Proceedings of the IEEE/CVF Conference on Computer Vision and Pattern Recognition*, pages 1518–1528, 2020.

[29] Wenxiao Wang, Cong Fu, Jishun Guo, Deng Cai, and Xiaofei He. Cop: Customized deep model compression via regularized correlation-based filter-level pruning. *arXiv preprint arXiv:1906.10337*, 2019.

[30] Gavin E Crooks. Survey of simple, continuous, univariate probability distributions. Technical report, Technical report, Lawrence Berkeley National Lab, 2013., 2012.

[31] Rodrigo R Pescim, Clarice GB Demétrio, Gauss M Cordeiro, Edwin MM Ortega, and Mariana R Urbano. The beta generalized half-normal distribution. *Computational statistics & data analysis*, 54(4):945–957, 2010.

[32] RL Graham. Applications of the fkg inequality and its relatives. In *Mathematical Programming The State of the Art*, pages 115–131. Springer, 1983.

[33] Lars Hormander. *The analysis of partial differential operators*. Springer, 1983.

[34] Zhuang Liu, Jianguo Li, Zhiqiang Shen, Gao Huang, Shoumeng Yan, and Changshui Zhang. Learning efficient convolutional networks through network slimming. In *The IEEE International Conference on Computer Vision (ICCV)*, Oct 2017.

[35] Yuandong Tian, Tina Jiang, Qucheng Gong, and Ari Morcos. Luck matters: Understanding training dynamics of deep relu networks. *arXiv preprint arXiv:1905.13405*, 2019.

[36] I Bellido and Emile Fiesler. Do backpropagation trained neural networks have normal weight distributions? In *International Conference on Artificial Neural Networks*, pages 772–775. Springer, 1993.

[37] Radford M Neal. *BAYESIAN LEARNING FOR NEURAL NETWORKS*. PhD thesis, University of Toronto, 1995.

[38] Jinwook Go, Byungjoon Baek, and Chulhee Lee. Analyzing weight distribution of feedforward neural networks and efficient weight initialization. In *Joint IAPR International Workshops on Statistical Techniques in Pattern Recognition (SPR) and Structural and Syntactic Pattern Recognition (SSPR)*, pages 840–849. Springer, 2004.

[39] Hubert W Lilliefors. On the kolmogorov-smirnov test for normality with mean and variance unknown. *Journal of the American statistical Association*, 62(318):399–402, 1967.

[40] Bradley Efron. Student's t-test under symmetry conditions. *Journal of the American Statistical Association*, 64(328):1278–1302, 1969.

[41] Kaiming He, Xiangyu Zhang, Shaoqing Ren, and Jian Sun. Deep residual learning for image recognition. In *The IEEE Conference on Computer Vision and Pattern Recognition (CVPR)*, June 2016.

[42] Ilya Sutskever, James Martens, George Dahl, and Geoffrey Hinton. On the importance of initialization and momentum in deep learning. In *International conference on machine learning*, pages 1139–1147, 2013.

[43] Karen Simonyan and Andrew Zisserman. Very deep convolutional networks for large-scale image recognition. *arXiv preprint arXiv:1409.1556*, 2014.

[44] Boris T Polyak and Anatoli B Juditsky. Acceleration of stochastic approximation by averaging. *SIAM journal on control and optimization*, 30(4):838–855, 1992.

[45] Alex Krizhevsky. One weird trick for parallelizing convolutional neural networks. *arXiv preprint arXiv:1404.5997*, 2014.

[46] Diederik P Kingma and Jimmy Ba. Adam: A method for stochastic optimization. *arXiv preprint arXiv:1412.6980*, 2014.

[47] Bing Xu, Naiyan Wang, Tianqi Chen, and Mu Li. Empirical evaluation of rectified activations in convolutional network. *arXiv preprint arXiv:1505.00853*, 2015.

[48] Gao Huang, Zhuang Liu, Laurens Van Der Maaten, and Kilian Q Weinberger. Densely connected convolutional networks. In *Proceedings of the IEEE conference on computer vision and pattern recognition*, pages 4700–4708, 2017.

[49] John Duchi, Elad Hazan, and Yoram Singer. Adaptive subgradient methods for online learning and stochastic optimization. *Journal of machine learning research*, 12(Jul):2121–2159, 2011.

[50] Senwei Liang, Yuehaw Khoo, and Haizhao Yang. Drop-activation: Implicit parameter reduction and harmonic regularization. *arXiv preprint arXiv:1811.05850*, 2018.

[51] Kaiming He, Xiangyu Zhang, Shaoqing Ren, and Jian Sun. Identity mappings in deep residual networks. In *European conference on computer vision*, pages 630–645. Springer, 2016.

[52] Ekin D Cubuk, Barret Zoph, Dandelion Mane, Vijay Vasudevan, and Quoc V Le. Autoaugment: Learning augmentation strategies from data. In *Proceedings of the IEEE conference on computer vision and pattern recognition*, pages 113–123, 2019.

[53] Sergey Zagoruyko and Nikos Komodakis. Wide residual networks. *arXiv preprint arXiv:1605.07146*, 2016.

[54] Matthew D Zeiler. Adadelta: an adaptive learning rate method. *arXiv preprint arXiv:1212.5701*, 2012.

[55] Terrance DeVries and Graham W Taylor. Improved regularization of convolutional neural networks with cutout. *arXiv preprint arXiv:1708.04552*, 2017.

[56] Saining Xie, Ross Girshick, Piotr Dollár, Zhuowen Tu, and Kaiming He. Aggregated residual transformations for deep neural networks. In *Proceedings of the IEEE conference on computer vision and pattern recognition*, pages 1492–1500, 2017.

[57] Sangdoo Yun, Dongyoon Han, Seong Joon Oh, Sanghyuk Chun, Junsuk Choe, and Youngjoon Yoo. Cutmix: Regularization strategy to train strong classifiers with localizable features. In *Proceedings of the IEEE International Conference on Computer Vision*, pages 6023–6032, 2019.

[58] Jie Hu, Li Shen, and Gang Sun. Squeeze-and-excitation networks. In *Proceedings of the IEEE conference on computer vision and pattern recognition*, pages 7132–7141, 2018.

[59] Kaiming He, Xiangyu Zhang, Shaoqing Ren, and Jian Sun. Delving deep into rectifiers: Surpassing human-level performance on imagenet classification. In *Proceedings of the IEEE international conference on computer vision*, pages 1026–1034, 2015.

[60] Alex Krizhevsky, Geoffrey Hinton, et al. Learning multiple layers of features from tiny images. 2009.

[61] Zhongzhan Huang, Senwei Liang, Mingfu Liang, and Haizhao Yang. Dianet: Dense-and-implicit attention network. *arXiv preprint arXiv:1905.10671*, 2019.

[62] HyunJae Lee, Hyo-Eun Kim, and Hyeonseob Nam. Srm: A style-based recalibration module for convolutional neural networks. In *Proceedings of the IEEE International Conference on Computer Vision*, pages 1854–1862, 2019.

[63] Xavier Glorot and Yoshua Bengio. Understanding the difficulty of training deep feedforward neural networks. In *Proceedings of the thirteenth international conference on artificial intelligence and statistics*, pages 249–256, 2010.

[64] Olga Russakovsky, Jia Deng, Hao Su, Jonathan Krause, Sanjeev Satheesh, Sean Ma, Zhiheng Huang, Andrej Karpathy, Aditya Khosla, Michael Bernstein, et al. Imagenet large scale visual recognition challenge. *International journal of computer vision*, 115(3):211–252, 2015.

[65] Sanghyun Woo, Jongchan Park, Joon-Young Lee, and In So Kweon. Cbam: Convolutional block attention module. In *Proceedings of the European Conference on Computer Vision (ECCV)*, pages 3–19, 2018.

[66] Yann LeCun, Léon Bottou, Yoshua Bengio, and Patrick Haffner. Gradient-based learning applied to document recognition. *Proceedings of the IEEE*, 86(11):2278–2324, 1998.

[67] Senwei Liang, Zhongzhan Huang, Mingfu Liang, and Haizhao Yang. Instance enhancement batch normalization: an adaptive regulator of batch noise. *arXiv preprint arXiv:1908.04008*, 2019.

[68] Andrew M Saxe, James L McClelland, and Surya Ganguli. Exact solutions to the nonlinear dynamics of learning in deep linear neural networks. *arXiv preprint arXiv:1312.6120*, 2013.

[69] Xiang Li, Xiaolin Hu, and Jian Yang. Spatial group-wise enhance: Improving semantic feature learning in convolutional networks. *arXiv preprint arXiv:1905.09646*, 2019.

[70] Vijay Badrinarayanan, Alex Kendall, and Roberto Cipolla. Segnet: A deep convolutional encoder-decoder architecture for image segmentation. *IEEE transactions on pattern analysis and machine intelligence*, 39(12):2481–2495, 2017.

[71] Shaoqing Ren, Kaiming He, Ross Girshick, and Jian Sun. Faster r-cnn: Towards real-time object detection with region proposal networks. In *Advances in neural information processing systems*, pages 91–99, 2015.

[72] Hengshuang Zhao, Jianping Shi, Xiaojuan Qi, Xiaogang Wang, and Jiaya Jia. Pyramid scene parsing network. In *Proceedings of the IEEE conference on computer vision and pattern recognition*, pages 2881–2890, 2017.

[73] Ning Xu, Brian Price, Scott Cohen, and Thomas Huang. Deep image matting. In *Proceedings of the IEEE Conference on Computer Vision and Pattern Recognition*, pages 2970–2979, 2017.

[74] Sebastian Lutz, Konstantinos Amplianitis, and Aljosa Smolic. Alphagan: Generative adversarial networks for natural image matting. *arXiv preprint arXiv:1807.10088*, 2018.

[75] Justin Johnson, Alexandre Alahi, and Li Fei-Fei. Perceptual losses for real-time style transfer and super-resolution. In *European conference on computer vision*, pages 694–711. Springer, 2016.

[76] Alec Radford, Luke Metz, and Soumith Chintala. Unsupervised representation learning with deep convolutional generative adversarial networks. *arXiv preprint arXiv:1511.06434*, 2015.

[77] Ilya Loshchilov and Frank Hutter. Sgdr: Stochastic gradient descent with warm restarts. *arXiv preprint arXiv:1608.03983*, 2016.

A Related Proposition

Proposition 3 (Amoroso distribution)**.** *The Amoroso distribution is a four parameter, continuous, univariate, unimodal probability density, with semi-infinite range [30]. And its probability density function is*

$$\mathbf{Amoroso}(X|a,\theta,\alpha,\beta) = \frac{1}{\Gamma(\alpha)}|\frac{\beta}{\theta}|(\frac{X-a}{\theta})^{\alpha\beta-1}\exp\left\{-(\frac{X-a}{\theta})^{\beta}\right\}, \tag{7}$$

for $x, a, \theta, \alpha, \beta \in \mathbb{R}, \alpha > 0$ and range $x \geq a$ if $\theta > 0$, $x \leq a$ if $\theta < 0$. The mean and variance of Amoroso distribution are

$$\mathbb{E}_{X\sim\mathbf{Amoroso}(X|a,\theta,\alpha,\beta)}X = a + \theta \cdot \frac{\Gamma(\alpha+\frac{1}{\beta})}{\Gamma(\alpha)}, \tag{8}$$

and

$$\mathbf{Var}_{X\sim\mathbf{Amoroso}(X|a,\theta,\alpha,\beta)}X = \theta^2\left[\frac{\Gamma(\alpha+\frac{2}{\beta})}{\Gamma(\alpha)} - \frac{\Gamma(\alpha+\frac{1}{\beta})^2}{\Gamma(\alpha)^2}\right]. \tag{9}$$

Proposition 4 (Half-normal distribution)**.** *Let random variable X follow a normal distribution $N(0,\sigma^2)$, then $Y = |X|$ follows a half-normal distribution [31]. Moreover, Y also follows $\mathbf{Amoroso}(x|0,\sqrt{2}\sigma,\frac{1}{2},2)$. By Eq. (8) and Eq. (9), the mean and variance of half-normal distribution are*

$$\mathbb{E}_{X\sim N(0,\sigma^2)}|X| = \sigma\sqrt{2/\pi}, \tag{10}$$

and

$$\mathbf{Var}_{X\sim N(0,\sigma^2)}|X| = \sigma^2\left(1-\frac{2}{\pi}\right). \tag{11}$$

Proposition 5 (Scaled Chi distribution)**.** *Let $X = (x_1, x_2, ...x_k)$ and $x_i, i = 1, ..., k$ are k independent, normally distributed random variables with mean 0 and standard deviation σ. The statistic $\ell_2(X) = \sqrt{\sum_{i=1}^{k} x_i^2}$ follows Scaled Chi distribution [30]. Moreover, $\ell_2(X)$ also follows $\mathbf{Amoroso}(x|0,\sqrt{2}\sigma,\frac{k}{2},2)$. By Eq. (8) and Eq. (9), the mean and variance of Scaled Chi distribution are*

$$\mathbb{E}_{X\sim N(\mathbf{0},\sigma^2\cdot\mathbf{I_k})}[\ell_2(X)]^j = 2^{j/2}\sigma^j \cdot \frac{\Gamma(\frac{k+j}{2})}{\Gamma(\frac{k}{2})}, \tag{12}$$

and

$$\mathbf{Var}_{X\sim N(\mathbf{0},\sigma^2\cdot\mathbf{I_k})}\ell_2(X) = 2\sigma^2\left[\frac{\Gamma(\frac{k}{2}+1)}{\Gamma(\frac{k}{2})} - \frac{\Gamma(\frac{k+1}{2})^2}{\Gamma(\frac{k}{2})^2}\right]. \tag{13}$$

Proposition 6 (Stirling's formula)**.** [6] *For big enough x and $x \in \mathbb{R}^+$, we have an approximation of Gamma function:*

$$\Gamma(x+1) \approx \sqrt{2\pi x}\left(\frac{x}{e}\right)^x. \tag{14}$$

Proposition 7 (FKG inequality)**.** *If f and g are increasing functions on $\mathbb{R}^n$ [32], we have*

$$\mathbb{E}(f)\mathbb{E}(g) \leq \mathbb{E}(fg). \tag{15}$$

Say that a function on $\mathbb{R}^n$ is increasing if it is an increasing function in each of its arguments.(i.e., for fixed values of the other arguments).

[6] `en.wikipedia.org/wiki/Stirling'sapproximation`

Proposition 8. *Let $f(X,Y)$ is a two dimensional differentiable function. According to Taylor theorem [33], we have*

$$f(X,Y) = f(\mathbb{E}(X),\mathbb{E}(Y)) + \sum_{cyc}(X-\mathbb{E}(X))\frac{\partial}{\partial X}f(\mathbb{E}(X),\mathbb{E}(Y)) + Remainder1, \tag{16}$$

$$\begin{aligned} f(X,Y) = f(\mathbb{E}(X),\mathbb{E}(Y)) + \sum_{cyc}(X-\mathbb{E}(X))\frac{\partial}{\partial X}f(\mathbb{E}(X),\mathbb{E}(Y)) + \\ \frac{1}{2}\sum_{cyc}(X-\mathbb{E}(X))^T\frac{\partial^2}{\partial X^2}f(\mathbb{E}(X),\mathbb{E}(Y))(X-\mathbb{E}(X)) + Remainder2 \end{aligned} \tag{17}$$

Lemma 1. *Let X and Y are random variables. Then we have such an estimation*

$$\mathbf{Var}\left(\frac{X}{Y}\right) \approx \left(\frac{\mathbb{E}(X)}{\mathbb{E}(Y)}\right)^2\left(\frac{\mathbf{Var}X}{\mathbb{E}(X)^2} + \frac{\mathbf{Var}Y}{\mathbb{E}(Y)^2} - 2\frac{\mathbf{Cov}(X,Y)}{\mathbb{E}(X)\mathbb{E}(Y)}\right). \tag{18}$$

Proof. Let $f(X,Y) = X/Y$, according to the definition of variance, we have

$$\begin{aligned} \mathbf{Var}f(X,Y) &= \mathbb{E}[f(X,Y) - \mathbb{E}(f(X,Y))]^2 \\ &\approx \mathbb{E}[f(X,Y) - \mathbb{E}\left\{f(\mathbb{E}(X),\mathbb{E}(Y)) + \sum_{cyc}(X-\mathbb{E}(X))\frac{\partial}{\partial X}f(\mathbb{E}(X),\mathbb{E}(Y))\right\}]^2 \\ &\qquad\qquad \text{from Eq. (16)} \\ &= \mathbb{E}[f(X,Y) - f(\mathbb{E}(X),\mathbb{E}(Y)) - \sum_{cyc}\mathbb{E}(X-\mathbb{E}(X))\frac{\partial}{\partial X}f(\mathbb{E}(X),\mathbb{E}(Y))]^2 \\ &= \mathbb{E}[f(X,Y) - f(\mathbb{E}(X),\mathbb{E}(Y))]^2 \\ &\approx \mathbb{E}[\sum_{cyc}(X-\mathbb{E}(X))\frac{\partial}{\partial X}f(\mathbb{E}(X),\mathbb{E}(Y))]^2 \qquad \text{from Eq. (16)} \\ &= 2\mathbf{Cov}(X,Y)\frac{\partial}{\partial X}f(\mathbb{E}(X),\mathbb{E}(Y))\frac{\partial}{\partial Y}f(\mathbb{E}(X),\mathbb{E}(Y)) + \sum_{cyc}[\frac{\partial}{\partial X}f(\mathbb{E}(X),\mathbb{E}(Y))]^2\cdot\mathbf{Var}X \\ &= 2\mathbf{Cov}(X,Y)\cdot\frac{1}{\mathbb{E}(Y)}\cdot\left(-\frac{\mathbb{E}(X)}{(\mathbb{E}(Y))^2}\right) + \frac{1}{(\mathbb{E}(Y))^2}\cdot\mathbf{Var}X + \frac{(\mathbb{E}X)^2}{(\mathbb{E}Y)^4}\cdot\mathbf{Var}Y \\ &= \left(\frac{\mathbb{E}(X)}{\mathbb{E}(Y)}\right)^2\left(\frac{\mathbf{Var}X}{\mathbb{E}(X)^2} + \frac{\mathbf{Var}Y}{\mathbb{E}(Y)^2} - 2\frac{\mathbf{Cov}(X,Y)}{\mathbb{E}(X)\mathbb{E}(Y)}\right). \end{aligned}$$

□

From Eq.(17) and **Lemma 1**, we also can obtain an estimation of $\mathbb{E}(\mathbf{A}/\mathbf{B})$, where $\mathbf{A}$ and $\mathbf{B}$ are two random variables. *i.e.*,

$$\mathbb{E}\left(\frac{\mathbf{A}}{\mathbf{B}}\right) \approx \frac{\mathbb{E}\mathbf{A}}{\mathbb{E}\mathbf{B}} + \mathbf{Var}(\mathbf{B})\cdot\frac{\mathbb{E}\mathbf{A}}{(\mathbb{E}\mathbf{B})^3}. \tag{19}$$

Lemma 2. *For big enough x and $x \in \mathbb{R}^+$, we have*

$$\lim_{x\to+\infty}\left[\frac{\Gamma(\frac{x+1}{2})}{\Gamma(\frac{x}{2})}\right]^2\cdot\frac{1}{x} = \frac{1}{2}. \tag{20}$$

And

$$\lim_{x\to+\infty}\frac{\Gamma(\frac{x}{2}+1)}{\Gamma(\frac{x}{2})} - \left[\frac{\Gamma(\frac{x+1}{2})}{\Gamma(\frac{x}{2})}\right]^2 = \frac{1}{4}. \tag{21}$$

Proof.

$$\begin{aligned}
\lim_{x\to+\infty}\left[\frac{\Gamma(\frac{x+1}{2})}{\Gamma(\frac{x}{2})}\right]^2\cdot\frac{1}{x} &\approx \lim_{x\to+\infty}\left(\frac{\sqrt{2\pi(\frac{x-1}{2})}\cdot(\frac{x-1}{2e})^{\frac{x-1}{2}}}{\sqrt{2\pi(\frac{x-2}{2})}\cdot(\frac{x-2}{2e})^{\frac{x-2}{2}}}\right)^2\cdot\frac{1}{x} \qquad \text{from Proposition. 6}\\
&= \lim_{x\to+\infty}\left(\frac{x-1}{x-2}\right)\cdot\frac{(\frac{x-1}{2e})^{x-2}}{(\frac{x-2}{2e})^{x-2}}\cdot\left(\frac{x-1}{2e}\right)\cdot\frac{1}{x}\\
&= \lim_{x\to+\infty}\left(1+\frac{1}{x-2}\right)^{x-2}\cdot\frac{x-1}{x-2}\cdot\frac{x-1}{2e}\cdot\frac{1}{x}\\
&= \frac{1}{2}
\end{aligned}$$

on the other hand, we have

$$\begin{aligned}
\lim_{x\to+\infty}\frac{\Gamma(\frac{x}{2}+1)}{\Gamma(\frac{x}{2})}-\left[\frac{\Gamma(\frac{x+1}{2})}{\Gamma(\frac{x}{2})}\right]^2 &= \lim_{x\to+\infty}\frac{x}{2}-\left(1+\frac{1}{x-2}\right)^{x-2}\cdot\frac{x-1}{x-2}\cdot\frac{x-1}{2e}\\
&= \lim_{x\to+\infty}\frac{x}{2e}\left(e-(1+\frac{1}{x})^x\right)\\
&= \frac{1}{2}\left(-\frac{\frac{1}{e}(-e)}{2}\right)\\
&= \frac{1}{4}
\end{aligned}$$

□

Proposition 9. *KL divergence between two distributions P and Q of a continuous random variable is given by $D_{KL}(p\|q)=\int_x p(x)\log\frac{p(x)}{q(x)}$. And probabilty density function of multivariate Normal distribution is given by $p(\mathbf{x})=\frac{1}{(2\pi)^{k/2}|\Sigma|^{1/2}}\exp\left(-\frac{1}{2}(\mathbf{x}-\boldsymbol{\mu})^T\Sigma^{-1}(\mathbf{x}-\boldsymbol{\mu})\right)$. Let our two Normal distributions be $\mathcal{N}\left(\boldsymbol{\mu_p},\Sigma_p\right)$ and $\mathcal{N}\left(\boldsymbol{\mu}_q,\Sigma_q\right)$, both k dimensional. we have*

$$D_{KL}(p\|q)=\frac{1}{2}\left[\log\frac{|\Sigma_q|}{|\Sigma_p|}-k+\left(\boldsymbol{\mu_p}-\boldsymbol{\mu_q}\right)^T\Sigma_q^{-1}\left(\boldsymbol{\mu_p}-\boldsymbol{\mu_q}\right)+\operatorname{tr}\left\{\Sigma_q^{-1}\Sigma_p\right\}\right]. \tag{22}$$

Proposition 10 (Jacobi's formula)**.** *If A is a differentiable map from the real numbers to $n\times n$ matrices,*

$$\frac{d}{dt}\det A(t)=\operatorname{tr}\left(\operatorname{adj}(A(t))\frac{dA(t)}{dt}\right). \tag{23}$$

Proposition 11. *For random variable X with μ and σ^2 as mean and variance, then we can use Taylor expansion to obtain:*

$$\begin{cases}\mathbb{E}(\log X)\approx\log\mu-\frac{\sigma^2}{2\mu^2}\\ \mathbf{Var}(\log X)\approx\frac{\sigma^2}{\mu^2}\end{cases}. \tag{24}$$

Proposition 12. *Given n normal distributions $N(0,\sigma_i^2), 1\le i\le n$ and $(X_{i1},X_{i2},...,X_{im})$ are sample from $N(0,\sigma_i^2), 1\le j\le m$. then*

$$\mathbf{Var}_{1\le i\le n,1\le j\le m}(X_{ij})=\frac{1}{n}\sum_{i=1}^{n}\sigma_i^2. \tag{25}$$

Proof.

$$
\begin{aligned}
\mathbf{Var}_{1\le i\le n, 1\le j\le m}(X_{ij}) &= \frac{1}{mn}\sum_{i=1}^{n}\sum_{j=1}^{m}[X_{ij}-\mathbb{E}(X_{ij})]^2 && (26)\\
&= \frac{1}{n}\{\frac{1}{m}\sum_{j=1}^{m}[X_{ij}-\mathbb{E}(X_{1j})]^2+...+\frac{1}{m}\sum_{j=1}^{m}[X_{nj}-\mathbb{E}(X_{nj})]^2\}\\
&\qquad \text{Since } \mathbb{E}(X_{ij})=0, 1\le i\le n, 1\le j\le m\\
&= \frac{1}{n}\{\sigma_1^2+...+\sigma_n^2\} && (27)
\end{aligned}
$$

□

Lemma 3. *For a matrix* $\mathbf{B}\in R^{n\times n}$ *and a small constant* ϵ*, we have:*

$$det(\mathbf{I}_n+\epsilon\mathbf{B}) = 1+\epsilon\,\mathrm{tr}(\mathbf{B})+O(\epsilon^2). \tag{28}$$

Proof. First, we regard $det(\mathbf{I}_n+\epsilon\mathbf{B})$ as a function w.r.t ϵ. Since Proposition 10, we have:

$$
\begin{aligned}
\frac{d}{d\epsilon}det(\mathbf{I}_n+\epsilon\mathbf{B})|_{\epsilon=0} &= \mathrm{tr}\{\mathrm{adj}(\mathbf{I}_n+\epsilon\mathbf{B})\mathbf{B}\}|_{\epsilon=0} && (29)\\
&= \mathrm{tr}\{det(\mathbf{I}_n+\epsilon\mathbf{B})\cdot(\mathbf{I}_n+\epsilon\mathbf{B})^{-1}\mathbf{B}\}|_{\epsilon=0} && (30)\\
&= det(\mathbf{I}_n+\epsilon\mathbf{B})\cdot\mathrm{tr}\{(\mathbf{I}_n+\epsilon\mathbf{B})^{-1}\mathbf{B}\}|_{\epsilon=0} && (31)\\
&= \mathrm{tr}(\mathbf{B}) && (32)
\end{aligned}
$$

Using Taylor expansion for $det(\mathbf{I}_n+\epsilon\mathbf{B})$, we have $\frac{d}{d\epsilon}det(\mathbf{I}_n+\epsilon\mathbf{B}) = det(\mathbf{I}_n)+\frac{d}{d\epsilon}det(\mathbf{I}_n+\epsilon\mathbf{B})|_{\epsilon=0}\cdot\epsilon+O(\epsilon^2)$. In other words, $det(\mathbf{I}_n+\epsilon\mathbf{B}) = 1+\epsilon\,\mathrm{tr}(\mathbf{B})+O(\epsilon^2)$.

□

A.1 The proof of Proposition 1

(**Proposition** 1) If the convolutional filters F_A in layer A meet CWDA, then we have following estimations:

Criterion	Mean	Variance
$\ell_1(F_A)$	$\sqrt{2/\pi}\sigma_A d_A$	$(1-\frac{2}{\pi})\sigma_A^2 d_A$
$\ell_2(F_A)$	$\sqrt{2}\sigma_A\Gamma(\frac{d_A+1}{2})/\Gamma(\frac{d_A}{2})$	$\sigma_A^2/2$
$\mathbf{Fermat}(F_A)$	$\sqrt{2}\sigma_A\Gamma(\frac{d_A+1}{2})/\Gamma(\frac{d_A}{2})$	$\sigma_A^2/2$

where d_A and σ_A^2 denote the dimension of F_A and the variance of the weights in layer A, respectively.

Proof. According to Appendix B, Eq. (21), Proposition 4 and Proposition 5, we can obtain the mean and variance of $\ell_1(F_A)$ and $\ell_2(F_A)$. Moreover, From the Theorem 3, we know that the Fermat point $\mathbf{F}$ of F_A and the origin $\mathbf{0}$ approximately coincide. According to Table 1, $||\mathbf{F}-F_A||_2 \approx ||\mathbf{0}-F_A||_2 = ||F_A||_2$. Therefore, the mean and variance of $\mathbf{Fermat}(F_A)$ are the same as $\ell_2(F_A)$'s in Proposition 1.

□

A.2 The proof of Proposition 2

(**Proposition** 2) If the convolutional filters F_A in layer A meet CWDA, then $\mathbb{E}[\ell_1(F_A)/\ell_2(F_A)]$ and $\mathbb{E}[\ell_2(F_A)/\ell_1(F_A)]$ only depend on their dimension d_A.

Proof. From Eq. (19), we have:

$$\begin{aligned}
\mathbb{E}[\frac{\ell_1(F_A)}{\ell_2(F_A)}] &\approx \frac{\mathbb{E}[\ell_1(F_A)]}{\mathbb{E}[\ell_2(F_A)]} + \mathbf{Var}[\ell_2(F_A)] \cdot \frac{\mathbb{E}[\ell_1(F_A)]}{\mathbb{E}[\ell_2(F_A)]^3} \\
&= \frac{\sqrt{2/\pi}\sigma_A d_A}{\sqrt{2}\sigma_A \Gamma(\frac{d_A+1}{2})/\Gamma(\frac{d_A}{2})} + \sigma_A^2/2 \cdot \frac{\sqrt{2/\pi}\sigma_A d_A}{[\sqrt{2}\sigma_A \Gamma(\frac{d_A+1}{2})/\Gamma(\frac{d_A}{2})]^3} \quad \text{from Proposition. 1} \\
&\approx O(\sqrt{d_A}) + O(\frac{1}{\sqrt{d_A}}) \quad \text{from Eq. (20)}
\end{aligned}$$

Similarly, we can prove that $\mathbb{E}[\ell_2(F_A)/\ell_1(F_A)]$ also only depend on their dimension d_A.

$$\begin{aligned}
\mathbb{E}[\frac{\ell_2(F_A)}{\ell_1(F_A)}] &\approx \frac{\mathbb{E}[\ell_2(F_A)]}{\mathbb{E}[\ell_1(F_A)]} + \mathbf{Var}[\ell_1(F_A)] \cdot \frac{\mathbb{E}[\ell_2(F_A)]}{\mathbb{E}[\ell_1(F_A)]^3} \\
&= \frac{\sqrt{2}\sigma_A \Gamma(\frac{d_A+1}{2})/\Gamma(\frac{d_A}{2})}{\sqrt{2/\pi}\sigma_A d_A} + (1-\frac{2}{\pi})\sigma_A^2 d_A \cdot \frac{\sqrt{2}\sigma_A \Gamma(\frac{d_A+1}{2})/\Gamma(\frac{d_A}{2})}{[\sqrt{2/\pi}\sigma_A d_A]^3} \\
&\qquad \text{from Proposition. 1} \\
&\approx O(\frac{1}{\sqrt{d_A}}) + O(\frac{1}{d_A^{1.5}}) \quad \text{from Eq. (20)}
\end{aligned}$$

□

B The relaxation for CWDA

(Convolution Weight Distribution Assumption) Let $F_{ij} \in \mathbb{R}^{N_i \times k \times k}$ be the j^{th} well-trained filter of the i^{th} convolutional layer. In general[7], in i^{th} layer, F_{ij} $(j = 1, 2, ..., N_{i+1})$ are i.i.d and follow such a distribution:

$$F_{ij} \sim \mathbf{N}(\mathbf{0}, \mathbf{\Sigma}^i_{\text{diag}} + \epsilon \cdot \mathbf{\Sigma}^i_{\text{block}}), \tag{33}$$

where $\mathbf{\Sigma}^i_{\text{block}} = \text{diag}(K_1, K_2, ..., K_{N_i})$ is a block diagonal matrix and the diagonal elements of $\mathbf{\Sigma}^i_{\text{block}}$ are 0. ϵ is a small constant. The values of the off-block-diagonal elements are 0 and $K_l \in R^{k^2 \times k^2}, l = 1, 2, ..., N_i$. $\mathbf{\Sigma}^i_{\text{diag}} = \text{diag}(a_1, a_2, ..., a_{N_i \times k \times k})$ is a diagonal matrix and the elements of $\mathbf{\Sigma}^i_{\text{diag}}$ are close enough.

In Section 2, we propose CWDA. In order to use this assumption conveniently, we give the following relaxation of CWDA:

(**Convolution Weight Distribution Assumption-Relaxation**) Let $F_{ij} \in \mathbb{R}^{N_i \times k \times k}$ be the j^{th} well-trained filter of the i^{th} convolutional layer. In general, in i^{th} layer, F_{ij} $(j = 1, 2, ..., N_{i+1})$ are i.i.d and follow such a distribution:

$$F_{ij} \sim \mathbf{N}(\mathbf{0}, \sigma^2_{\text{layer}} \cdot \mathbf{I}_{N_i \times k \times k}), \tag{34}$$

where σ^2_{layer} is the variance of the weights in i^{th} convolutional layer.

Next, we analyze the gap between CWDA and CWDA-Relaxation, *i.e.,* the difference between $\mathbf{N}(\mathbf{0}, \mathbf{\Sigma}^i_{\text{diag}} + \epsilon \cdot \mathbf{\Sigma}^i_{\text{block}})$ and $\mathbf{N}(\mathbf{0}, \sigma^2_{\text{layer}} \cdot \mathbf{I}_{N_i \times k \times k})$.

Lemma 4. *Given two n-dimension Gaussian distributions $\mathbf{N}(\mathbf{0}, \mathbf{\Sigma}_{diag} + \epsilon \cdot \mathbf{\Sigma}_{block})$ and $\mathbf{N}(\mathbf{0}, \mathbf{\Sigma}_{diag})$, we can estimate the KL divergence of them:*

$$\text{KL}[\mathbf{N}(\mathbf{0}, \mathbf{\Sigma}_{diag} + \epsilon \cdot \mathbf{\Sigma}_{block}) || \mathbf{N}(\mathbf{0}, \mathbf{\Sigma}_{diag})] \approx \frac{1}{2} \log[\frac{1}{1 + O(\epsilon^2)}] \tag{35}$$

[7] In Section 6, we make further discussion and analysis on the conditions for CWDA to be satisfied.

where $\mathbf{\Sigma}_{block} = \operatorname{diag}(K_1, K_2, ..., K_{N_i})$ is a block diagonal matrix and the diagonal elements of $\mathbf{\Sigma}_{block}$ are 0. ϵ is a small constant. The values of the off-block-diagonal elements are 0 and $K_l \in R^{k^2 \times k^2}, l = 1, 2, ..., N_i$. $\mathbf{\Sigma}_{diag} = \operatorname{diag}(a_1, a_2, ..., a_{N_i \times k \times k})$ is a diagonal matrix and the elements of $\mathbf{\Sigma}_{diag}$ are close enough. $n = N_i \times k \times k$.

Proof. Since Proposition 9, we have:

$$2\,\mathrm{KL} = \log \frac{det[\mathbf{\Sigma}_{\text{diag}}]}{det[\mathbf{\Sigma}_{\text{diag}} + \epsilon \cdot \mathbf{\Sigma}_{\text{block}}]} - n + 0 + \operatorname{tr}\{\mathbf{\Sigma}_{\text{diag}}^{-1}(\mathbf{\Sigma}_{\text{diag}} + \epsilon \cdot \mathbf{\Sigma}_{\text{block}})\} \tag{36}$$

$$= \log \frac{det[\mathbf{\Sigma}_{\text{diag}}]}{det[\mathbf{\Sigma}_{\text{diag}} + \epsilon \cdot \mathbf{\Sigma}_{\text{block}}]} - n + \operatorname{tr}\{\mathbf{I}_k + \epsilon \mathbf{\Sigma}_{\text{diag}}^{-1} \mathbf{\Sigma}_{\text{block}}\} \tag{37}$$

$$= \log \frac{det[\mathbf{\Sigma}_{\text{diag}}]}{det[\mathbf{\Sigma}_{\text{diag}} + \epsilon \cdot \mathbf{\Sigma}_{\text{block}}]} \qquad \text{Since the diagonal elements of } \mathbf{\Sigma}_{\text{block}} \text{ are 0} \tag{38}$$

Let $\mathbf{\Sigma}_{\text{diag}} = \operatorname{diag}(S_1, S_2, ..., S_{N_i})$, where $S_j = \operatorname{diag}(a_{(j-1)k^2+1}, a_{(j-1)k^2+2}, ..., a_{(j-1)k^2+k^2}), j = 1, 2, ..., N_i$.

$$2\,\mathrm{KL} = \log \frac{det[\mathbf{\Sigma}_{\text{diag}}]}{det[\mathbf{\Sigma}_{\text{diag}} + \epsilon \cdot \mathbf{\Sigma}_{\text{block}}]} \tag{39}$$

$$= \log \prod_{j=1}^{n} a_k - \log\{\prod_{h=1}^{N_i} det[S_h + \epsilon K_h]\} \tag{40}$$

$$= \log \prod_{j=1}^{n} a_k - \log\{\prod_{h=1}^{N_i} det[S_h] det[\mathbf{I}_{k^2} + \epsilon S_h^{-1} K_h]\} \qquad \text{Since } S_h \succeq 0 \tag{41}$$

Note that S_h is a diagonal matrix and the diagonal elements of K_h are all zero. Therefore

$$\operatorname{tr}(S_h^{-1} K_h) = 0. \tag{42}$$

Next,

$$2\,\mathrm{KL} = \log \prod_{j=1}^{n} a_k - \log\{\prod_{h=1}^{N_i} det[S_h] det[\mathbf{I}_{k^2} + \epsilon S_h^{-1} K_h]\} \tag{43}$$

$$= \log \prod_{j=1}^{n} a_k - \log\{\prod_{h=1}^{N_i} det[S_h] \cdot (1 + \epsilon \operatorname{tr}(S_h^{-1} K_h) + O(\epsilon^2))\} \qquad \text{Since Lemma 3}$$

$$= \log \prod_{j=1}^{n} a_k - \log\{\prod_{h=1}^{N_i} det[S_h] \cdot (1 + O(\epsilon^2))\} \qquad \text{Since Eq. (42)}$$

$$= \log \prod_{j=1}^{n} a_k - \log \prod_{j=1}^{n} a_k (1 + O(\epsilon^2)) \tag{44}$$

$$= \log[\frac{1}{1 + O(\epsilon^2)}] \tag{45}$$

□

According to Statistical test (2) in Section 2.1, $\mathbf{N}(\mathbf{0}, \mathbf{\Sigma}_{\text{diag}})$ can be approximate to $\mathbf{N}(\mathbf{0}, \frac{1}{n} \operatorname{tr}(\mathbf{\Sigma}_{\text{diag}}) \mathbf{I}_n)$. In addition, from Propsition 12 and Lemma 4, while ϵ is small enough, the distribution $\mathbf{N}(\mathbf{0}, \mathbf{\Sigma}_{\text{diag}} + \epsilon \cdot \mathbf{\Sigma}_{\text{block}})$ can be approximate to $\mathbf{N}(\mathbf{0}, \sigma_{\text{layer}}^2 \cdot \mathbf{I}_{N_i \times k \times k})$. The analysis in this paper are based on *Convolution Weight Distribution Assumption-Relaxation* and we use it to explain successfully many phenomena in the Similarity and Applicability problem of pruning criteria.

C Proof of Theorem 1

Theorem 1. Let $n-$dimension random variable X meet CWDA, and the pair of criteria (C_1, C_2) is one of (ℓ_1, ℓ_2), $(\ell_2, \mathbf{Fermat})$ or $(\mathbf{Fermat}, \mathbf{GM})$, we have

$$\mathbf{max}\left\{\mathbf{Var}_X\left(\frac{\widehat{C}_2(X)}{\widehat{C}_1(X)}\right), \mathbf{Var}_X\left(\frac{\widehat{C}_1(X)}{\widehat{C}_2(X)}\right)\right\} \lesssim B(n). \tag{46}$$

where $\widehat{C}_1(X)$ denotes $C_1(X)/\mathbb{E}(C_1(X))$ and $\widehat{C}_2(X)$ denotes $C_2(X)/\mathbb{E}(C_2(X))$. $B(n)$ denotes the upper bound of left-hand side and when n is large enough, $B(n) \to 0$.

For i^{th} layer, we use v_j to represent F_{ij}, $j = 1, 2, ...N$. And v_j meets CWDA. Since Appendix B, we use the following three points to prove Theorem 1.

(1) For (ℓ_2, ℓ_1). In fact, $\ell_2 \cong \ell_1$ (their importance rankings are similar) is not trivial. Generally speaking, for convolutional filters, $\mathbf{dim}(v_j)$ is large enough. Since v_i satisfies CWDA, from Theorem 2, we know that the variance of ratio between $\widehat{\ell_1}$ and $\widehat{\ell_2}$ have a bound $O(\mathbf{dim}(v_j)^{-1})$, which means ℓ_2 and ℓ_1 are *appropriate monotonic*. Specific numerical validation is shown in Fig. 9 of Appendix D).

Theorem 2. *Let $X \sim N(\mathbf{0}, c^2 \cdot \mathbf{I}_n)$, we have*

$$\mathbf{max}\left\{\mathbf{Var}_X\left(\frac{\widehat{\ell}_2(X)}{\widehat{\ell}_1(X)}\right), \mathbf{Var}_X\left(\frac{\widehat{\ell}_1(X)}{\widehat{\ell}_2(X)}\right)\right\} \lesssim \frac{1}{n}. \tag{47}$$

where $\widehat{\ell}_1(X)$ denotes $\ell_1(X)/\mathbb{E}(\ell_1(X))$ and $\widehat{\ell}_2(X)$ denotes $\ell_2(X)/\mathbb{E}(\ell_2(X))$. c is a constant.

Proof. (See Appendix D). □

(2) For $(\ell_2, \mathbf{Fermat})$. Since v_i satisfies CWDA, from Theorem 3, we know that the Fermat point of v_i and the origin $\mathbf{0}$ approximately coincide. According to Table 2, $||\mathbf{Fermat} - v_i||_2 \approx ||\mathbf{0} - v_i||_2 = ||v_i||_2$. Therefore, from Theorem 2, the bound $B(n)$ for the (ℓ_1, $\mathbf{Fermat}$) and (ℓ_2, $\mathbf{Fermat}$) are $\frac{1}{n}$ and 0, respectively. Moreover, since CWDA, the centroid of v_i is $\mathbf{G} = \frac{1}{n}\sum_{i=1}^{N} v_i = \mathbf{0}$. Hence,

$$\mathbf{G} = \mathbf{0} \approx \mathbf{Fermat}. \tag{48}$$

Theorem 3. *Let random variable $v_i \in \mathbb{R}^k$ and they are i.i.d and follow normal distribution $N(\mathbf{0}, \sigma^2\mathbf{I}_k)$. For $F \in \mathbb{R}^k$, we have $\mathbf{argmin}_F \left\{\mathbb{E}_{v_i \sim N(\mathbf{0}, \sigma^2\mathbf{I}_k)} \sum_{i=1}^{n} ||F - v_i||_2\right\} = \mathbf{0}$.*

Proof. (See Appendix E). □

(3) For $(\mathbf{GM}, \mathbf{Fermat})$. First, we show the following two theorems:

Theorem 4. *For n random variables $a_i \in \mathbb{R}^k$ follow $N(\mathbf{0}, c^2 \cdot \mathbf{I}_k)$.When k is large enough, we have such an estimation:*

$$\mathbf{Var}_{a_i}\frac{F_1(a_i)}{F_2(a_i)} \approx \frac{1}{2nk}, \quad \mathbf{Var}_{a_i}\frac{F_2(a_i)}{F_1(a_i)} \approx \frac{1}{2nk}, \tag{49}$$

where $F_1(a_i) = \sum_{i=1}^{n} ||a_i||_2/\mathbb{E}(\sum_{i=1}^{n} ||a_i||_2)$ and $F_2(a_i) = \sum_{i=1}^{n} ||a_i||_2^2/\mathbb{E}(\sum_{i=1}^{n} ||a_i||_2^2)$.

Proof. (See Appendix F). □

Theorem 5. *Let $v_0, v_1, ..., v_k$ be the $k+1$ vectors in n dimensional Euclidean space $\mathbb{E}^n$. For all P in $\mathbb{E}^n$,*

$$\sum_{i=0}^{k} ||P - v_i||_2^2 = \sum_{i=0}^{k} ||G - v_i||_2^2 + (k+1)||P - G||_2^2, \tag{50}$$

where G is the centroid of v_i, will hold if it satisfies one of the following conditions:

(1)if $k \geq n$ and $\mathbf{rank}(v_1 - v_0, v_2 - v_0, ..., v_k - v_0) = n$.

(2)if $k < n$ and $(v_1 - v_0, v_2 - v_0, ..., v_k - v_0)$ are linearly independent.

(3)if $v_i \sim N(\mathbf{0}, c^2 \cdot \mathbf{I}_n)$, Eq.(50) holds with probability 1.

Proof. (See Appendix G). □

Let $P \in \{v_1, v_2, ..., v_N\}$. Since $v_i \sim N(\mathbf{0}, c^2 \cdot \mathbf{I})$, we can obtain that $a_i = P - v_i \sim N(\mathbf{0}, 2c^2 \cdot \mathbf{I})$ if $P \neq v_i$. According to the analysis in Section 3.1 and Theorem 4, we have

$$\sum_{i=1}^{n} ||a_i||_2 \cong \sum_{i=1}^{n} ||a_i||_2^2, \tag{51}$$

Next, we can prove $(k+1)||P - F||_2^2$ (**Fermat**) and $\sum_{i=1}^{N} ||P - v_i||_2$ (**GM**) are *approximately monotonic*, where $P \in \{v_1, v_2, ..., v_N\}$.

$$\begin{aligned}
(k+1)||P - F||_2^2 &\cong (k+1)||P - G||_2^2 && \text{Since Eq. (48)} \\
&= \sum_{i=1}^{N} ||P - v_i||_2^2 - \sum_{i=1}^{N} ||G - v_i||_2^2 && \text{Since Theorem 5} \\
&\cong \sum_{i=1}^{N} ||P - v_i||_2 - \sum_{i=1}^{N} ||G - v_i||_2^2 && \text{Since Eq. (51)} \\
&\cong \sum_{i=1}^{N} ||P - v_i||_2 && (52)
\end{aligned}$$

The reason for the last equation is that $\sum_{i=1}^{N} ||G - v_i||_2^2$ is a constant for given v_i.

D Proof of Theorem 2

Theorem 2 Let $X \sim N(\mathbf{0}, c^2 \cdot \mathbf{I}_n)$, we have

$$\mathbf{max}\left\{\mathbf{Var}_X\left(\frac{\widehat{\ell}_2(X)}{\widehat{\ell}_1(X)}\right), \mathbf{Var}_X\left(\frac{\widehat{\ell}_1(X)}{\widehat{\ell}_2(X)}\right)\right\} \lesssim \frac{1}{n}.$$

where $\widehat{\ell}_1(X)$ denotes $\ell_1(X)/\mathbb{E}(\ell_1(X))$ and $\widehat{\ell}_2(X)$ denotes $\ell_2(X)/\mathbb{E}(\ell_2(X))$.

Proof. For the ratio $\widehat{\ell}_2(X)/\widehat{\ell}_1(X)$, we have

$$\begin{aligned}
\mathbf{Var}\left(\frac{\widehat{\ell}_2(X)}{\widehat{\ell}_1(X)}\right) &= \left(\frac{\mathbb{E}(\ell_1(X))}{\mathbb{E}(\ell_2(X))}\right)^2 \mathbf{Var}\left(\frac{\ell_2(X)}{\ell_1(X)}\right) \\
&\approx \left(\frac{\mathbb{E}(\ell_1(X))}{\mathbb{E}(\ell_2(X))}\right)^2 \left(\frac{\mathbb{E}(\ell_2(X))}{\mathbb{E}(\ell_1(X))}\right)^2 \left(\frac{\mathbf{Var}\ell_2(X)}{\mathbb{E}(\ell_2(X))^2} + \frac{\mathbf{Var}\ell_1(X)}{\mathbb{E}(\ell_1(X))^2} - 2\frac{\mathbf{Cov}(\ell_2(X), \ell_1(X))}{\mathbb{E}(\ell_2(X))\mathbb{E}(\ell_1(X))}\right) \\
& \qquad \text{from Lemma. 1} \\
&\leq \left(\frac{\mathbf{Var}\ell_2(X)}{\mathbb{E}(\ell_2(X))^2} + \frac{\mathbf{Var}\ell_1(X)}{\mathbb{E}(\ell_1(X))^2}\right). && \text{from Proposition. 7}
\end{aligned}$$

similarly, we also have

$$\mathbf{Var}\left(\frac{\widehat{\ell}_1(X)}{\widehat{\ell}_2(X)}\right) \leq \left(\frac{\mathbf{Var}\ell_2(X)}{\mathbb{E}(\ell_2(X))^2} + \frac{\mathbf{Var}\ell_1(X)}{\mathbb{E}(\ell_1(X))^2}\right). \tag{53}$$

Therefore,

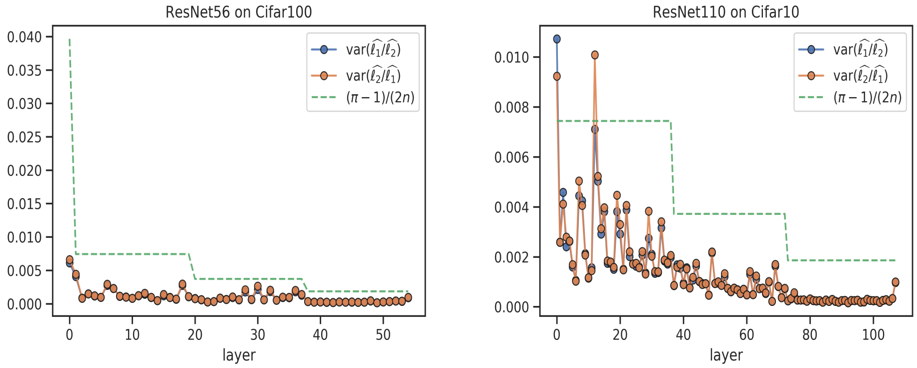

Figure 9: The approximation of **Theorem 2**: (Left) the example about ResNet56; (Right) the example about ResNet110.

$$
\begin{aligned}
\mathbf{max}\left\{\mathbf{Var}_X\left(\frac{\widehat{\ell}_2(X)}{\widehat{\ell}_1(X)}\right), \mathbf{Var}_X\left(\frac{\widehat{\ell}_1(X)}{\widehat{\ell}_2(X)}\right)\right\} &\leq \left(\frac{\mathbf{Var}\ell_2(X)}{\mathbb{E}(\ell_2(X))^2}+\frac{\mathbf{Var}\ell_1(X)}{\mathbb{E}(\ell_1(X))^2}\right) \\
&= \frac{2\sigma^2\left[\frac{\Gamma(\frac{n}{2}+1)}{\Gamma(\frac{n}{2})}-\frac{\Gamma(\frac{n+1}{2})^2}{\Gamma(\frac{n}{2})^2}\right]}{(\sqrt{2}\sigma\cdot\frac{\Gamma(\frac{n+1}{2})}{\Gamma(\frac{n}{2})})^2}+\frac{\sigma^2\left(1-\frac{2}{\pi}\right)n}{(n\cdot\sigma\sqrt{2/\pi})^2} \\
&\qquad\text{from Proposition. 5 and 4} \\
&\approx \left(\frac{1}{2n}+(\frac{\pi}{2}-1)\frac{1}{n}\right) \qquad\text{from Lemma 2} \\
&= \frac{\pi-1}{2n}
\end{aligned}
$$

□

Because the approximation is widely used in the proof of Theorem 1, it is necessary to verify it numerically. As shown in Fig. 9, we use ResNet56 on Cifar100 and ResNet110 on Cifar10 respectively to verify Theorem 1. From Fig. 9, we find that the estimationn of Theorem 1 is reliable, *i.e.*, the estimation $O(\frac{1}{n})$ for $\mathbf{max}\left\{\mathbf{Var}_X\left(\frac{\widehat{\ell}_2(X)}{\widehat{\ell}_1(X)}\right), \mathbf{Var}_X\left(\frac{\widehat{\ell}_1(X)}{\widehat{\ell}_2(X)}\right)\right\}$ is appropriate.

E Proof of Theorem 3

Proposition 13. *Let $L_p^{(\alpha)}(x)$ denotes generalized Laguerre function, and it have following properties:*

$$\frac{\partial^n}{\partial x^n}L_p^{(\alpha)}=(-1)^nL_{p-n}^{(\alpha+n)}(x), \tag{54}$$

and for $\alpha>0$,

$$L_{-\frac{1}{2}}^{(\alpha)}(x)>0. \tag{55}$$

Theorem 3. Let random variable $v_i\in\mathbb{R}^k$. They are i.i.d and follow normal distribution $N(\mathbf{0},\sigma^2\mathbf{I}_k)$. For F in $\mathbb{R}^k$, we have

$$\mathbf{argmin}_F\left\{\mathbb{E}_{v_i\sim N(\mathbf{0},\sigma^2\mathbf{I}_k)}\sum_{i=1}^n||F-v_i||_2\right\}=\mathbf{0}.$$

Proof. Let $w_i = F - v_i$ and we have $w_i \sim N(F, \sigma^2\mathbf{I}_k)$, then

$$\begin{aligned}
\mathbb{E}_{v_i \sim N(\mathbf{0},\sigma^2\mathbf{I}_k)} \sum_{i=1}^{n} ||F - v_i||_2 &= \sum_{i=1}^{n} \mathbb{E}_{v_i \sim N(\mathbf{0},\sigma^2\mathbf{I}_k)} ||F - v_i||_2 \\
&= \sum_{i=1}^{n} \mathbb{E}_{w_i \sim N(F,\sigma^2\mathbf{I}_k)} ||w_i||_2 \\
&= n \cdot \sigma^2 \sqrt{\frac{\pi}{2}} \cdot L_{\frac{1}{2}}^{(\frac{k}{2}-1)} \left(-\frac{||F||_2^2}{2\sigma^2} \right)
\end{aligned}$$

The reason for the last equation is that $||w_i||_2$ follows scaled noncentral chi distribution[8] when $w_i \sim N(F, \sigma^2\mathbf{I}_k)$. Let $T(x) = L_{\frac{1}{2}}^{(\frac{k}{2}-1)} \left(-\frac{x^2}{2\sigma^2} \right)$, we calculate the minimum of $T(x)$. From Eq. (54),

$$\frac{d}{dx} T(x) = \frac{x}{\sigma^2} \cdot L_{-\frac{1}{2}}^{(\frac{k}{2})} \left(-\frac{x^2}{2\sigma^2} \right). \tag{56}$$

Since Eq. (55), we find that $\frac{d}{dx}T(x) > 0$ when $x > 0$ and if $x \leq 0$, then $\frac{d}{dx}T(x) \leq 0$. It means that $T(x)$ gets the minimizer at $||F||_2 = 0$, *i.e.*, $F = \mathbf{0}$.

□

F Proof of Theorem 4

Lemma 5. *For two random variables $X, Y \in \mathbb{R}^k$ follow $N(\mathbf{0}, c^2 \cdot \mathbf{I}_k)$ and they are i.i.d. When k is large enough, we have:*

$$\mathbb{E}\left(\frac{(||X||_2^2 - ||Y||_2^2)^2}{2||X||_2 \cdot ||Y||_2} \right) \approx 2c^2 + \frac{4c^2k + 1}{2k^2}, \tag{57}$$

and

$$\mathbf{Var}\left(\frac{(||X||_2^2 - ||Y||_2^2)^2}{2||X||_2 \cdot ||Y||_2} \right) \lesssim 8c^4 + \frac{16c^4k + c^2}{k^2}, \tag{58}$$

Proof. According to **Proposition 3** and **Lemma 2**, it is easy to know, when k is large enough, that

$$\mathbb{E}\left(2||X||_2 \cdot ||Y||_2\right) = 2c^2k, \quad \mathbf{Var}\left(2||X||_2 \cdot ||Y||_2\right) = c^2 + 4c^4k, \tag{59}$$

and

$$\mathbb{E}\left((||X||_2^2 - ||Y||_2^2)^2\right) = 4c^4k, \quad \mathbf{Var}\left((||X||_2^2 - ||Y||_2^2)^2\right) = 16c^8(2k^2 + 3k). \tag{60}$$

Since Lemma 1, we have an estimation

$$\begin{aligned}
\mathbf{Var}\left(\frac{(||X||_2^2 - ||Y||_2^2)^2}{2||X||_2 \cdot ||Y||_2} \right) &\leq \left(\frac{\mathbb{E}(||X||_2^2 - ||Y||_2^2)^2}{\mathbb{E}2||X||_2 \cdot ||Y||_2} \right)^2 \left(\frac{\mathbf{Var}(||X||_2^2 - ||Y||_2^2)^2}{\mathbb{E}(||X||_2^2 - ||Y||_2^2)^2} + \frac{\mathbf{Var}(2||X||_2 \cdot ||Y||_2)^2)}{\mathbb{E}(2||X||_2 \cdot ||Y||_2)^2} \right) \\
&\approx \left(\frac{4c^4k}{2c^2k} \right)^2 \cdot \left(\frac{c^2 + 4c^4k}{4c^4k} + \frac{16c^8(2k^2 + 3k)}{16c^8k^2} \right) \\
&\qquad \text{Since Eq.(59) and Eq.(60)} \\
&= 8c^4 + \frac{16c^4k + c^2}{k^2}.
\end{aligned}$$

Therefore,

$$\begin{aligned}
\mathbb{E}\left(\frac{(||X||_2^2 - ||Y||_2^2)^2}{2||X||_2 \cdot ||Y||_2} \right) &\approx \frac{\mathbb{E}(||X||_2^2 - ||Y||_2^2)^2}{\mathbb{E}2||X||_2 \cdot ||Y||_2} + \mathbf{Var}(2||X||_2 \cdot ||Y||_2) \cdot \frac{\mathbb{E}(||X||_2^2 - ||Y||_2^2)^2}{(\mathbb{E}2||X||_2 \cdot ||Y||_2)^3} \\
&\qquad \text{Since Eq.(19)} \\
&\approx \frac{4c^4k}{2c^2k} + \frac{4c^4k}{8c^6k^3} \cdot (c^2 + 4c^4k) \qquad \text{Since Eq.(59) and Eq.(60)} \\
&= 2c^2 + \frac{4c^2k + 1}{2k^2}.
\end{aligned}$$

□

[8] Survey of simple,continuous,uniariate probability distribution and Wikipredia.

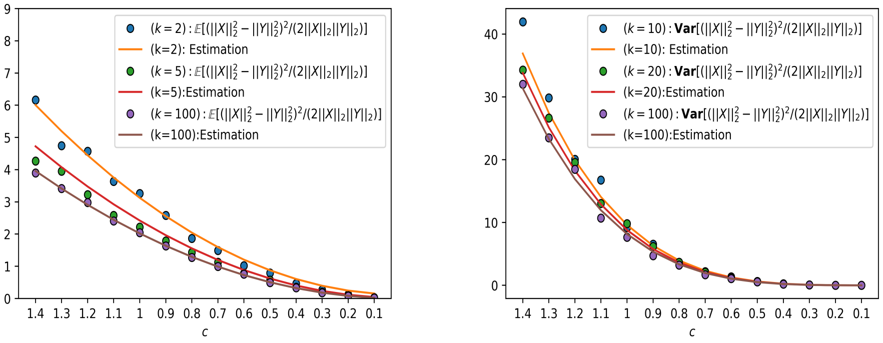

Figure 10: (Left) The numerical verification of Eq.(57) and (Right) The numerical verification of Eq.(58). X and Y follow $N(\mathbf{0}, c^2 \cdot I_k)$.

Note that, the approximation is widely used in the proof of Eq.(57) and Eq.(58). Hence, it is also necessary to verify it numerically. As shown in Fig. 10, the estimation is appropriate. According to **Lemma** 5, the mathematical expectation and variance of the ratio of $(||X||_2^2 - ||Y||_2^2)^2$ and $2||X||_2 \cdot ||Y||_2$ are both close to 0 when k is large enough and c is small enough. that is,

$$2(||X||_2 \cdot ||Y||_2) \gg (||X||_2^2 - ||Y||_2^2)^2. \tag{61}$$

By the way, the convolutional filters easily meet the condition that k is large enough.

Theorem 4. For n random variables $a_i \in \mathbb{R}^k$ follow $N(\mathbf{0}, c^2 \cdot \mathbf{I}_k)$.When k is large enough, we have such an estimation:

$$\mathbf{Var}_{a_i} \frac{F_1(a_i)}{F_2(a_i)} \approx \frac{1}{2nk}, \quad \mathbf{Var}_{a_i} \frac{F_2(a_i)}{F_1(a_i)} \approx \frac{1}{2nk}.$$

where $F_1(a_i) = \sum_{i=1}^n ||a_i||_2 / \mathbb{E}(\sum_{i=1}^n ||a_i||_2)$ and $F_2(a_i) = \sum_{i=1}^n ||a_i||_2^2 / \mathbb{E}(\sum_{i=1}^n ||a_i||_2^2)$.

Proof. Since Eq. (12) and Eq. (13), we have

$$\mathbf{Var}_{a_i} \frac{F_1(a_i)}{F_2(a_i)} = \left(\frac{nc^2k}{nc\sqrt{k}}\right)^2 \cdot \mathbf{Var}_{a_i}\left(\frac{\sum_{i=1}^n ||a_i||_2}{\sum_{i=1}^n ||a_i||_2^2}\right). \tag{62}$$

and

$$\mathbf{Var}_{a_i} \frac{F_2(a_i)}{F_1(a_i)} = \left(\frac{nc\sqrt{k}}{nc^2k}\right)^2 \cdot \mathbf{Var}_{a_i}\left(\frac{\sum_{i=1}^n ||a_i||_2^2}{\sum_{i=1}^n ||a_i||_2}\right). \tag{63}$$

According to Lagrange's identity, we have

$$\begin{aligned}
\left(\sum_{i=1}^n ||a_i||_2^2\right)\left(\sum_{i=1}^n 1\right) &= \left(\sum_{i=1}^n ||a_i||_2\right)^2 + \sum_{1 \le i < j \le n} (||a_i||_2^2 - ||a_j||_2^2)^2 \\
&= \sum_{i=1}^n ||a_i||_2^2 + \sum_{1 \le i < j \le n} (||a_i||_2 \cdot ||a_j||_2) + 2 \sum_{1 \le i < j \le n} (||a_i||_2^2 - ||a_j||_2^2)^2 \\
&\approx \sum_{i=1}^n ||a_i||_2^2 + 2 \sum_{1 \le i < j \le n} (||a_i||_2 \cdot ||a_j||_2) && \text{Since Eq. (61)} \\
&= \left(\sum_{i=1}^n ||a_i||_2\right)^2
\end{aligned}$$

so we have

$$\mathbf{Var}_{a_i \sim N(\mathbf{0}, c^2 \cdot \mathbf{I}_k)} \frac{\sum_{i=1}^n ||a_i||_2}{\sum_{i=1}^n ||a_i||_2^2} \approx \mathbf{Var}_{a_i \sim N(\mathbf{0}, c^2 \cdot \mathbf{I}_k)} \frac{n}{\sum_{i=1}^n ||a_i||_2} \tag{64}$$

By central limit theorem, we have $\sqrt{n}(\frac{1}{n}\sum_{i=1}^{n}||a_i||_2 - \mu) \sim N(\mathbf{0}, \sigma^2)$. And let $g(x) = \frac{1}{x}$, we can use Delta method[9] to find the distribution of $g(\frac{1}{n}\sum_{i=1}^{n}||a_i||_2)$:

$$\sqrt{n}\left(g(\frac{\sum_{i=1}^{n}||a_i||_2}{n}) - g(\mu))\right) \sim N(0, \sigma^2 \cdot [g\prime(\mu)]^2) = N(0, \sigma^2 \cdot \frac{1}{\mu^4}). \tag{65}$$

where μ and σ^2 denote the mean and variance of $||a_i||_2$ respectively. From Eq. (64), we have

$$\begin{aligned}
\mathbf{Var}_{a_i \sim N(\mathbf{0}, c^2 \cdot \mathbf{I}_k)} \frac{\sum_{i=1}^{n}||a_i||_2}{\sum_{i=1}^{n}||a_i||_2^2} &\approx \mathbf{Var}_{a_i \sim N(\mathbf{0}, c^2 \cdot \mathbf{I}_k)} \frac{n}{\sum_{i=1}^{n}||a_i||_2} \\
&= \sigma^2 \cdot \frac{1}{\mu^4 \cdot n} && \text{Since Eq. (65)} \\
&= 2c^2 \left[\frac{\Gamma(\frac{k}{2}+1)}{\Gamma(\frac{k}{2})} - \frac{\Gamma(\frac{k+1}{2})^2}{\Gamma(\frac{k}{2})^2}\right] \cdot \frac{1}{(\sqrt{2}c \cdot \frac{\Gamma(\frac{k+1}{2})}{\Gamma(\frac{k}{2})})^4 \cdot n} \\
& && \text{Since Eq. (12) and Eq. (13)} \\
&= \frac{1}{2c^2 \cdot nk^2} && \text{Since Lemma. 2}
\end{aligned}$$

Since Eq. (62), we have

$$\mathbf{Var}_{a_i} \frac{F_1(a_i)}{F_2(a_i)} = \left(\frac{nc^2k}{nc\sqrt{k}}\right)^2 \cdot \mathbf{Var}_{a_i} \left(\frac{\sum_{i=1}^{n}||a_i||_2}{\sum_{i=1}^{n}||a_i||_2^2}\right) \approx \frac{1}{2nk}. \tag{66}$$

Similar to Eq. (64),

$$\mathbf{Var}_{a_i \sim N(\mathbf{0}, c^2 \cdot \mathbf{I}_k)} \frac{\sum_{i=1}^{n}||a_i||_2^2}{\sum_{i=1}^{n}||a_i||_2} \approx \mathbf{Var}_{a_i \sim N(\mathbf{0}, c^2 \cdot \mathbf{I}_k)} \frac{\sum_{i=1}^{n}||a_i||_2}{n} \tag{67}$$

$$\begin{aligned}
\mathbf{Var}_{a_i \sim N(\mathbf{0}, c^2 \cdot \mathbf{I}_k)} \frac{\sum_{i=1}^{n}||a_i||_2^2}{\sum_{i=1}^{n}||a_i||_2} &\approx \mathbf{Var}_{a_i \sim N(\mathbf{0}, c^2 \cdot \mathbf{I}_k)} \frac{\sum_{i=1}^{n}||a_i||_2}{n} && \text{Similar to Eq. (64)} \\
&= \sigma^2 \cdot \frac{1}{n} && \text{Since central limit theorem} \\
&= 2c^2 \left[\frac{\Gamma(\frac{k}{2}+1)}{\Gamma(\frac{k}{2})} - \frac{\Gamma(\frac{k+1}{2})^2}{\Gamma(\frac{k}{2})^2}\right] \cdot \frac{1}{n} && \text{Since Eq. (13)} \\
&= \frac{c^2}{2n} && \text{Since Lemma. 2}
\end{aligned}$$

Since Eq. (63), we have

$$\mathbf{Var}_{a_i} \frac{F_2(a_i)}{F_1(a_i)} = \left(\frac{nc\sqrt{k}}{nc^2k}\right)^2 \cdot \mathbf{Var}_{a_i} \left(\frac{\sum_{i=1}^{n}||a_i||_2^2}{\sum_{i=1}^{n}||a_i||_2}\right) \approx \frac{1}{2nk}. \tag{68}$$

From Eq.(66) and Eq.(68), **Theorem 4** holds.

□

In Fig. 11, we also show a numerical verification of **Theorem 4**.

[9] https://en.wikipedia.org/wiki/Delta_method

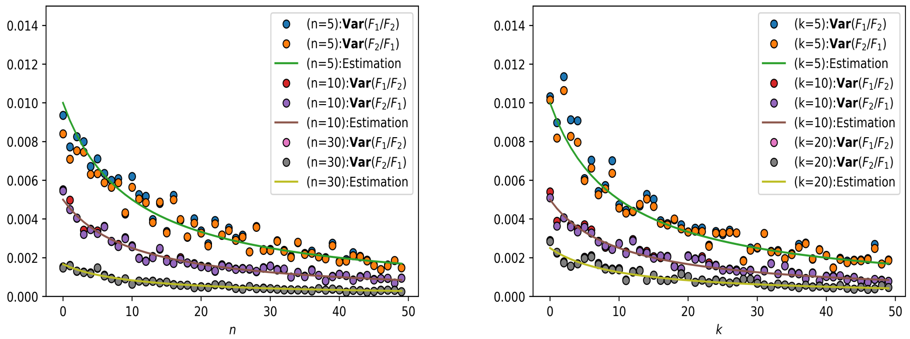

Figure 11: A numerical verification of **Theorem 4**, where $F_1 = \sum_{i=1}^{n} ||a_i||_2 / \mathbb{E}(\sum_{i=1}^{n} ||a_i||_2)$ and $F_2 = \sum_{i=1}^{n} ||a_i||_2^2 / \mathbb{E}(\sum_{i=1}^{n} ||a_i||_2^2)$. a_i follow $N(\mathbf{0}, 0.01^2 \cdot I_k)$.

G Proof of Theorem 5

Proposition 14. *For a $n \times m$ random matrix $(a_{ij})_{n\times m}$, where $a_{ij} \sim N(0, \sigma^2)$. And Eq. (14) holds with probability 1.*

$$\mathbf{rank}((a_{ij})_{n\times m}) = \mathbf{min}(m, n). \tag{69}$$

Lemma 6. *Let $v_0, v_1, ..., v_k$ be the $k+1$ vectors in n dimensional Euclidean space V and $k \leq n$. If $\mathbf{rank}(v_1 - v_0, v_2 - v_0, ..., v_k - v_0) = n$, then $\forall x \in V$, $\exists \lambda_i (0 \leq i \leq k)$, s.t.*

$$x = \sum_{i=0}^{k} \lambda_i \cdot v_i, \tag{70}$$

and $\sum_{i=0}^{k} \lambda_i = 1$. We call $\lambda = (\lambda_0, \lambda_1, ..., \lambda_k)$ the generalized barycentric coordinate with respect to $(v_0, v_1, ..., v_k)$. (In general, barycentric coordinate is a concept in Polytope)

Proof. Note that v_i is the element of n dimensional linear space V and $\mathbf{rank}(v_1 - v_0, v_2 - v_0, ..., v_k - v_0) = n$. It means $(v_1 - v_0, v_2 - v_0, ..., v_k - v_0)$ form a set of basis in the linear space V. $\forall x \in V$, $x - v_0$ can be expressed linearly by them, *i.e.*,$\exists t_i (1 \leq i \leq k)$ s.t.

$$\begin{aligned} x &= v_0 + \sum_{i=1}^{k} t_i (v_i - v_0) \\ &= (1 - \sum_{i=1}^{k} t_i) v_0 + \sum_{i=1}^{k} t_i v_i. \end{aligned}$$

Let $\lambda_0 = (1 - \sum_{i=1}^{k} t_i)$ and $\lambda_i = t_i (1 \leq i \leq k)$, Lemma 6 holds. □

Lemma 7. *Let $v_0, v_1, ..., v_k$ be the $k+1$ vectors in n dimensional Euclidean space V. $\forall a, b \in V$, and the generalized barycentric coordinate of a, b with respect to $(v_0, v_1, ..., v_k)$ are $\lambda = (\lambda_0, \lambda_1, ..., \lambda_k)^T$ and $\mu = (\mu_0, \mu_1, ..., \mu_k)^T$,respectively. Then*

$$||a - b||_2^2 = (\lambda - \mu)^T D (\lambda - \mu), \tag{71}$$

where $D = (-\frac{1}{2} d_{ij})_{(k+1)\times(k+1)}$, and $d_{ij} = ||v_i - v_j||_2^2$.

Proof. Since Lemma 6, let $R = [v_0, v_1, ..., v_k]_{n\times(k+1)}$, and we have $a = R\lambda$ and $b = R\mu$. Moreover,

$$\begin{aligned} ||a - b||_2^2 &= (a - b)^T (a - b) && (72) \\ &= [R(\lambda - \mu)]^T [R(\lambda - \mu)] && (73) \\ &= (\lambda - \mu)^T R^T R (\lambda - \mu). && (74) \end{aligned}$$

Note that, for $D = (-\frac{1}{2}d_{ij})_{(k+1)\times(k+1)}$,

$$-\frac{1}{2}d_{ij} = -\frac{1}{2}(v_i - v_j)^T(v_i - v_j) \tag{75}$$

$$= v_i^T v_j - \frac{1}{2}(v_i^T v_i + v_j^T v_j). \tag{76}$$

So we have $D = R^T R - \frac{1}{2}\left((v_i^T v_i + v_j^T v_j)_{(k+1)\times(k+1)}\right)$. It can be further simplified to $D = R^T R - \frac{1}{2}(V\alpha^T + \alpha V^T)$, where $V = (v_0^T v_0, ..., v_k^T v_k)^T$ and $\alpha = (1, ..., 1)^T$. So

$$||a - b||_2^2 = (\lambda - \mu)^T R^T R(\lambda - \mu) \tag{77}$$

$$= (\lambda - \mu)^T(D + \frac{1}{2}(V\alpha^T + \alpha V^T))(\lambda - \mu) \tag{78}$$

$$= (\lambda - \mu)^T D(\lambda - \mu) + \frac{1}{2}(\lambda - \mu)^T(V\alpha^T + \alpha V^T)(\lambda - \mu), \tag{79}$$

therefore, we only need to prove $(\lambda - \mu)^T(V\alpha^T + \alpha V^T)(\lambda - \mu) = 0$. From Lemma 6, we have $\alpha^T(\lambda - \mu) = (\lambda - \mu)^T\alpha = 0$ and the Lemma 7 holds.

□

Definition 1 (Ultra dimension)**.** *For a set U composed of vectors in a n dimensional linear space V, we define $\widehat{\mathbf{dim}}(U)$ as the Ultra dimension of U. The definition is that if U has k linearly independent vectors and there are no more, then $\widehat{\mathbf{dim}}(U) = k$.*

In fact, if U is a linear subspace in V, then the Ultra dimension and the dimensions of the linear subspace are equivalent. If U is a linear manifold, $U = \{x + v_0 | x \in W\}$, where v_0 and W are non-zero vectors and linear subspaces in V, respectively. And $\mathbf{dim}(W) = r$. Then

$$\widehat{\mathbf{dim}}(U) = \begin{cases} r, \quad v_0 \in W \\ r+1, v_0 \notin W \end{cases} \tag{80}$$

In other words, $\widehat{\mathbf{dim}}(U) \geq \widehat{\mathbf{dim}}(W)$ always holds.

Lemma 8. *For arbitrary k $(1 \leq k \leq n-1)$, let $a_1, a_2, ..., a_k$ be k linearly independent vectors in n dimensional linear space V. Consider one $n-1$ dimensional linear subspace W in V and a non-zero vector v_0 in V. They form a linear manifold $P = \{v_0 + \alpha | \alpha \in W\}$. If $a_1, a_2, ..., a_k$ do not all belong to P, then there must exist $n-k$ vectors $p_1, p_2, ..., p_{n-k}$ from P, s.t $(a_1, a_2, ..., a_k, p_1, p_2, ..., p_{n-k})$ are a set of basis for the linear space V.*

Proof. we use mathematical induction. First, show that the Lemma 8 holds for $n - k = 1$. it means we need to find a vector $p_1 \in P$ s.t. $a_1, a_2, ..., a_k, p_1$ linearly independent. If p_1 does not exist, then $\forall p \in P$ would be linearly represented by $a_1, a_2, ..., a_k$. In other word,

$$P \subset L = \mathbf{span}(a_1, a_2, ..., a_k), \tag{81}$$

① For the linear manifold P, if $v_0 \in W$. This means that P is equal to the linear subspace W. Since Eq. (81), we have $W \subset L$ and $\widehat{\mathbf{dim}}(W) = \widehat{\mathbf{dim}}(L)$. Hence, $P = W = L$. However, $a_1, a_2, ..., a_k$ do not all belong to P, a contradiction.

② For the linear manifold P, if $v_0 \notin W$, then $\widehat{\mathbf{dim}}(P) = n$. Because $v_0 \notin W$, that is, v_0 cannot be represented by a set of basis of W. In other words, v_0 and a set of basis of W are linearly independent. However, the dimension of W is $n - 1$, hence $\widehat{\mathbf{dim}}(P) = n$. From Eq. (81), we have $P \subset L$, so

$$n = \widehat{\mathbf{dim}}(P) \leq \widehat{\mathbf{dim}}(L) = k = n - 1, \tag{82}$$

a contradiction. Therefore, Lemma 8 holds for $n - k = 1$. Assume the induction hypothesis that Lemma 8 is true when $n - k = l$, where $1 \leq l$. when $n - k = l + 1$, *i.e.*, $k = n - (l + 1)$, we also can find a vector $p_1 \in P$ s.t. $a_1, a_2, ..., a_k, p_1$ linearly independent. Otherwise, $\forall p \in P$ would be linearly represented by $a_1, a_2, ..., a_k$. Similarly, we have Eq. (81). Note that, from Definition 1, $\widehat{\mathbf{dim}}(P) \geq n - 1$, hence

$$n - 1 \leq \widehat{\mathbf{dim}}(P) \leq \widehat{\mathbf{dim}}(L) = k = n - (l + 1). \tag{83}$$

a contradiction. At this time, we have $k+1 = n-(l+1)+1 = n-l$ vectors $a_1, a_2, ..., a_k, p_1$ which are not all on P. Note that $n-(n-l) = l$, using the induction hypothesis, the Lemma 8 also holds for $n-k = l$. In summary, Lemma 8 holds.

□

Theorem 5. Let $v_0, v_1, ..., v_k$ be the $k+1$ vectors in n dimensional Euclidean space $\mathbb{E}^n$. For all P in $\mathbb{E}^n$,

$$\sum_{i=0}^{k} ||P - v_i||_2^2 = \sum_{i=0}^{k} ||G - v_i||_2^2 + (k+1)||P - G||_2^2.$$

where G is the centroid of v_i, will hold if it satisfies one of the following conditions:

(1)if $k \geq n$ and $\mathbf{rank}(v_1 - v_0, v_2 - v_0, ..., v_k - v_0) = n$.

(2)if $k < n$ and $(v_1 - v_0, v_2 - v_0, ..., v_k - v_0)$ are linearly independent.

(3)if $v_i \sim N(\mathbf{0}, c \cdot \mathbf{I}_n)$, Eq.(50) holds with probability 1 where c is a constant.

Proof. **For Theorem 5 (1)**. From Lemma 6, $\forall P \in E^n$,$\exists \gamma = (\gamma_0, ..., \gamma_k)$, s.t. P can be represented by $\sum_{i=0}^{k} \gamma_i v_i$, where $\sum_{i=0}^{k} \gamma_i = 1$. In fact, for each v_i, it also can be respresented by $\sum_{j=0}^{k} \beta_{ij} v_i$, where $\sum_{i=0}^{k} \beta_{ij} = 1$. We just take $(\beta_{i0}, \beta_{i1}, ..., \beta_{ik})$ as one of the standard orthogonal basis $\epsilon_i = (0, 0, ..., 1_i, ...0)$. According to lemma 7,

$$\begin{aligned} ||P - v_i||_2^2 &= (\gamma - \epsilon_i)^T D(\gamma - \epsilon_i) && (84) \\ &= \gamma^T D\gamma - 2\gamma^T D\epsilon_i + \epsilon_i^T D\epsilon_i && (85) \\ &= \gamma^T D\gamma - 2\gamma^T D\epsilon_i. && (86) \end{aligned}$$

The final equation is because the diagonal elements of the matrix are all 0. On the other hand, we have

$$\begin{aligned} ||G - v_i||_2^2 &= (\frac{1}{k+1}\sum_{i=0}^{k} \epsilon_i - \epsilon_i)^T D(\frac{1}{k+1}\sum_{i=0}^{k} \epsilon_i - \epsilon_i) && (87) \\ &= \frac{1}{(k+1)^2}\alpha^T D\alpha - \frac{2}{k+1}\alpha^T D\epsilon_i + \epsilon_i^T D\epsilon_i && (88) \\ &= \frac{1}{(k+1)^2}\alpha^T D\alpha - \frac{2}{k+1}\alpha^T D\epsilon_i, && (89) \end{aligned}$$

where $\alpha = \sum_{i=0}^{k} \epsilon_i$, *i.e.*,$\alpha = (1, 1, ..., 1)$. Next, we consider $||P - G||_2^2$.

$$\begin{aligned} ||P - G||_2^2 &= (\gamma - \frac{1}{k+1}\alpha)^T D(\gamma - \frac{1}{k+1}\alpha) && (90) \\ &= \gamma^T D\gamma + \frac{1}{(k+1)^2}\alpha^T D\alpha - \frac{2}{k+1}\gamma^T D\alpha. && (91) \end{aligned}$$

In summary, we have

$$\begin{aligned} \sum_{i=0}^{k} ||P - v_i||_2^2 - ||G - v_i||_2^2 &= (k+1)\gamma^T D\gamma - 2\gamma^T D\alpha + \frac{1}{k+1}\alpha^T D\alpha && (92) \\ &= (k+1)||P - G||_2^2 && (93) \end{aligned}$$

Therefore, Theorem 5 (1) holds.

For Theorem 5 (2). Next, we prove the case of $k < n$. Obviously, Lemma 6 does not hold. We consider about such a linear space $W_1 = \mathbf{span}(P - G)$, *i.e.*, a linear space expanded by $P - G$, and its orthogonal complement $W_1^{\perp}$ (in E^n). Since dimension formula from linear space, it is easy to konw that $\mathbf{dim}(W_1^{\perp}) = n - 1$.

Two linear manifolds T_1 and T_2 are constructed as follows,

$$T_1 = \{x + G | x \in W_1^{\perp}\} \tag{94}$$

$$T_2 = \{x + G - v_0 | x \in W_1^{\perp}\} \tag{95}$$

$\forall v_i \in T_1$, we have $(v_i - G)^T(P - G) = 0$, Furthermore,

$$||P - v_i||_2^2 = ||v_i - G||_2^2 + ||P - G||_2^2. \tag{96}$$

It is easy to know that $G - v_0$ is not 0. If $v_1 - v_0, ..., v_k - v_0$ are all belong to T_2, it means $v_1, .., v_k$ are all in T_1. Hence, we have Eq. (96). By summing both sides of Eq. (96) for i, it is obvious find that Theorem 5 (2) holds. If $v_1 - v_0, ..., v_k - v_0$ are not all belong to T_2, since Lemma 8, there are $n - k$ vectors $p_1 - v_0, p_2 - v_0, .., p_{n-k} - v_0$ from T_2 s.t. they and $v_1 - v_0, ..., v_k - v_0$ are linearly independent, where p_i obviously belongs to manifold T_1.

At the same time, we have $2G - p_i \in T_1$, we can also construct $n - k$ new vectors $2G - p_i - v_0 \in T_2$ and calculate the rank that

$$\begin{aligned} &\mathbf{rank}(v_1 - v_0, ..., v_k - v_0, p_1 - v_0, ..., p_{n-k} - v_0, 2G - p_1 - v_0, ..., 2G - p_{n-k} - v_0) \\ &= \mathbf{rank}(v_1 - v_0, ..., v_k - v_0, p_1 - v_0, ..., p_{n-k} - v_0, 2(G - v_0), ..., 2(G - v_0)) && (97) \\ &= \mathbf{rank}(v_1 - v_0, ..., v_k - v_0, p_1 - v_0, ..., p_{n-k} - v_0, 0, ..., 0) && (98) \\ &= n && (99) \end{aligned}$$

The reason of the final equation is that $\sum_{i=1}^{k}(v_i - v_0) = (k + 1)(G - v_0)$. Note that there are a total of $k + (n - k) + (n - k) = n + (n - k) \geq n$ vectors, meets the lemma 6 condition. For the convenience of description, we define

$$L_i^{(1)} = v_i, (0 \leq i \leq k), \tag{100}$$

$$L_i^{(2)} = p_i, (1 \leq i \leq n - k), \tag{101}$$

$$L_i^{(3)} = 2G - p_i, (1 \leq i \leq n - k). \tag{102}$$

And their centroid is

$$\begin{aligned} G' &= \frac{1}{2n - k + 1}\left(\sum_{i=0}^{k} v_i + \sum_{i=1}^{n-k}(L_i^{(2)} + L_i^{(3)})\right) && (103) \\ &= \frac{1}{2n - k + 1}((k + 1)G + 2(n - k)G) && (104) \\ &= G && (105) \end{aligned}$$

That is, the newly added vector does not change the centroid of v_i. On the other hand, since both $L_i^{(2)}$ and $L_i^{(3)}$ are in the linear manifold T_1, and it meets the conditions of the Eq.(96). Similar to the derivation in the Theorem 5 (1), we have

$$\begin{aligned} (2n - k + 1)||P - G||_2^2 &= \sum_{t = L_i^{(1)}, L_i^{(2)}, L_i^{(3)}} \left(||P - t||_2^2 - ||G - t||_2^2\right) && (106) \\ &= \sum_{i=0}^{k}\left(||P - v_i||_2^2 - ||G - v_i||_2^2\right) + \sum_{t = L_i^{(2)}, L_i^{(3)}} \left(||P - t||_2^2 - ||G - t||_2^2\right) && (107) \\ &= \sum_{i=0}^{k}\left(||P - v_i||_2^2 - ||G - v_i||_2^2\right) + 2(n - k)||P - G||_2^2 && (108) \end{aligned}$$

The final equation is because both $L_i^{(2)}$ and $L_i^{(3)}$ are in the linear manifold T_1 and satisfy Eq. (96). To simplify Eq. (108), we obtain $\sum_{i=0}^{k}\left(||P - v_i||_2^2 - ||G - v_i||_2^2\right) = (k + 1)||P - G||_2^2$. Therefore, Theorem 5 (2) holds.

For Theorem 5 (3). When $k \geq n$, from Proposition 14, we know that $\mathbf{rank}(v_1 - v_0, v_2 - v_0, ..., v_k - v_0)$ = n holds with probability 1. Hence, if we use the similar deduction from Theorem 5 (1), we can find that Theorem 5 (3) holds when $k \geq n.$ On the other hand, when $k < n$, we can get the same result also according to Proposition 14. The reason is that $(v_1 - v_0, v_2 - v_0, ..., v_k - v_0)$ are linearly independent with probability 1.

□

H The result of Sp

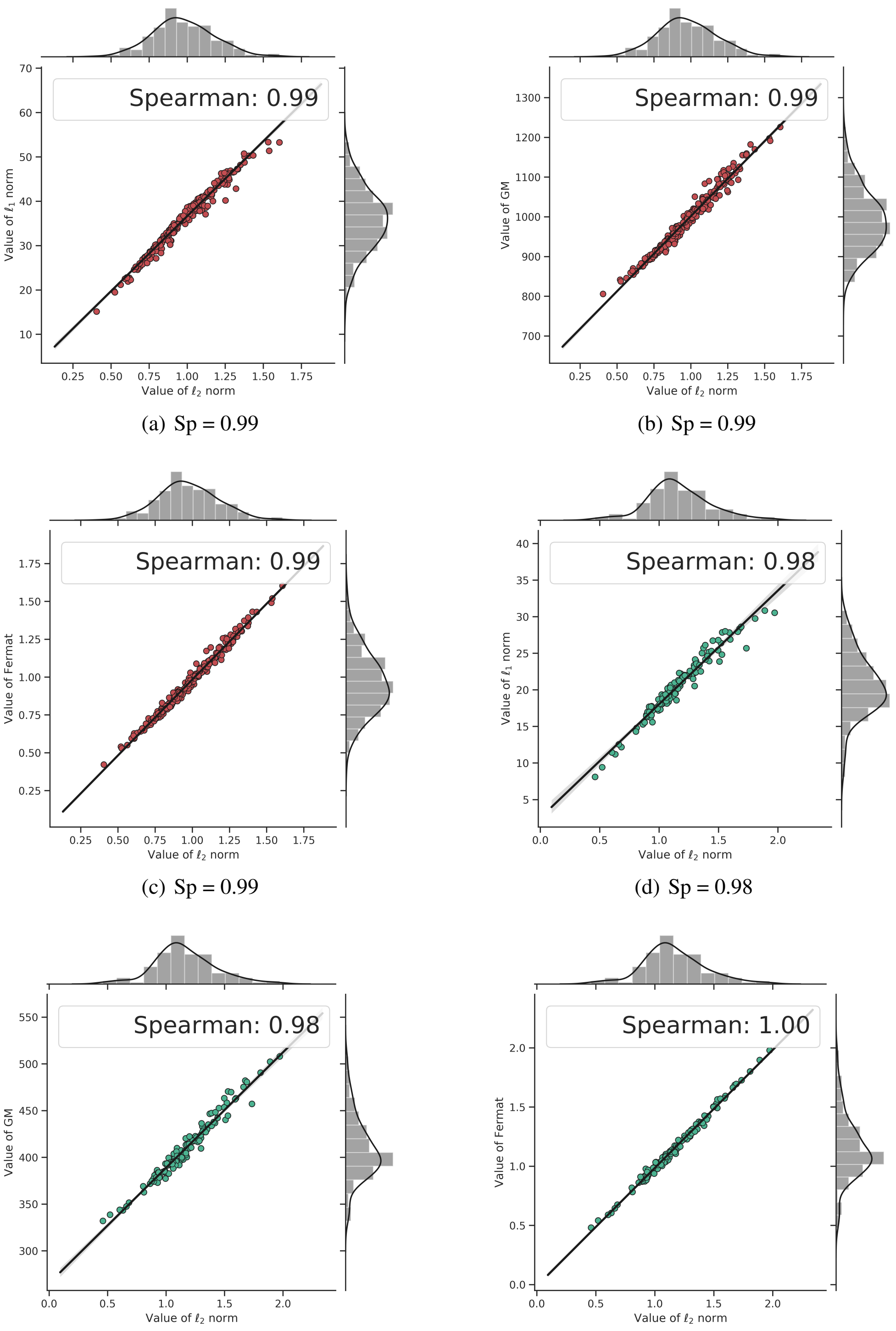

(a) Sp = 0.99

(b) Sp = 0.99

(c) Sp = 0.99

(d) Sp = 0.98

(e) Sp = 0.98

(f) Sp = 1.00

Figure 12: The Spearman's rank correlation coefficient (Sp) for different criteria. (a-c) are Sp between ℓ_1 and ℓ_2, $\mathbf{GM}$ and ℓ_2, $\mathbf{Fermat}$ and ℓ_2 from ResNet18 (12^{th} Conv), respectively. The results of VGG16 (3^{rd} Conv) are shown in (d-f). If the Sp of two pruning criteria is close to 1, then the sequence of their pruned filters may have strong similarity.

I Other result

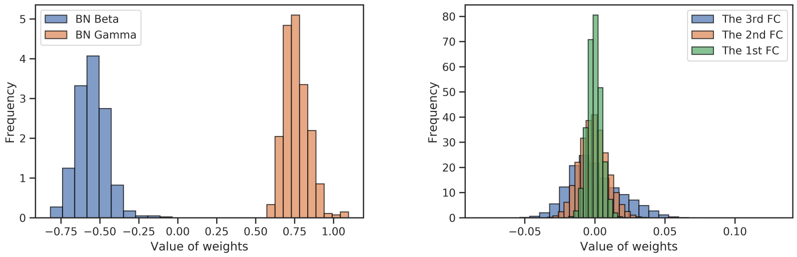

Figure 13: The distribution about other learnable parameters. (Left): The disrtibution about the learnable parameters of batch normalization. (Rihgt): The parameters distribution of the fully-connected layers (FC). For FC, the Sp between the criteria in Table2 are greater than 0.9.

In Fig 13, we show the other learnable parameters (*i.e.* Batch normalization (BN) and fully connected neural network (FC)) in VGG16-BN. For BN, the distribution of its parameters does not satisfy CWDA, and similar results are shown in [34, 35]. Moreover, the learnable parameters of fully-connected layers also do not follow a Gaussian-alike distribution, which is consistent with the conclusion in previous work [36, 37, 38].

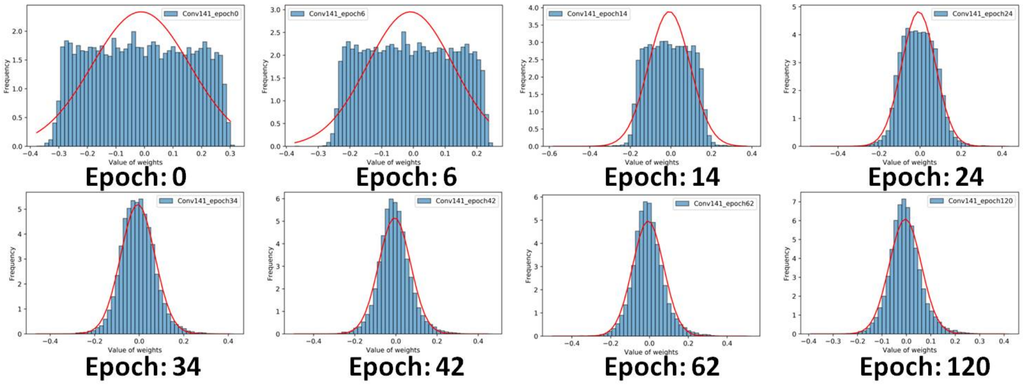

Figure 14: The distribution of the convolutional filter (141$^{\text{th}}$ Conv) with kaiming-uniform initialization for each epoch.

J An interesting case for *Importance Score* measured by different criteria

The following results are the index of pruned filters obtained by the filters' *Importance Score* from different types of pruning criteria. We take VGG16 (2^{nd}) as an example. The 5^{th} filter in this layer is regarded as a redundant convolutional filter for APoZ criterion, but other criteria consider it to be almost the most important.

Taylor ℓ_1: [27, 36, 25, 11, 6, 23, 24, 16, 0, 57, 48, 53, 1, 61, 18, 55, 34, 15, 51, 58, 31, 3, 12, 21, 59, 30, 7, 38, 41, 50, 10, 33, 17, 46, 62, 13, 49, 43, 42, 47, 2, 32, 44, 20, 39, 52, 56, 40, 9, 26, 37, 22, 29, 54, 60, 8, 14, 45, 4, 63, 19, 35, 28, **5**]

Taylor ℓ_2: [23, 32, 36, 11, 62, 16, 30, 59, 10, 13, 2, 50, 38, 0, 46, 43, 21, 26, 15, 22, 7, 51, 39, 33, 14, 58, 9, 40, 57, 6, 61, 44, 20, 48, 3, 53, 41, 56, 17, 12, 18, 31, 4, 1, 25, 19, 63, 24, 54, 45, 52, 37, 55, 47, 34, 35, 8, 29, 42, 27, 49, 28, 60, **5**]

BN_β: [52, 46, 32, 21, 14, 29, 17, 0, 19, 36, 1, 51, 44, 40, 41, 60, 57, 27, 22, 53, 63, 8, 30, 26, 23, 58, 39, 18, 9, 47, 31, 35, 11, 37, 55, 45, 3, 61, 6, 4, 33, 25, 15, 48, 43, 28, 56, 2, 13, 16, 34, 20, 59, 10, 7, 24, 50, 62, 12, 49, 38, 42, **5**, 54]

APoZ: [**5**, 10, 38, 42, 62, 24, 13, 12, 7, 28, 59, 15, 23, 11, 16, 56, 34, 35, 57, 19, 2, 49, 43, 25, 6, 63, 61, 36, 9, 27, 33, 20, 48, 58, 55, 18, 51, 31, 1, 0, 53, 37, 26, 29, 47, 60, 8, 44, 41, 46, 21, 17, 14, 32, 52, 22, 39, 3, 40, 30, 4, 45, 50, 54]

K The details of other pruning criteria

For notation, we denote i^{th} convolutional filter in layer l as F_i^l and the input feature maps in layer l as $\mathbf{I}^l \in \mathbb{R}^{N \times I^l \times H^l \times W^l}$, where N, I^l, H^l, W_l mean the train set size, number of channels, height and width respectively, $i = 1, 2, \cdots, \lambda_l$, and $l = 1, 2, \cdots, L$. The formulation of the filters' *Importance Score* under each pruning criteria are illustrated as follows:

Norm-based criteria:

- ℓ_1-Norm [5]: $||F_i^l||_1$;
- ℓ_2-Norm [7]: $||F_i^l||_2$;

BN-based criteria [12]:

- BN_γ: $|\gamma_i^l|$, where γ_i^l is the scaling factor in the Batch Normalization layer l;
- BN_β: $|\beta_i^l|$, where β_i^l is the shifting factor in the Batch Normalization layer l.

Activation-based criteria:

- APoZ [8]: $\frac{\sum_{p,q} \mathbb{1}\left((|\mathbf{I}^l * F_i^l|)_{p,q} > \sigma\right)}{N \times I^l \times H^l \times W^l}$, where we set $\sigma = 0.0001$ same as [9], and $\mathbb{1}(\cdot)$ is the indicator function, $*$ is convolution operator and $\mathbf{I}^l * F_i^l$ is the i-th output feature map;
- Entropy [9]: we first prepare $\mathbf{G}_i^l = GAP(\mathbf{I}^l * F_i^l)$, where $\mathbf{G}_i^l \in \mathbb{R}^{N \times 1}$ and $GAP(\cdot)$ is the Global Average Pooling. Then, we estimate statistical distribution for $\mathbf{G}_i^l$ by dividing all elements in $\mathbf{G}_i^l$ into m bins. Let p_j is the probability of bin j, and the the *Importance Score* score is $-\sum_{j=1}^{m} p_j \log p_j$.

First order Taylor based criteria [10, 11, 26]:

- Taylor ℓ_1-Norm: $||\frac{\partial loss}{\partial F_i^l} \cdot F_i^l||_1$;
- Taylor ℓ_2-Norm: $||\frac{\partial loss}{\partial F_i^l} \cdot F_i^l||_2$;

The $loss$ is the Cross Entropy Loss on the split training set from the original training set.

L Additional experiments about image clasification

Table 5: The accuracy(%) of several networks and datasets using different pruning criteria.

		Experiment (1)			Experiment (2)			Experiment (3)		
		Trained	Pruned	Fine-tuned	Trained	Pruned	Fine-tuned	Trained	Pruned	Fine-tuned
CIFAR10	ℓ_1	93.61	61.21	93.51	93.21	54.31	93.22	93.26	57.74	93.32
VGG16	ℓ_2	93.61	63.41	93.32	93.21	54.61	93.42	93.26	57.42	93.29
	GM	93.61	61.22	93.41	93.21	53.71	93.25	93.26	57.46	93.36
CIFAR100	ℓ_1	72.67	25.91	71.50	72.99	20.43	71.36	72.56	24.01	71.07
VGG16	ℓ_2	72.67	27.07	71.28	72.99	22.31	71.12	72.56	24.45	70.92
	GM	72.67	26.37	71.27	72.99	21.67	71.26	72.56	24.26	70.78
ImageNet	ℓ_1	71.58	30.33	71.02	71.33	40.33	70.12	72.01	28.07	70.93
VGG16	ℓ_2	71.58	29.47	70.83	71.33	40.45	70.13	72.01	27.89	71.02
	GM	71.58	30.76	70.95	71.33	39.86	70.33	72.01	28.01	70.74
CIFAR10	ℓ_1	92.98	77.73	93.08	92.97	76.02	92.82	93.01	79.93	92.81
ResNet56	ℓ_2	92.98	79.02	92.83	92.97	77.91	92.72	93.01	82.43	92.81
	GM	92.98	74.26	92.77	93.2	73.93	92.61	93.01	80.48	92.84
CIFAR100	ℓ_1	71.36	50.64	70.15	70.02	52.41	69.19	70.48	52.19	69.77
ResNet56	ℓ_2	71.36	53.44	70.16	70.02	52.73	69.31	70.48	52.16	69.62
	GM	71.36	45.12	70.22	70.02	52.62	69.54	70.48	50.74	69.69
ImageNet	ℓ_1	73.31	62.22	73.06	73.16	54.24	72.99	73.21	63.12	73.02
ResNet34	ℓ_2	73.31	62.02	72.91	73.16	53.64	72.78	73.21	62.98	72.86
	GM	73.31	61.88	72.96	73.16	53.48	72.94	73.21	62.36	73.04

All the setting of these experiments are under can be found in `https://github.com/bearpaw/pytorch-classification`. Specifically, for pruning ratio:

VGG16 on CIFAR10, CIFAR100 and ImageNet:

`https://github.com/Eric-mingjie/rethinking-network-pruning/blob/master/cifar/l1-norm-pruning/vggprune.py#L84`

ResNet56 on CIFAR10 and CIFAR100:

`https://github.com/Eric-mingjie/rethinking-network-pruning/blob/master/cifar/l1-norm-pruning/res56prune.py#L94`

ResNet34 on ImageNet:

`https://github.com/Eric-mingjie/rethinking-network-pruning/blob/master/imagenet/l1-norm-pruning/prune.py#L138`

M About weight decay

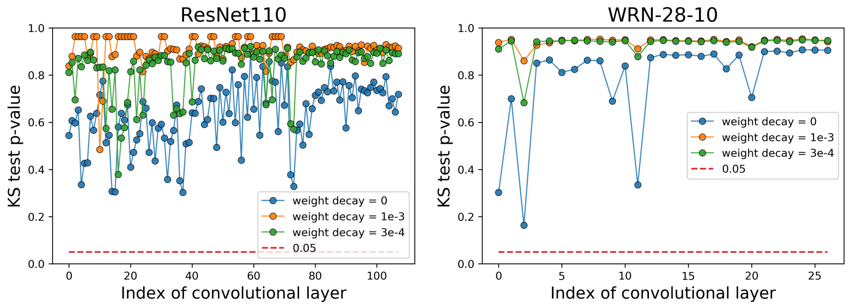

Figure 15: KS test [39] while using different settings of weight decay.

We train the ResNet110 and WRN-28-10 on CIFAR100 with different weight decay (1e-3, 3e-4 and 0) and use KS test to verify whether the parameters of different layers follow a normal distribution. In Fig. 15, we can find

(1) When weight decay (wd) is non-zero, the normality is higher than that when weight decay is 0.

(2) If weight decay is 0, the p-value can still be much greater than 0.05, which means that the regularization of weight decay may not be the key reason for CWDA. The distribution of the parameters in these two networks (weight decay is 0) are shown in Fig. 17 and Fig. 16.

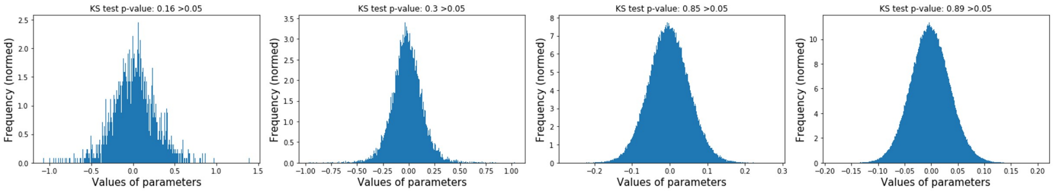

Figure 16: The distribution of parameters in different convolutional filters (WRN-28-10, wd = 0).

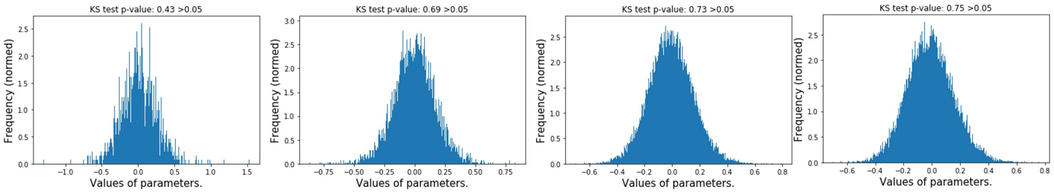

Figure 17: The distribution of parameters in different convolutional filters (ResNet110, wd = 0).

N More visualizations of correlation matrix

N.1 VGG16

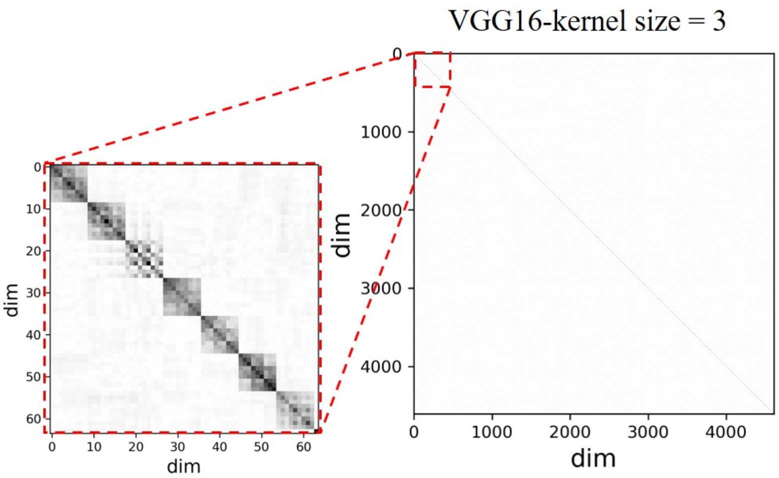
VGG16-kernel size = 3

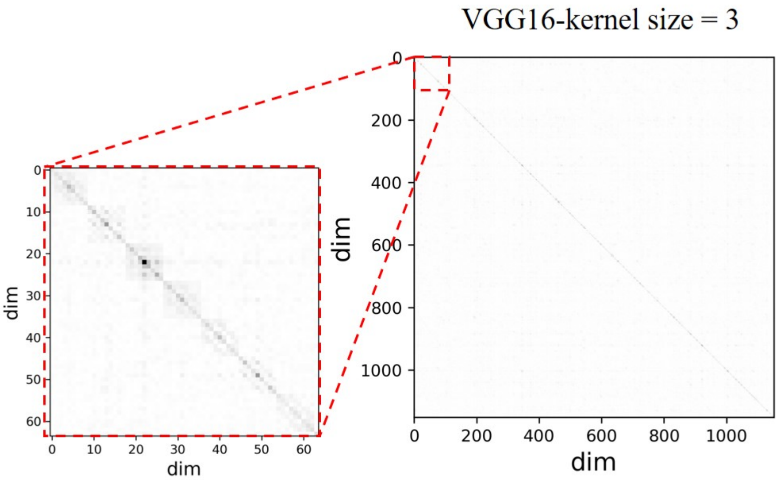
VGG16-kernel size = 3

N.2 VGG19

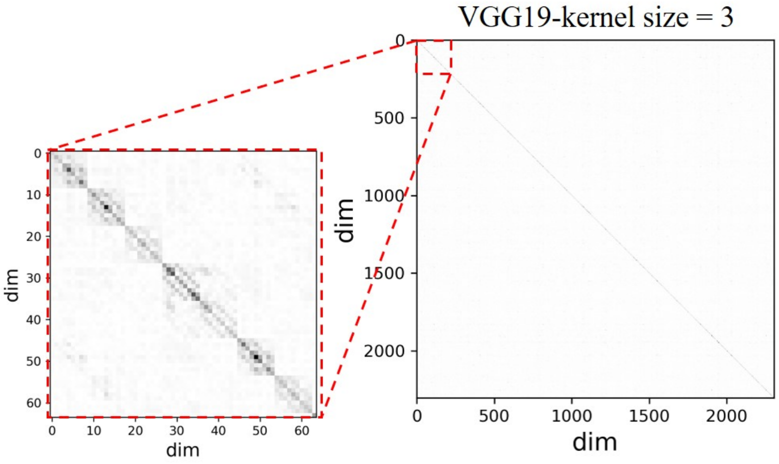
VGG19-kernel size = 3
0
500
1000
1500
2000
dim
0
500
1000
1500
2000
dim
0
10
20
30
40
50
60
dim
0
10
20
30
40
50
60
dim

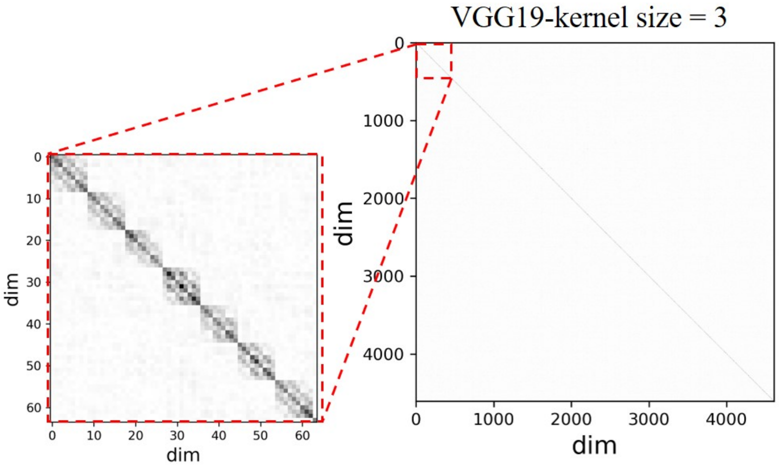
VGG19-kernel size = 3
0
1000
2000
3000
4000
dim
0
1000
2000
3000
4000
dim
0
10
20
30
40
50
60
dim
0
10
20
30
40
50
60
dim

N.3 ResNet18

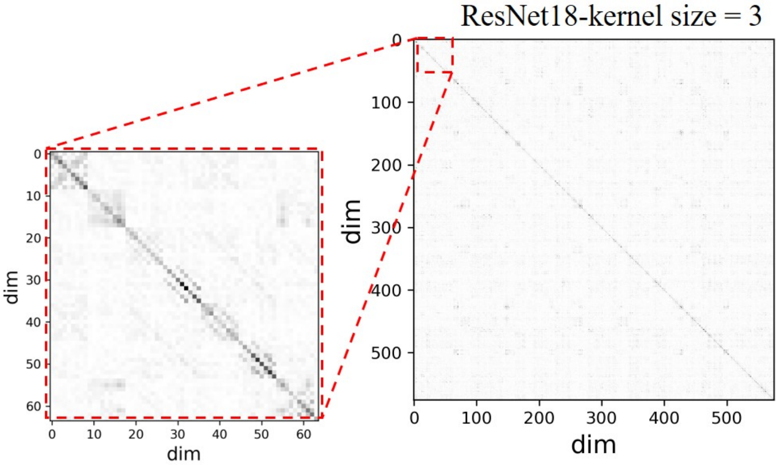

ResNet18-kernel size = 3
dim
dim
0
100
200
300
400
500
0
100
200
300
400
500
dim
dim
0
10
20
30
40
50
60
0
10
20
30
40
50
60

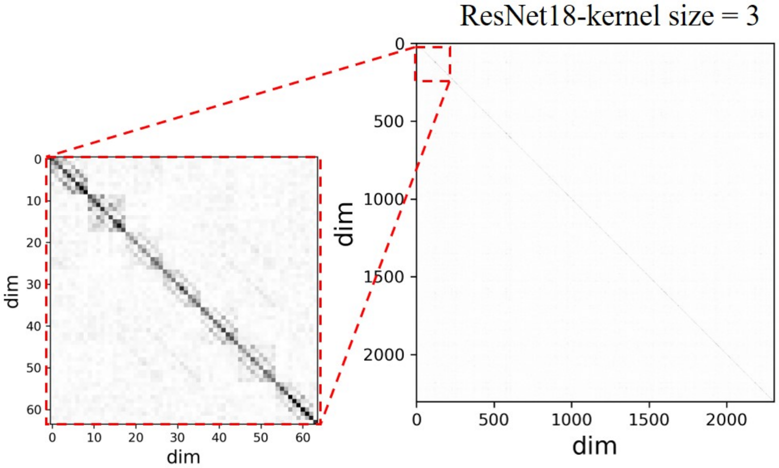

ResNet18-kernel size = 3
dim
dim
0
500
1000
1500
2000
0
500
1000
1500
2000
dim
dim
0
10
20
30
40
50
60
0
10
20
30
40
50
60

N.4 ResNet50

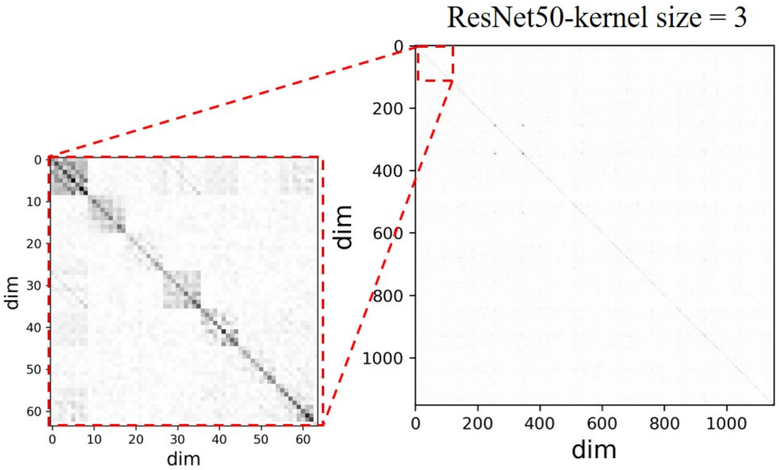
ResNet50-kernel size = 3

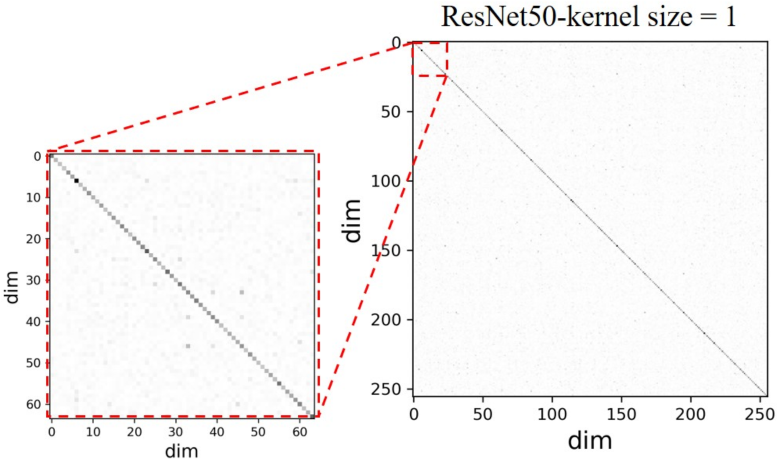
ResNet50-kernel size = 1

N.5 AlexNet

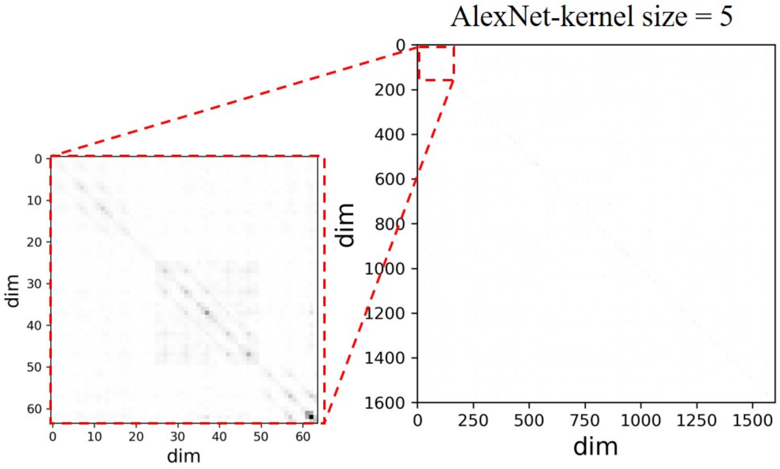
AlexNet-kernel size = 5
0
200
400
600
800
1000
1200
1400
1600
0
250
500
750
1000
1250
1500
dim
dim
0
10
20
30
40
50
60
dim
dim

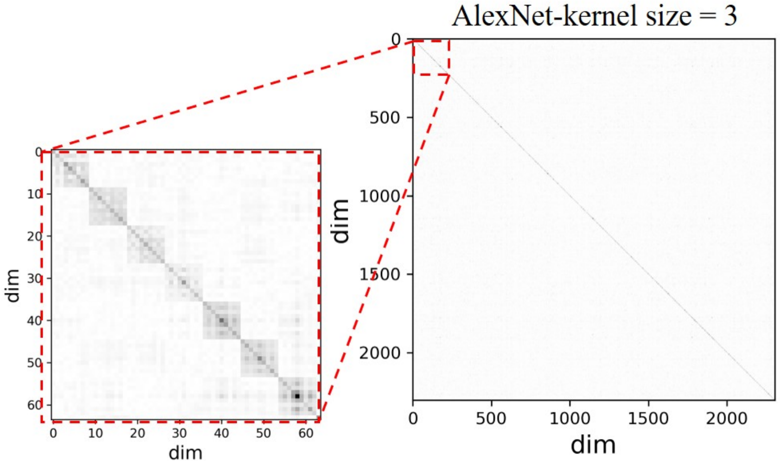
AlexNet-kernel size = 3
0
500
1000
1500
2000
dim
dim
0
10
20
30
40
50
60
dim
dim

N.6 DenseNet

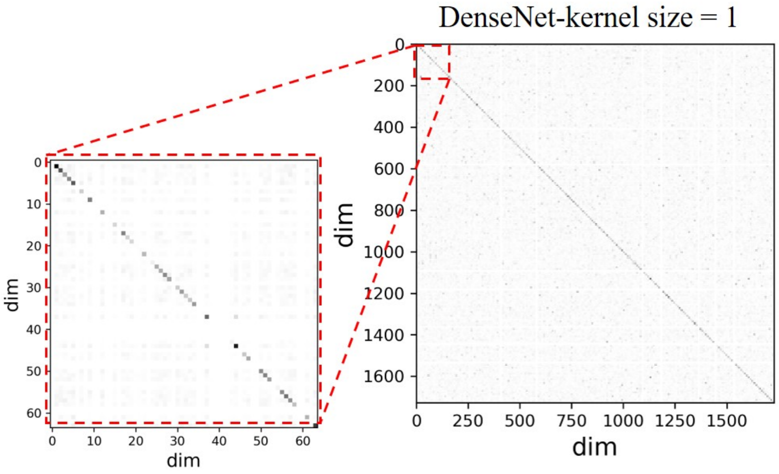
DenseNet-kernel size = 1

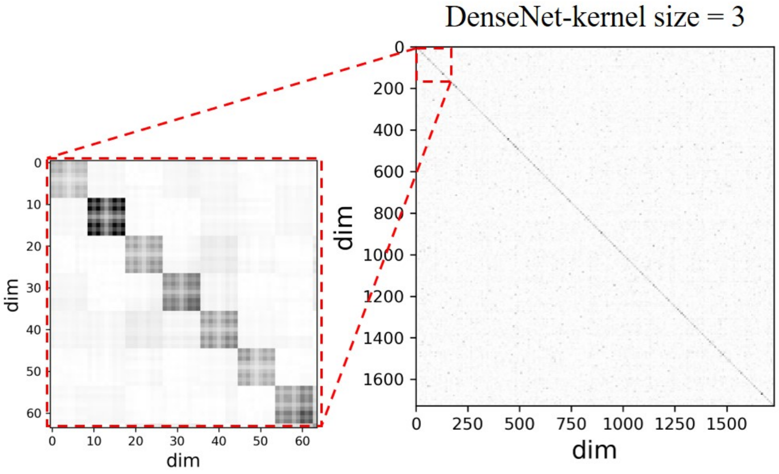
DenseNet-kernel size = 3

N.7 ResNext

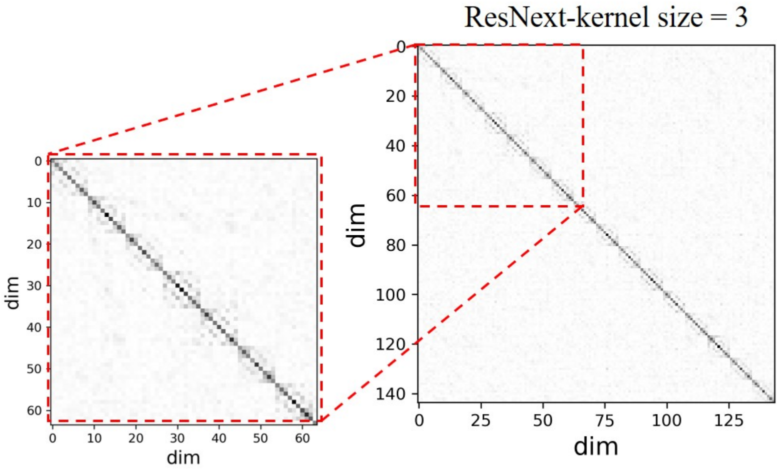
ResNext-kernel size = 3
0
20
40
60
80
100
120
140
dim
0
25
50
75
100
125
dim
0
10
20
30
40
50
60
dim
0
10
20
30
40
50
60
dim

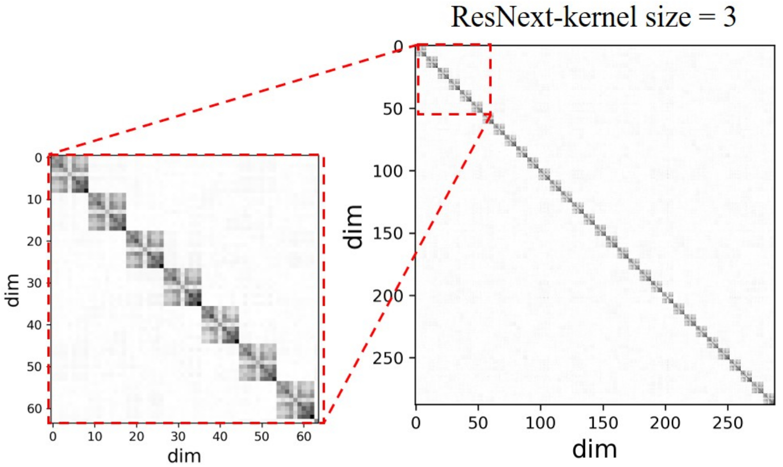
ResNext-kernel size = 3
0
50
100
150
200
250
dim
0
50
100
150
200
250
dim
0
10
20
30
40
50
60
dim
0
10
20
30
40
50
60
dim

N.8 MobileNet

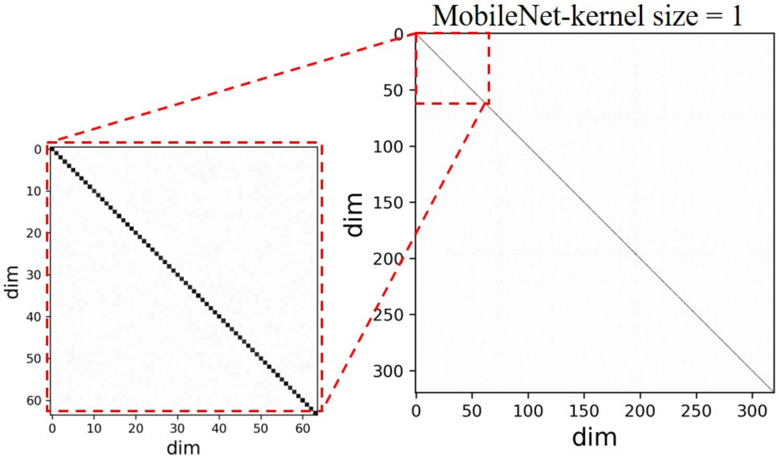

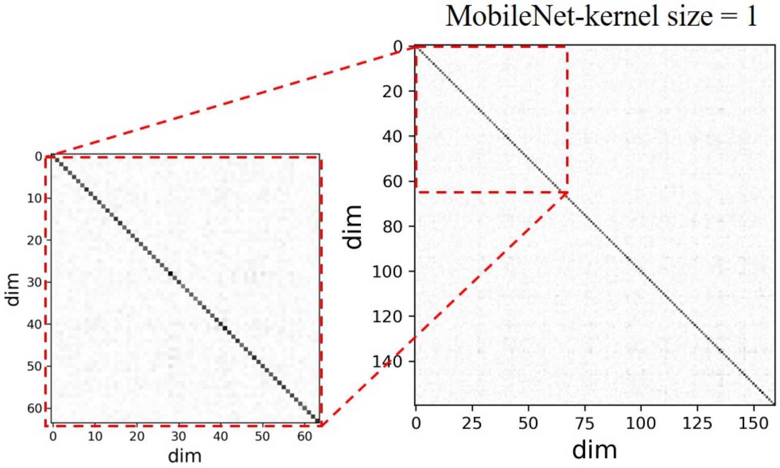

O More experiments for supporting our analysis in global pruning

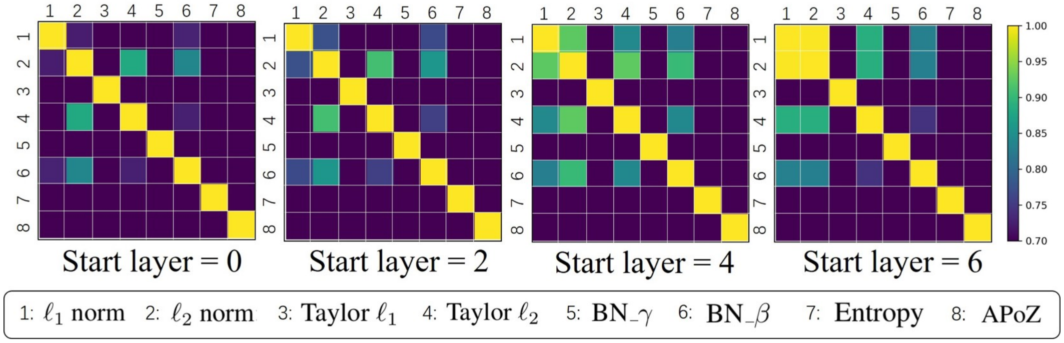

Figure 18: Global pruning with different start layer.

For VGG16. As shown in Fig.6 (a-b), compared with ResNet56, VGG16 has some layers with different dimensions but similar *Importance Score* measured by ℓ_1 or ℓ_2, such as "layer 2" and "layer 8" for ℓ_2 criterion in Fig.6 (a). From Table 3 (3-4), these pairs of layers make the Sp small, which explain why the result of ℓ_1 and ℓ_2 pruning is not similar in Fig. 5 (e) for VGG16. We consider a special class of global pruning, *i.e.,* the convolutional filters from one middle layer (called "Start layer") to the last layer are pruned globally. According to our analysis and Fig.6 (a-b), we can deduce that when "Start layer" ≥ 4, the Sp between ℓ_1 and ℓ_2 is large enough. The experiments in Fig.18 are consistent with our analysis, which imply our analysis is reasonable.

P Statistical Test

In this section, according to Section 2.1, we have a series of statistical tests for the necessary conditions of CWDA. let $F_{ij} \in \mathbb{R}^{N_i \times k \times k}$ represent the j^{th} filter of the i^{th} convolutional layer.[10]

(1) **Gaussian**. We verify whether F_{ij} approximatively follow a Gaussian-alike distribution. In i^{th} layer, we use Kolmogorov–Smirnov (KS) test [39] to check if all the weights in the same layer follow a normal distribution.

(2) **Variance**. We verify whether the variance of the diagonal elements of Σ_{diag} are small enough. Since Appendix B, Let σ_j denotes the standard deviation of all the weights of filter F_{ij} in i^{th} layer. We use Student's t test [40] to check if the variance of these σ_j is small enough. The null hypothesis H_0 and the alternative hypothesis H_1 are:

$$H_0 : \mathbf{Var}(\sigma_1^2, \sigma_2^2, .., \sigma_{N_i}^2) \leq \sigma_0^2, \qquad H_1 : \mathbf{Var}(\sigma_1^2, \sigma_2^2, .., \sigma_{N_i}^2) > \sigma_0^2.$$

where N_i denotes the number of the filters in i^{th} layer and σ_0 is a given real number which is small enough, like $\sigma_0^2 = 0.0001$.

(3) **Mean**. We verify whether the mean of F_{ij} is 0. Let the mean of all the weights in the same layer is μ. We use Student's t test [40] to check if μ is close to 0. First, we check the upper bound (Mean-Left) of μ, *i.e.*,

$$H_0 : \mu \leq \epsilon_0, \qquad H_1 : \mu > \epsilon_0.$$

where ϵ_0 is a small constant, like $\epsilon_0 = 0.01$. Next, we check the lower bound (Mean-Right) and the null hypothesis H_0 and the alternative hypothesis H_1 are:

$$H_0 : \mu \geq -\epsilon_0, \qquad H_1 : \mu < -\epsilon_0.$$

(4) **Magnitude**. We verify whether ϵ is small enough. Let h denote the mean of the off-diagonal elements of $\mathbf{\Sigma}_{\text{diag}} + \epsilon \cdot \mathbf{\Sigma}_{\text{block}}$.

$$H_0 : h \leq \epsilon_0, \qquad H_1 : h > \epsilon_0.$$

Table 6: The experiments for having the comprehensive statistical tests on CWDA.

NETWORK STRUCTURE	**OPTIMIZER**	**REGULARIZATION**
ResNet [41]	SGD [42]	L1 norm
VGG [43]	ASGD [44]	L2 norm
AlexNet [45]	Adam [46]	RReLu [47]
DenseNet [48]	Adagrad [49]	Dropact [50]
PreResNet [51]	Adamax [46]	Autoaug [52]
WRN [53]	Adadelta [54]	Cutout [55]
ResNext [56]		Cutmix [57]
ATTENTION MECHANISM	**INITIALIZATION**	**DATASET**
SENet [58]	Kaiming-normal [59]	CIFAR10 [60]
DIANet [61]	Kaiming-uniform [59]	CIFAR100 [60]
SRMNet [62]	Xavier-normal [63]	ImageNet [64]
CBAM [65]	Xavier-uniform [63]	MNIST [66]
IEBN [67]	Orthogonal [68]	
SGENet [69]		
SEGMENTATION	**DETECTION**	**BATCH NORMALIZATION**
SegNet [70]	Faster RCNN [71]	VGG
PSPNet [72]		VGG-bn
PYTORCH PRETRAIN	**MATTING**	**LEARNING RATE**
ResNet18/34/50	Deep image matting [73]	Schedule150-225
VGG11/16/19	AlphaGAN matting [74]	Schedule82-164
STYLE TRANSFER	**GAN**	Schedule60-120
Fast neural style [75]	DCGAN [76]	Cos-lr [77]

[10] The statistical tests about the situation with or without weight decay can be found in Appendix M.

Next, we show the passing rate about the statistical tests for different situations. “in the front of network” denotes whether all the failed cases are the layers whose position is in the front of the network.

For Network structure: `https://github.com/bearpaw/pytorch-classification`.

Table 7: **Network structure**.

Experiments	Remark	Gaussian	Variance	Mean	Magnitude	in the front of network?
ResNet164	CIFAR100	98.77%	97.55%	100%	97.55%	✓
VGG16	CIFAR100	100%	93.75%	100%	100%	✓
AlexNet	CIFAR100	100%	100%	100%	100%	✓
DenseNet-BC-100-12	CIFAR100	100%	98.99%	100%	98.99%	✓
PreResNet110	CIFAR100	100%	99.08%	100%	100%	✓
WRN28-10	CIFAR100	100%	100%	100%	100%	✓
ResNext-16x64d	CIFAR100	100%	100%	100%	100%	✓
ResNet164	CIFAR10	100.00%	97.55%	100%	97.55%	✓
VGG16	CIFAR10	100%	93.75%	100%	93.75%	✓
AlexNet	CIFAR10	100%	100%	100%	100%	✓
DenseNet-BC-100-12	CIFAR10	100%	100%	100%	98.99%	✓
PreResNet110	CIFAR10	100%	99.08%	100%	100%	✓
WRN28-10	CIFAR10	100%	100%	100%	100%	✓
ResNext-16x64d	CIFAR10	100%	100%	100%	100%	✓

For Optimizer: `https://pytorch.org/docs/master/optim.html#torch-optim`.

Table 8: **Optimizer**

Experiments	Remark	Gaussian	Variance	Mean	Magnitude	in the front of network?
ASGD	ResNet164	100%	99.39%	99.39%	100%	✓
Adam	ResNet164	99.39%	90.18%	100%	99.39%	✗
Adagrad	ResNet164	100%	99.39%	100%	100%	✓
Adamax	ResNet164	100%	96.93%	100%	99.39%	✗
Adadelta	ResNet164	100%	100%	100%	100%	✓
SGD	ResNet164	98.77%	97.55%	100%	97.53%	✓
ASGD	VGG16	100%	100%	93.75%	100%	✓
Adam	VGG16	93.75%	93.75%	100%	100.00%	✓
Adagrad	VGG16	100%	100%	100%	100%	✓
Adamax	VGG16	100%	100%	100%	93.75%	✗
Adadelta	VGG16	100%	100%	100%	100%	✓
SGD	VGG16	100%	93.75%	100%	100%	✓
ASGD	AlexNet	100%	100%	100%	100%	✓
Adam	AlexNet	100%	100%	100%	100%	✓
Adagrad	AlexNet	100%	100%	100%	100%	✓
Adamax	AlexNet	100%	100%	100%	100%	✓
Adadelta	AlexNet	100%	100%	100%	100%	✓
SGD	AlexNet	100%	100%	100%	100%	✓

For Regularization:`https://github.com/LeungSamWai/Drop-Activation`

`https://github.com/uoguelph-mlrg/Cutout`

`https://github.com/clovaai/CutMix-PyTorch`

`https://github.com/DeepVoltaire/AutoAugment`

For Attention:`https://github.com/moskomule/senet.pytorch`

`https://github.com/gbup-group/DIANet`

`https://github.com/EvgenyKashin/SRMnet`

Table 9: **Regularization**

Experiments	Remark	Gaussian	Variance	Mean	Magnitude	in the front of network?
L1 norm	ResNet164	100%	99.39%	99.39%	100%	✓
L2 norm	ResNet164	98.77%	97.53%	100%	97.53%	✓
RReLU	ResNet164	100%	99.39%	100%	100%	✓
Dropact	ResNet164	100%	96.93%	100%	99.39%	✓
Autoaugment	ResNet164	100%	96.93%	100%	99.39%	✓
Cutout	ResNet164	100%	100%	100%	100%	✓
Cutmix	ResNet164	98.77%	97.53%	100%	97.53%	✓
L1 norm	WRN28-10	100%	96.43%	100%	96.43%	✓
L2 norm	WRN28-10	100%	100%	100%	100%	✓
RReLU	WRN28-10	100%	96.43%	100%	100%	✓
Dropact	WRN28-10	100%	96.43%	100%	100%	✓
Autoaugment	WRN28-10	100%	96.43%	100%	100%	✓
Cutout	WRN28-10	100%	96.43%	100%	100%	✓
Cutmix	WRN28-10	100%	100%	100%	100%	✓
L1 norm	VGG16	100%	93.75%	100%	100%	✓
L2 norm	VGG16	100%	93.75%	100%	100%	✓
RReLU	VGG16	100%	93.75%	100%	93.75%	✓
Dropact	VGG16	100%	93.75%	100%	100%	✓
Autoaugment	VGG16	100%	93.75%	100%	100%	✓
Cutout	VGG16	100%	93.75%	93.75%	93.75%	✓
Cutmix	VGG16	100%	93.75%	100%	100%	✓
L1 norm	PreResNet110	100%	99.08%	100%	100%	✓
L2 norm	PreResNet110	100%	99.08%	100%	100%	✓
RReLU	PreResNet110	100%	100%	100%	100%	✓
Dropact	PreResNet110	100%	99.08%	100%	100%	✓
Autoaugment	PreResNet110	100%	100%	100%	100%	✓
Cutout	PreResNet110	100%	99.08%	99.08%	99.08%	✓
Cutmix	PreResNet110	100%	99.08%	100%	100%	✓
L1 norm	AlexNet	100%	100%	100%	100%	✓
L2 norm	AlexNet	100%	100%	100%	100%	✓
RReLU	AlexNet	100%	100%	100%	100%	✓
Dropact	AlexNet	100%	100%	100%	100%	✓
Autoaugment	AlexNet	100%	100%	100%	100%	✓
Cutout	AlexNet	100%	100%	100%	100%	✓
Cutmix	AlexNet	100%	100%	100%	100%	✓
L1 norm	DenseNet-BC-100-12	100%	98.99%	100%	98.99%	✓
L2 norm	DenseNet-BC-100-12	100%	98.99%	100%	98.99%	✓
RReLU	DenseNet-BC-100-12	100%	98.99%	100%	98.99%	✓
Dropact	DenseNet-BC-100-12	98.99%	98.99%	98.99%	98.99%	✓
Autoaugment	DenseNet-BC-100-12	100%	98.99%	100%	98.99%	✓
Cutout	DenseNet-BC-100-12	100%	98.99%	98.99%	98.99%	✓
Cutmix	DenseNet-BC-100-12	100%	98.99%	100%	98.99%	✓

`https://github.com/luuuyi/CBAM.PyTorch`

`https://github.com/gbup-group/IEBN`

`https://github.com/implus/PytorchInsight`

Table 10: **Attention**

Experiments	Remark	Gaussian	Variance	Mean	Magnitude	in the front of network?
SENet	ResNet164	99.39%	99.39%	100%	100%	✓
DIANet	ResNet164	99.39%	99.39%	100%	100%	✓
SRMNet	ResNet164	99.39%	97.55%	100%	99.39%	✓
CBAM	ResNet164	99.39%	99.39%	100%	100%	✓
IEBN	ResNet164	99.39%	99.39%	99.39%	99.39%	✓
SGENet	ResNet164	99.39%	98.77%	100%	100%	✓
SENet	VGG16	100%	93.75%	100%	100%	✓
DIANet	VGG16	100%	93.75%	100%	93.75%	✓
SRMNet	VGG16	100%	100%	100%	100%	✓
CBAM	VGG16	100%	93.75%	100%	100%	✓
IEBN	VGG16	100%	93.75%	93.75%	93.75%	✓
SGENet	VGG16	100%	93.75%	100%	100%	✓
SENet	PreResNet110	99.08%	100%	100%	100%	✓
DIANet	PreResNet110	100%	99.08%	100%	100%	✓
SRMNet	PreResNet110	100%	99.08%	99.08%	100%	✓
CBAM	PreResNet110	100%	100%	100%	100%	-
IEBN	PreResNet110	100%	99.08%	100%	99.08%	✓
SGENet	PreResNet110	100%	100%	100%	99.08%	✓
SENet	DenseNet-BC-100-12	100%	100%	100%	100%	✓
DIANet	DenseNet-BC-100-12	98.99%	98.99%	100%	100%	✓
SRMNet	DenseNet-BC-100-12	100%	98.99%	98.99%	98.99%	✓
CBAM	DenseNet-BC-100-12	100%	100%	100%	98.99%	✓
IEBN	DenseNet-BC-100-12	100%	98.99%	100%	100%	✓
SGENet	DenseNet-BC-100-12	100%	100%	98.99%	100%	✓
SENet	WRN28-10	100%	96.43%	100%	100%	✓
DIANet	WRN28-10	100%	96.43%	100%	100%	✓
SRMNet	WRN28-10	100%	96.43%	100%	100%	✓
CBAM	WRN28-10	100%	96.43%	100%	100%	✓
IEBN	WRN28-10	100%	96.43%	100%	100%	✓
SGENet	WRN28-10	100%	96.43%	100%	100%	✓

For initialization:

`https://pytorch.org/docs/master/nn.init.html#nn-init-doc.`

For dataset:

For other tasks:

`https://github.com/meetshah1995/pytorch-semse`

`https://github.com/jwyang/faster-rcnn.pytorch`

`https://github.com/speedinghzl/pytorch-segmentation-toolbox`

`https://github.com/foamliu/Deep-Image-Matting-PyTorch`

`https://github.com/CDOTAD/AlphaGAN-Matting`

`https://github.com/abhiskk/fast-neural-style`

Table 11: **Initialization**

Experiments	Remark	Gaussian	Variance	Mean	Magnitude	in the front of network?
Kaiming-uniform	ResNet164	98.77%	97.55%	100%	100%	✓
Kaiming-normal	ResNet164	98.77%	97.53%	100%	97.55%	✓
Xavier-normal	ResNet164	98.77%	96.32%	100%	97.55%	✓
Xarier-uniform	ResNet164	98.16%	96.32%	100%	99.39%	✓
Orthogonal	ResNet164	97.55%	96.32%	100%	100%	✓
Kaiming-uniform	VGG16	100%	93.75%	100%	100%	✓
Kaiming-normal	VGG16	100%	93.75%	100%	100%	✓
Xavier-normal	VGG16	100%	93.75%	100%	93.75%	✓
Xarier-uniform	VGG16	100%	93.75%	100%	93.75%	✓
Orthogonal	VGG16	100%	93.75%	93.75%	93.75%	✓
Kaiming-uniform	WRN28-10	100%	96.43%	100%	100%	✓
Kaiming-normal	WRN28-10	100%	100%	100%	100%	✓
Xavier-normal	WRN28-10	100%	96.43%	100%	100%	✓
Xarier-uniform	WRN28-10	100%	96.43%	100%	100%	✓
Orthogonal	WRN28-10	100%	96.43%	100%	100%	✓
Kaiming-uniform	PreResNet110	100%	99.08%	100%	100%	✓
Kaiming-normal	PreResNet110	100%	99.08%	100%	100%	✓
Xavier-normal	PreResNet110	100%	100%	100%	100%	✓
Xarier-uniform	PreResNet110	100%	99.08%	100%	100%	✓
Orthogonal	PreResNet110	100%	100%	100%	100%	✓
Kaiming-uniform	AlexNet	100%	100%	100%	100%	✓
Kaiming-normal	AlexNet	100%	100%	100%	100%	✓
Xavier-normal	AlexNet	100%	100%	100%	100%	✓
Xarier-uniform	AlexNet	100%	100%	100%	100%	✓
Orthogonal	AlexNet	100%	100%	100%	100%	✓
Kaiming-uniform	DenseNet-BC-100-12	100%	98.99%	100%	98.99%	✓
Kaiming-normal	DenseNet-BC-100-12	100%	98.99%	100%	98.99%	✓
Xavier-normal	DenseNet-BC-100-12	100%	98.99%	100%	98.99%	✓
Xarier-uniform	DenseNet-BC-100-12	98.99%	98.99%	98.99%	98.99%	✓
Orthogonal	DenseNet-BC-100-12	100%	98.99%	100%	98.99%	✓

Table 12: **Dataset**

Experiments	Remark	Gaussian	Variance	Mean	Magnitude	in the front of network?
CIFAR10	WRN28-10	100%	96.43%	100%	100%	✓
CIFAR100	WRN28-10	100%	100%	100%	100%	✓
ImageNet	WRN28-10	100%	96.43%	100%	100%	✓
MINIST	WRN28-10	100%	96.43%	100%	96%	✓

`https://github.com/csinva/gan-pretrained-pytorch`

Table 13: **Other tasks**

Experiments	Remark	Gaussian	Variance	Mean	Magnitude	in the front of network?
SgeNet(Cityscapes)	Segmentation	100%	100%	100%	100%	✓
PSPNet(Cityscapes)	Segmentation	100%	99.12%	100%	99.12%	✓
ResNet101(COCO)	Faster RCNN	100%	99.05%	100%	100%	✗
ResNet101(VOC2007)	Faster RCNN	100%	99.05%	100%	100%	✗
VGG16(Visual Genome)	Faster RCNN	100%	93.75%	100%	100%	✓
AlphaGAN	Image matting	100%	95.00%	100%	95.00%	✓
Deep image matting	Image matting	100%	100%	100%	100%	✓
Fast neural style	candy	86.67%	100%	100%	100%	✗
Fast neural style	mosaic	93.33%	100%	100%	100%	✓
Fast neural style	starry night	86.67%	100%	100%	100%	✗
Fast neural style	udnie	66.67%	100%	100%	100%	✗
DCGAN(MNIST)	GAN	100%	100%	100%	100%	✓
DCGAN(CIFAR10)	GAN	100%	100%	100%	100%	✓
DCGAN(CIFAR100)	GAN	100%	100%	100%	100%	✓
VGG19(CIFAR10)	without BN	100%	100%	100%	100%	✓
VGG19(CIFAR10)	with BN	93.75%	100%	100%	100%	✓
VGG19(CIFAR10-lr)	schedule(82-164)	93.75%	100%	100%	100%	✓
VGG19(CIFAR10-lr)	schedule(60-120)	93.75%	100%	100%	100%	✓
VGG19(CIFAR10-lr)	coslr	93.75%	100%	100%	100%	✓

For pytorch pretrain:`http://pytorch.org/docs/master/torchvision/index.html`.

Table 14: **Pytorch pretrian**

Experiments	Remark	Gaussian	Variance	Mean	Magnitude	in the front of network?
VGG11	ImageNet	100%	75.00%	100%	75.00%	✓
VGG16	ImageNet	100%	84.62%	100%	100%	✓
VGG19	ImageNet	100%	87.50%	100%	100%	✓
ResNet18	ImageNet	100%	88.24%	100%	100%	✓
ResNet34	ImageNet	100%	88.24%	100%	96.97%	✓
ResNet50	ImageNet	100%	83.67%	100%	100%	✗

Q Training through slimming

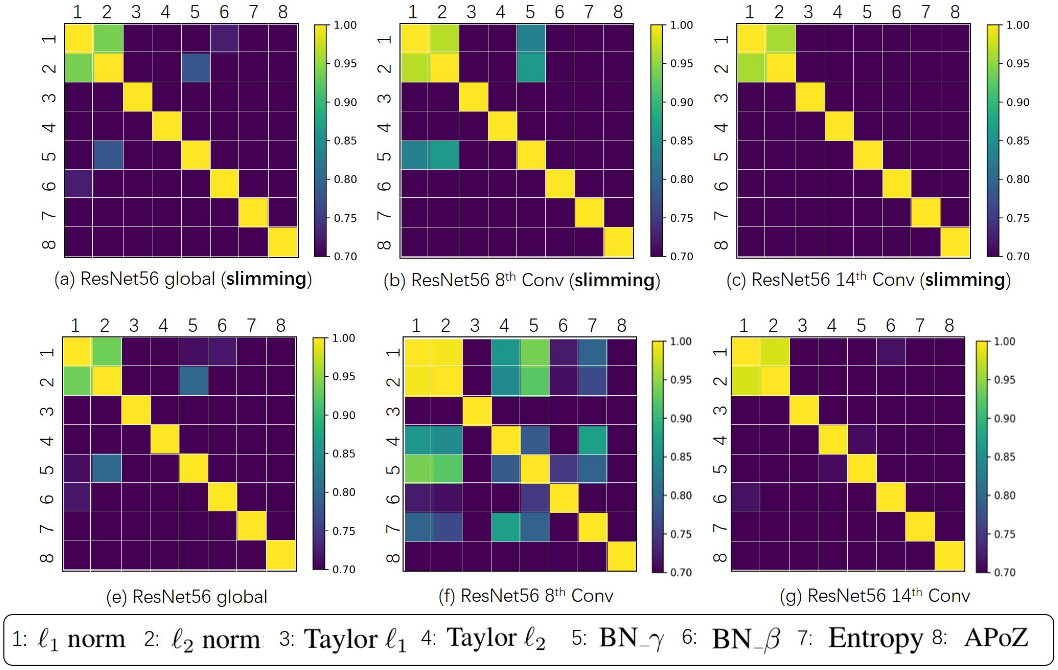

(a) ResNet56 global (**slimming**)

(b) ResNet56 8th Conv (**slimming**)

(c) ResNet56 14th Conv (**slimming**)

(e) ResNet56 global

(f) ResNet56 8th Conv

(g) ResNet56 14th Conv

Figure 19: The Similarity for different criteria with/without slimming [34].

As a representative of the BN-based pruning method, slimming pruning[34] can not be directly compared with the criteria mentioned in the paper because it adopts a special training method. Therefore, we use the training method in [34] to train another ResNet56 on cifar100. Then, the analysis of similarities between 8 different pruning criteria on such a model is shown in Fig. 19.

In this situation, the fifth criterion BN_γ is the method introduced in [34]. From Fig. 19, there is no significant difference in the result of the similarity between ResNet56 obtained by slimming method and resnet56 trained in general.

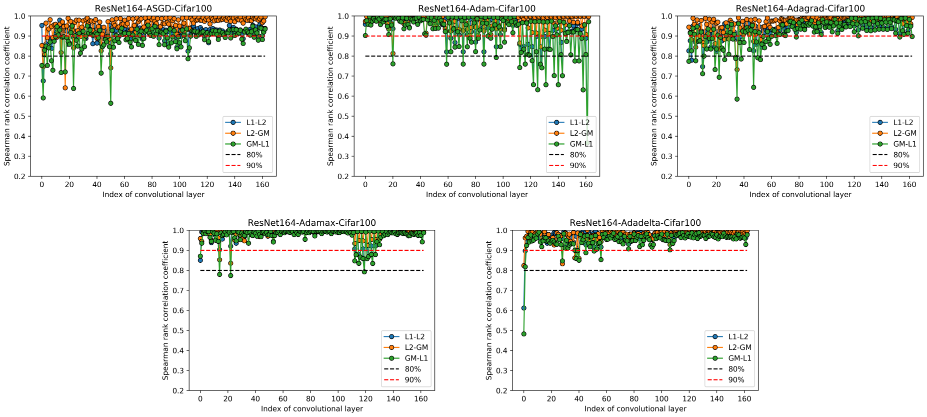

Figure 21: Optimizer

R More experiments of Sp in Norm-based criteria

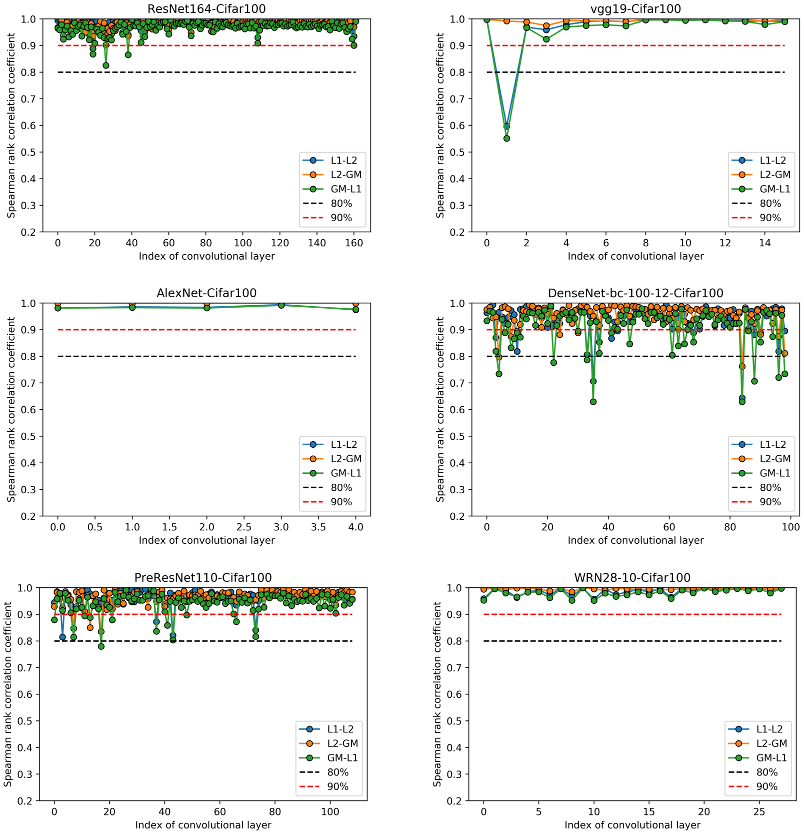

Figure 20: Network Structure

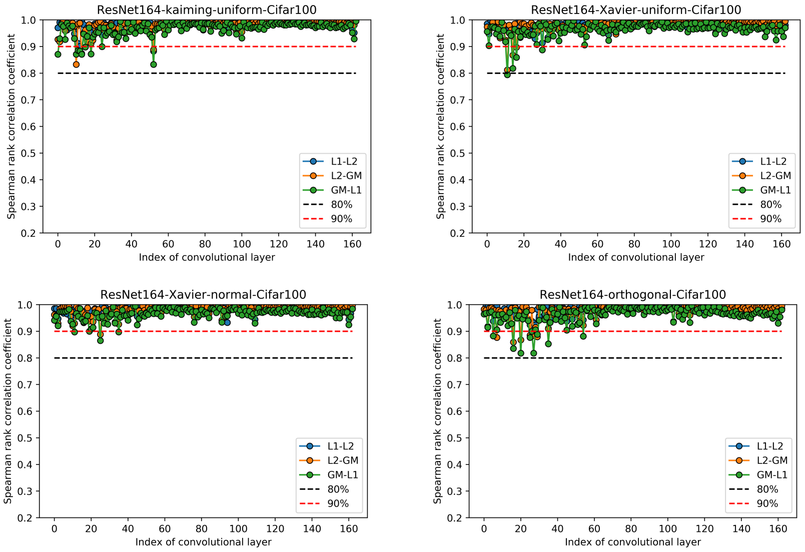

Figure 22: Initialization

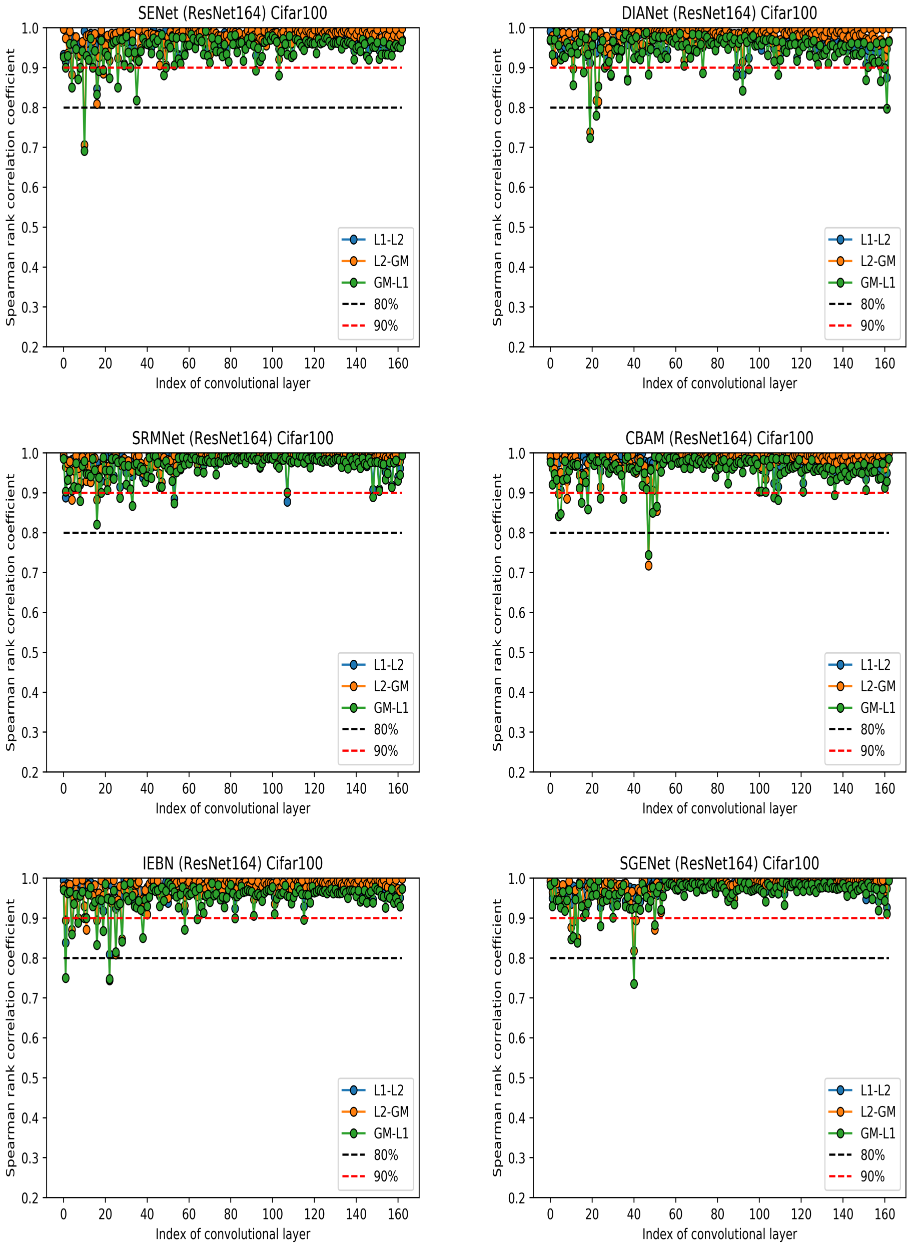

Figure 23: Attention mechanism

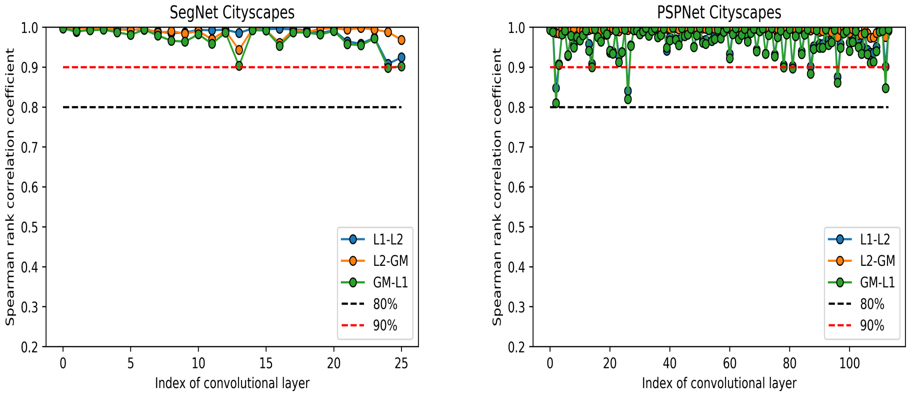

Figure 24: Other task: segmentation

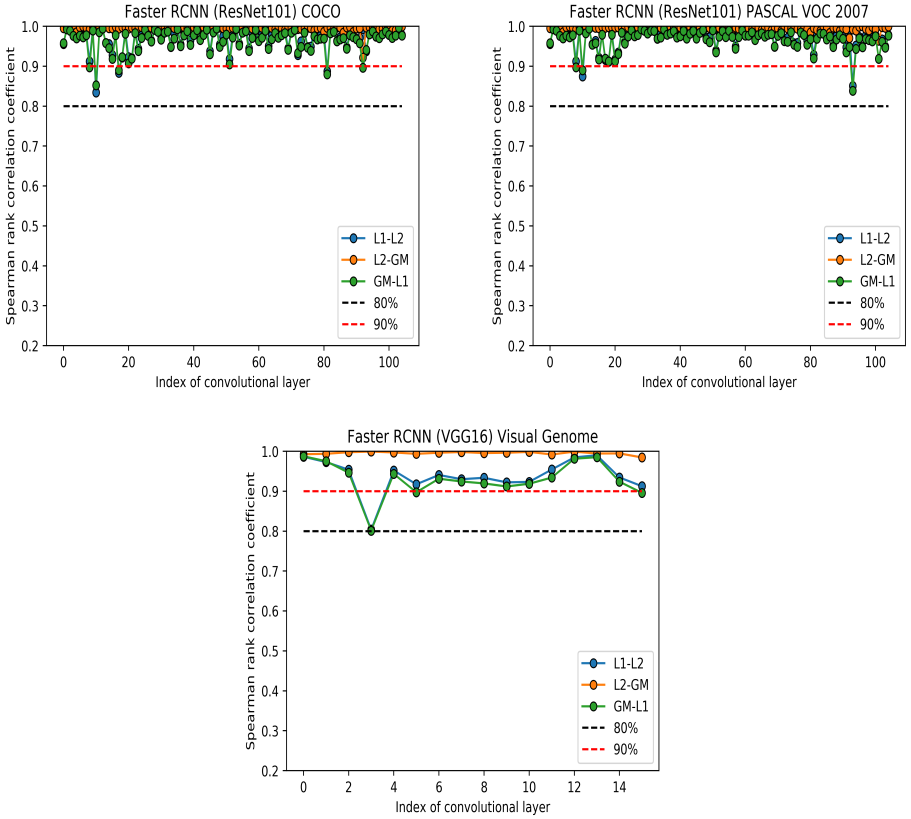

Figure 25: Other task: Faster RCNN

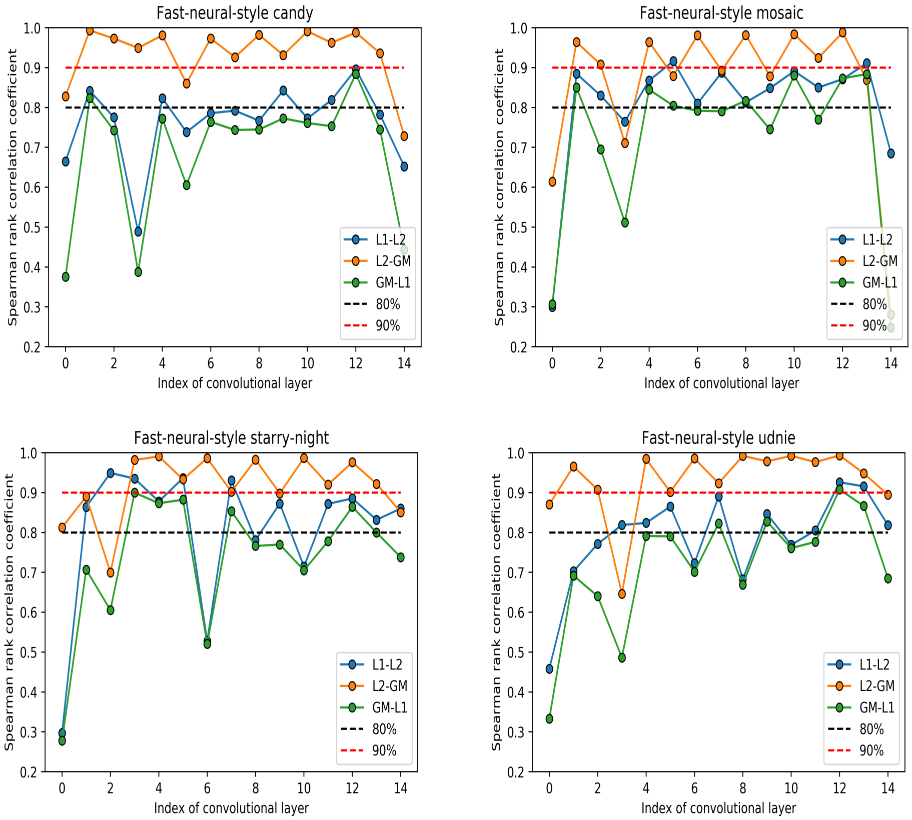

Figure 26: Other task: style transfer

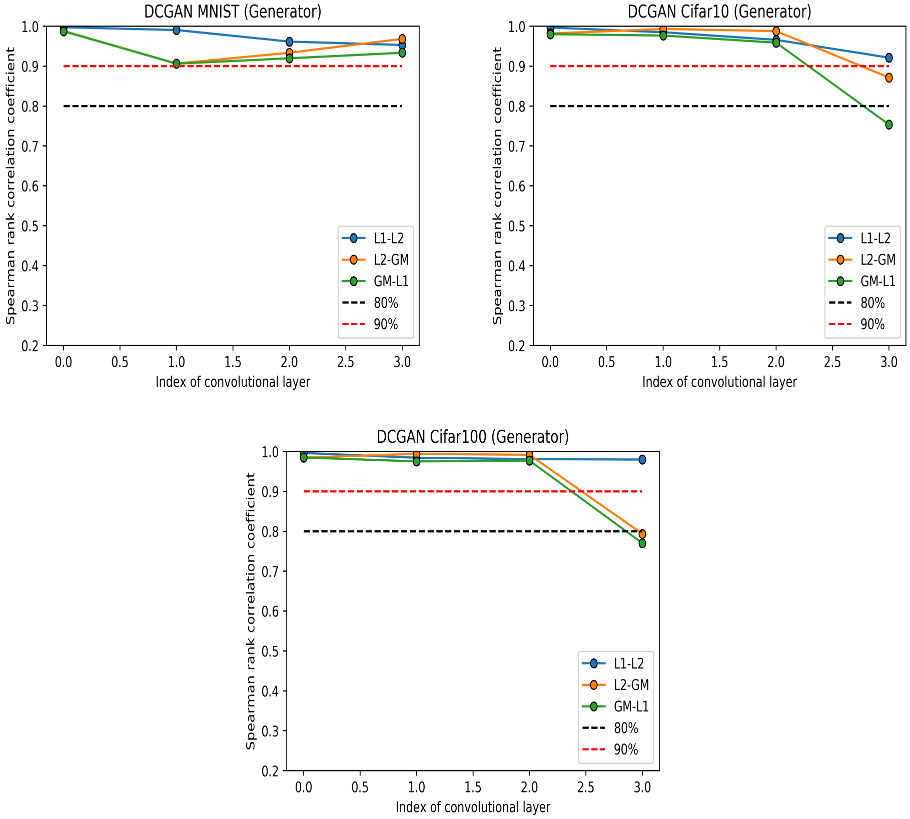

Figure 27: Other task: GAN

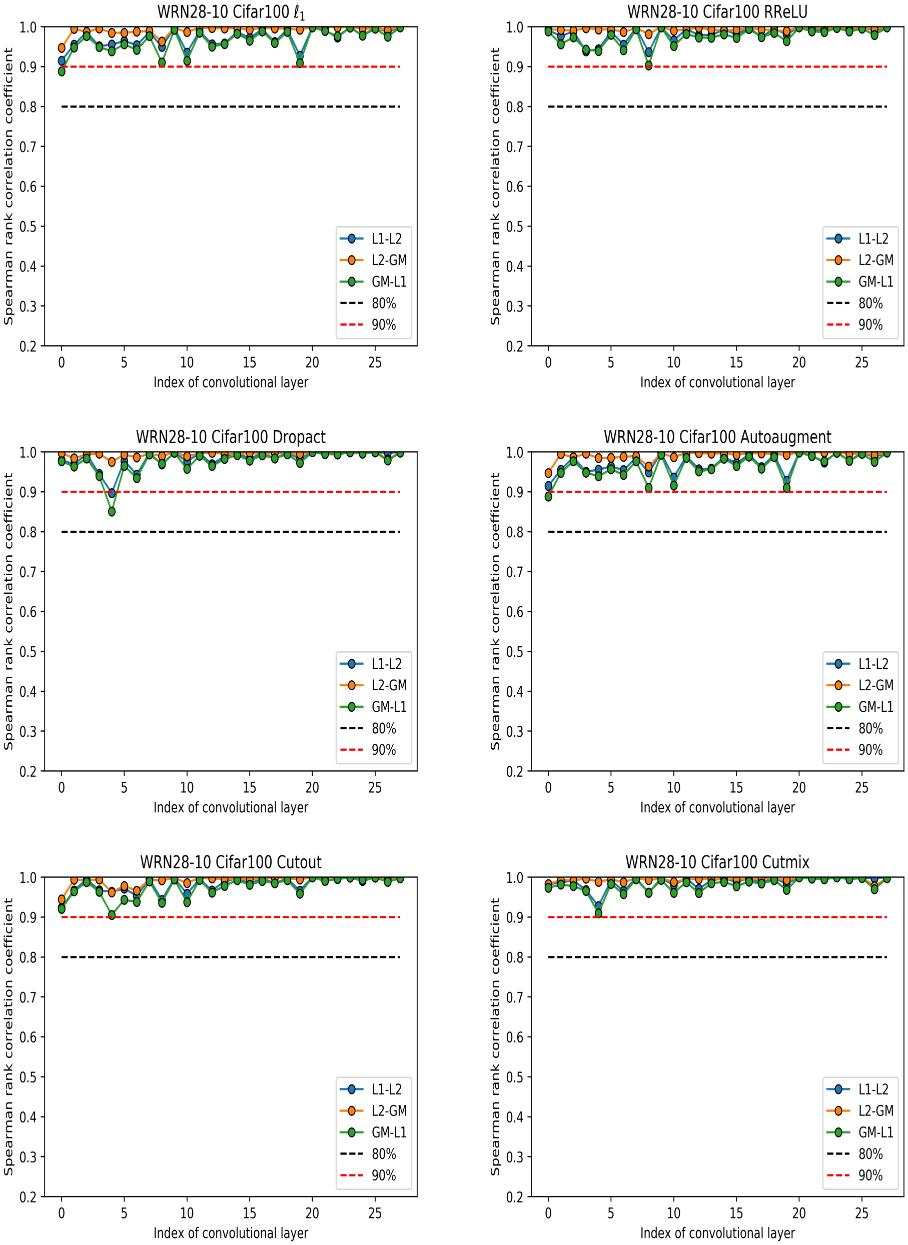

Figure 28: Other task: Regularization

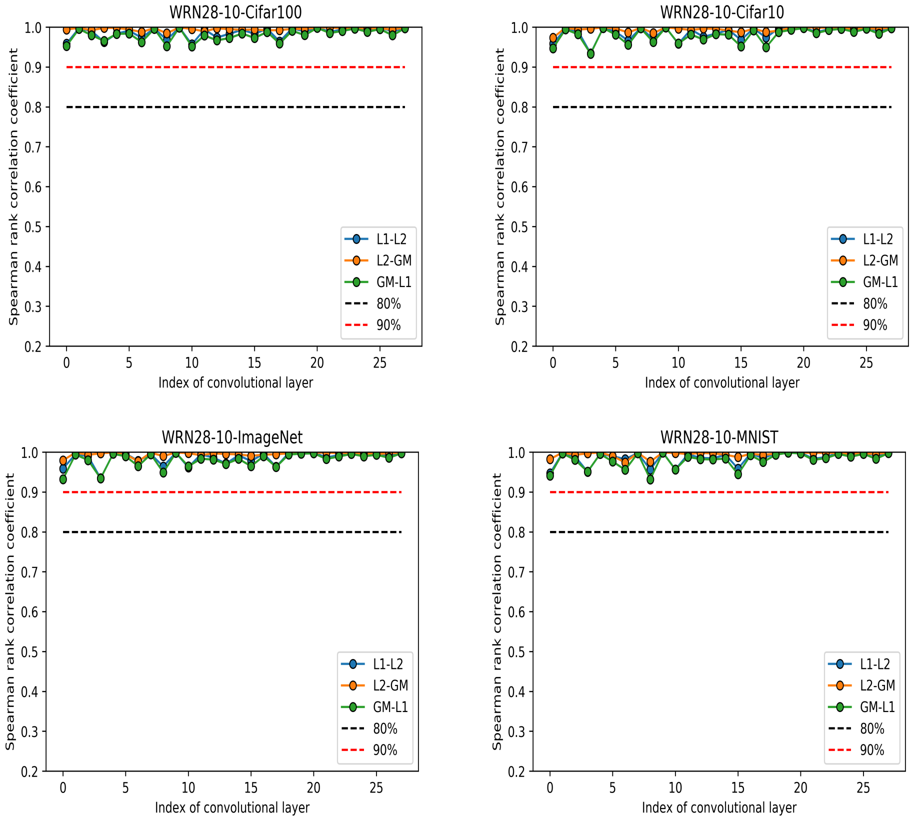

Figure 29: Dataset

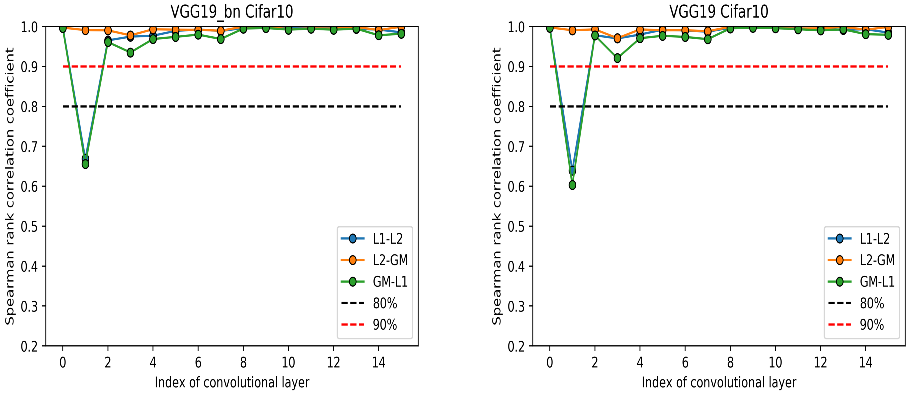

Figure 30: Batch normalization

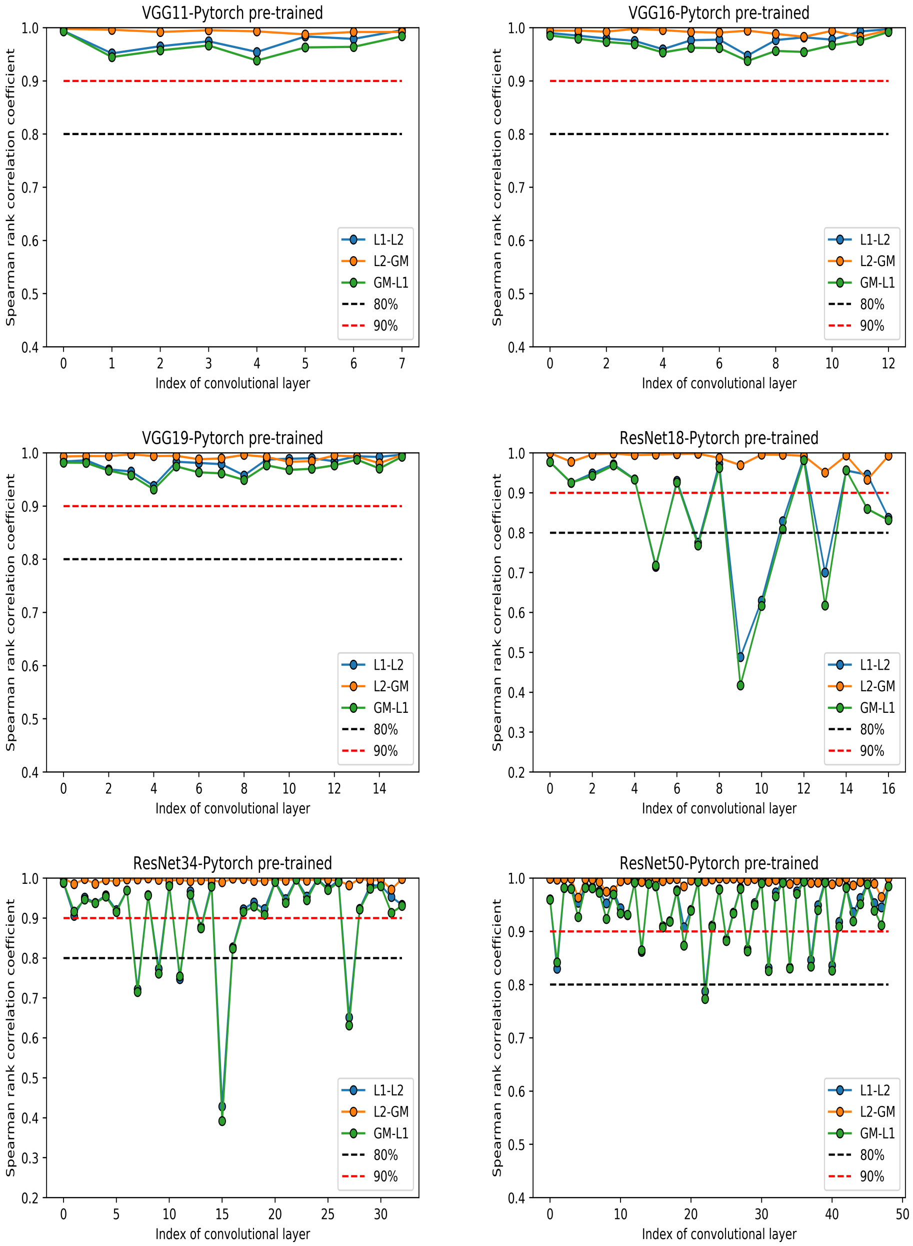

Figure 31: Pytorch pre-trained Model

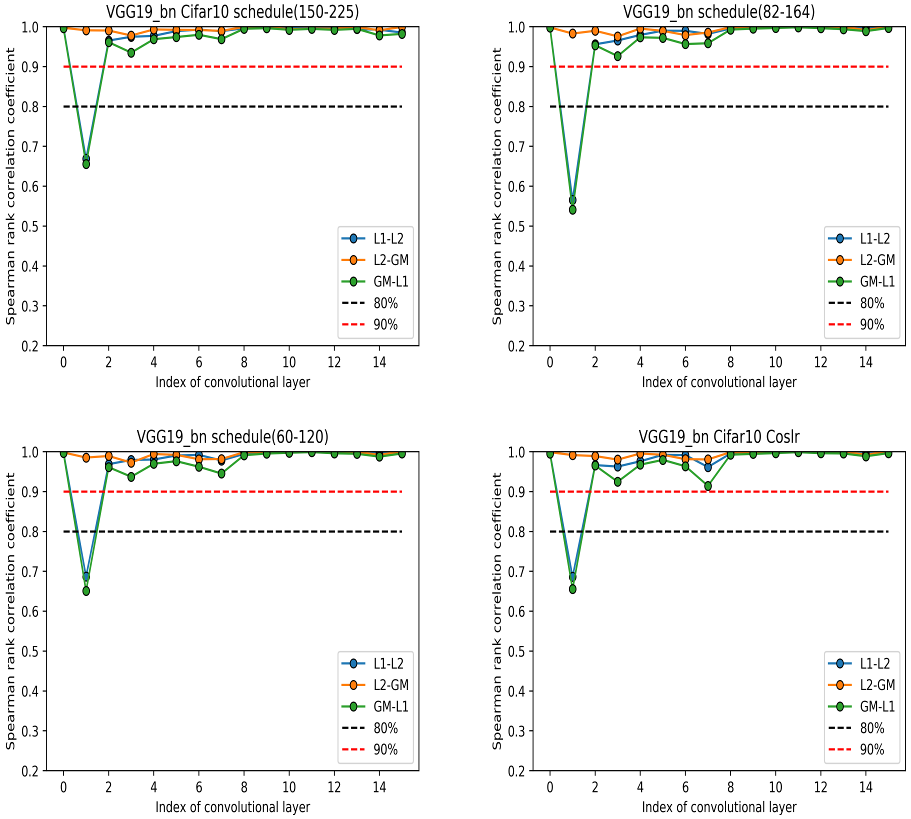

Figure 32: Learning rate